

## Seismic survey and geological model update of the Haaksbergen area of interest

Final report

**Ordered by** AkzoNobel Industrial Chemicals B.V.  
**Author** MWH B.V.  
**Project number** M11B0186  
**Document name** S:\data\Project\M11\M11B0186\2 (T ) Inhoudelijk - Technisch\T4 Deliverables\5\_Report\Isidorushoeve\m11b0186.r01\_ISH\_def.doc  
**Date** 18 November 2011

**Postal address**

PO Box 5076  
6802 EB ARNHEM  
Nederland  
T +31(0)26 7513800  
F +31(0)26 7513818

**Address**

Westervoortsedijk 50  
6827 AT ARNHEM  
Nederland  
[www.mwhglobal.nl](http://www.mwhglobal.nl)

KVK Haaglanden 27 18 43 23  
ING Bank Delft 65 93 74 331  
IBAN NL 63 ING B 0659 374331/BIC INGBNL2A  
MWH is ISO 9001:2008 en VCA\* gecertificeerd



## Table of contents

Executive summary	7
1 Introduction	15
1.1 Background	15
1.2 Seismic study and subsequent geological model update	16
1.3 This report	17
2 Description of the study area	19
2.1 Introduction	19
2.2 Location	19
2.3 Geological setting of the Zechstein salt deposits	19
2.4 Salt resources and reserves in the Haaksbergen area of interest	22
3 Seismic survey and data processing (DMT)	25
3.1 Introduction and location of the seismic lines	25
3.2 Seismic data acquisition	26
3.3 Data processing	34
3.4 Data delivery	41
4 Seismic data interpretation (T&A Survey)	43
4.1 Introduction	43
4.2 Data	44
4.3 Methods	44
4.4 Evaluation study	48
4.5 Recommendations	51
4.6 Reliability	52
5 Geological modeling	53
5.1 Introduction and objectives	53
5.2 Results of the manual interpolation	53
5.3 Fault orientation analysis	56
5.4 Data preparation	57
5.5 Modeling method	59
5.6 Modeling results	63
5.7 Profiles through the salt pillow	69
5.8 Discussion of the implications of the geological modeling results	72
5.9 Quality and reliability	74

6	Resources and reserves	79
6.1	Introduction	79
6.2	Salt resources	80
6.3	Salt reserves	83
6.4	Dip angle of the Zechstein Z1 Halite	86
7	Hydrocarbon risks	89
7.1	Introduction	89
7.2	General discussion of hydrocarbon risks within the study area	89
7.3	Main results of the PanTerra hydrocarbon and H <sub>2</sub> S risk evaluations	90
7.4	Further evaluation of hydrocarbon and H <sub>2</sub> S risks	91
	References	97

## Appendices

Appendix I:	Survey area and all geophone- and source positions
Appendix II:	All figures related to seismic data processing referred to in section 3.3
Appendix III:	All appendices related to related to seismic data interpretation referred to in chapter 4
Appendix IV:	Results of the manual interpolation of the depth of the base of the Zechstein Z1 Halite
Appendix V:	Results of the manual interpolation of the depth of the top of the Zechstein Z1 Halite
Appendix VI:	Modeled depth of the base of the Zechstein Z1 Halite
Appendix VII:	Modeled depth of the base of the Zechstein Z1 Halite (concession area Isidorushoeve)
Appendix VIII:	Modeled depth of the top of the Zechstein Z1 Halite
Appendix IX:	Modeled depth of the top of the Zechstein Z1 Halite (concession area Isidorushoeve)
Appendix X:	Modeled thickness of the Zechstein Z1 Halite with indicated profile lines
Appendix XI:	Modeled thickness of the Zechstein Z1 Halite with indicated profile lines (concession area Isidorushoeve)
Appendix XII:	Modeled depth of the base of the Triassic deposits
Appendix XIII:	Modeled depth of the base of the Triassic deposits (concession area Isidorushoeve)
Appendix XIV:	Modeled thickness of the Z2 to Z4 deposits
Appendix XV:	Modeled thickness of the Z2 to Z4 deposits (concession area Isidorushoeve)
Appendix XVI:	Modeled depth of the base of the Tertiary deposits

Appendix XVII:	Modeled depth of the base of the Tertiary deposits (concession area Isidorushoeve)
Appendix XVIII:	Longitudinal WNW-ESE section through the elongated salt pillow (Profile A)
Appendix XIX:	SW-NE cross section through the western part of the elongated salt pillow (Profile B)
Appendix XX:	SW-NE cross section through the middle part of the elongated salt pillow (Profile C)
Appendix XXI:	SW-NE cross section through the eastern part of the elongated salt pillow (Profile D)
Appendix XXII a-b:	Distance to closest shot point for the base (a) and the top (b) of the Zechstein Z1 Halite models
Appendix XXIII :	Shot point density for the top of the Zechstein Z1 Halite model
Appendix XXIV:	Zechstein Z1 salt thickness within the concession area for which Zechstein Z1 Halite resources are calculated, the developed areas of Sint Isidorushoeve and Haaksbergen within the concession area and indication of the 60 m buffer around seismic surveys and exploration boreholes acquired specifically for the purpose of salt mining
Appendix XXV:	Zechstein Z1 Halite thickness within the concession area with labeled potential caverns
Appendix XXVI:	Modeled depth of the top of the Zechstein Z1 Halite (reserves area)
Appendix XXVII:	List of all potential caverns with key data for each individual cavern
Appendix XXVIII:	Calculated dip angle of the top of the Zechstein Z1 Halite within the concession area
Appendix XXIX:	Calculated dip angle of the base of the Zechstein Z1 Halite within the concession area
Appendix XXX:	Slope of the base of the Triassic combined with isopachs for the depth of the base of the Triassic with potential caverns
Appendix XXXI:	Modeled depth of the base of the Triassic with potential caverns



## Executive summary

### Background

AkzoNobel has been mining salt in concession areas near the cities of Hengelo and Enschede since 1933. Using solution mining, Triassic Röt salt is being mined from caverns at depths ranging from 300 to 500 meters situated within the Twenthe-Rijn, Twenthe-Rijn Uitbreiding and Helmerzijde concession areas. As salt reserves are nearing depletion in these locations, AkzoNobel is investigating salt mining possibilities in new areas in the eastern Netherlands, and from other geological formations, such as the deeper, Permian, Zechstein salt to gain insight into its future salt mining possibilities.

Since 2006, AkzoNobel has been investigating the geological situation in the area around Hengelo and Enschede to gain insight in its future salt mining possibilities. Initial studies in 2006 and 2007 on the geological situation in the area around Hengelo and Enschede indicated that the best prospects for future salt mining were located in the Haaksbergen area of interest, just west of the town of Haaksbergen (Respec, 2006; MWH, 2007b). In this area salt mining from relatively shallow Zechstein salt resources seemed very promising. In 2008 AkzoNobel initiated a more detailed study of the geological situation in the Haaksbergen area of interest in support of the decision-making process for further exploratory research (MWH, 2008b). This study was based on all available and usable (mainly seismic) subsurface data in and around the Haaksbergen area of interest, and indicated that Zechstein salt resources are present with an elongated, pillow-like geometry at relatively shallow depths ranging from 600 to 900 meters below NAP. In the thickest parts of the salt pillow the thickness of the Zechstein Z1 Halite salt layers (the primary target), adds up to almost 400 meters. Based on the information available at that time, the top of the salt pillow was modeled as having two local highs (peaks), a western and an eastern one, with a low (saddle) in-between.

Following the positive results of the 2008 study, in April 2009 AkzoNobel applied for a production permit under Dutch Mining Law. The permit was granted in March 2010. In early 2011 an exploration well was drilled near Haaksbergen (borehole ISH-01), just south of the eastern high on seismic line 6073 (see Figure 1). The top of the Zechstein Z1 Halite deposits was found at a depth of just over 600 meters and the thickness of the Zechstein Z1 Halite deposits measured approximately 335 meters. These results matched extremely well with the modeled depth and thickness. The exploration well was also drilled to obtain more information on the salt pillow, the overlying deposits, and to be able to measure the chemical composition of the salt to establish the level of purity (grade). Therefore, several well logs, cuttings and cores from the borehole were made, which offered a lot of additional insight in the salt pillow, such as information on the quality of the Zechstein salt and the geological and geophysical characteristics of the different deposits. Following the positive results obtained from the exploration well, AkzoNobel applied for a production permit for the concession area 'Isidorushoeve' under Dutch Mining Law in 2011.

### Objectives and general method

Once the production permit is granted, a mining plan must be submitted to the authorities detailing how the salt will be mined such that the risks to the environment are minimized. Mining of the salt in the Haaksbergen area of interest requires more detailed knowledge on the location, geometry, thickness, and grade of the salt resource and on the presence of faults than was available from the previous studies. Therefore, AkzoNobel decided to conduct a seismic survey along two seismic lines of approximately 6.2 and 2.8 kilometers length to acquire higher resolution information, especially in

areas that had low data coverage. Interpretation of the newly acquired seismic data and integration into the existing geological model of the salt pillow in the Haaksbergen area of interest reduced the level of uncertainty in estimates of salt resources and reserves to a level that facilitates the decision-making process with respect to mining of the salt and planning thereof. In particular, additional insight was gained with respect to the risk at encountering hydrocarbons when drilling wells to develop caverns.

### Seismic survey and processing method and results

The 2D reflection seismic survey was carried out by DMT GmbH & Co. KG (DMT), from Essen, Germany using ground vibrators as the energy source. The survey started on July 28, 2011 with topographical surveying and was completed on August 4, 2011. The survey area is located at the northwestern edge of the town of Haaksbergen close to the village of Sint Isidorushoeve and the town of Hengevelde in the eastern area. The total length of the two seismic lines was 8.975 km (see Figure 1). Following data acquisition, data processing was performed by DMT.

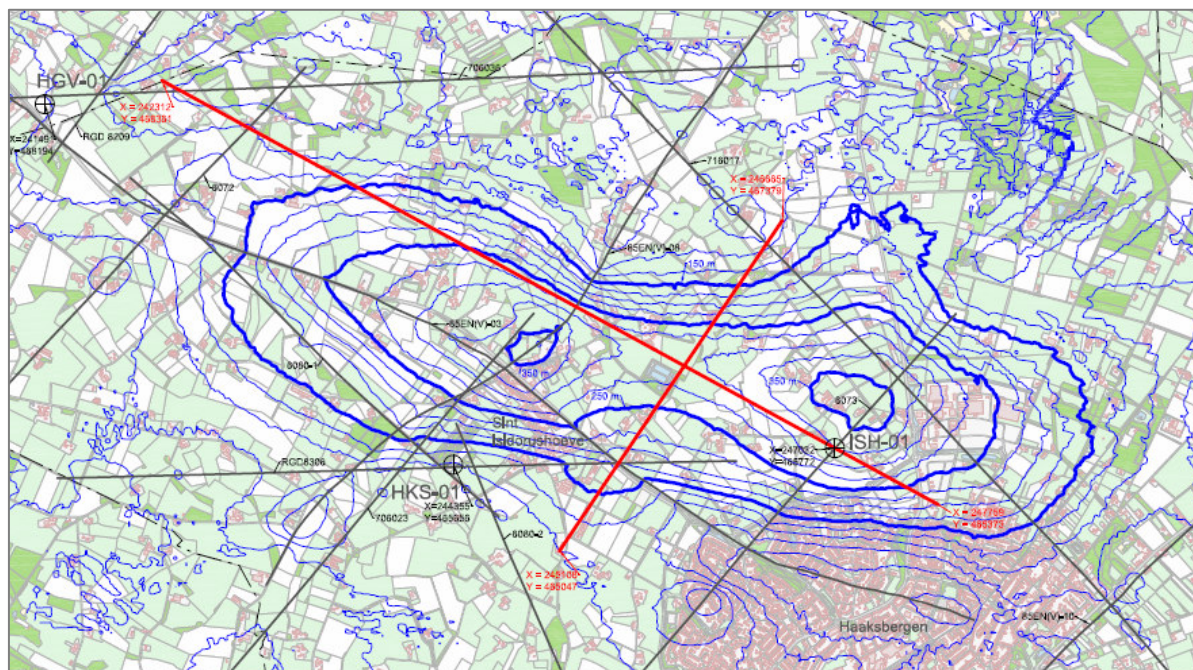


Figure 1: Survey area with location of the seismic lines.

### Seismic data interpretation method and results

T&A Survey was contracted to interpret the newly acquired seismic lines 11-AK-ISH-01 (ISH-01) and 11-AK-ISH-02 (ISH-02) in September and October 2011, to integrate this interpretation into the framework of previously interpreted seismic lines and to incorporate the seismic velocity and other information from exploration well Isidorushoeve-1 (ISH-01). Together with the wells Hengevelde-1 (HGV-01) and Haaksbergen-1 (HKS-01), it was used to tie in and check the seismic data interpretation, and to convert the seismic interpretation of the different formations from the time domain to a depth below surface.

Figure 2 displays the seismic profile (in time) with interpreted horizons for seismic line ISH-01. Figure 3 displays the seismic profile (in time) with interpreted horizons for seismic line ISH-02.



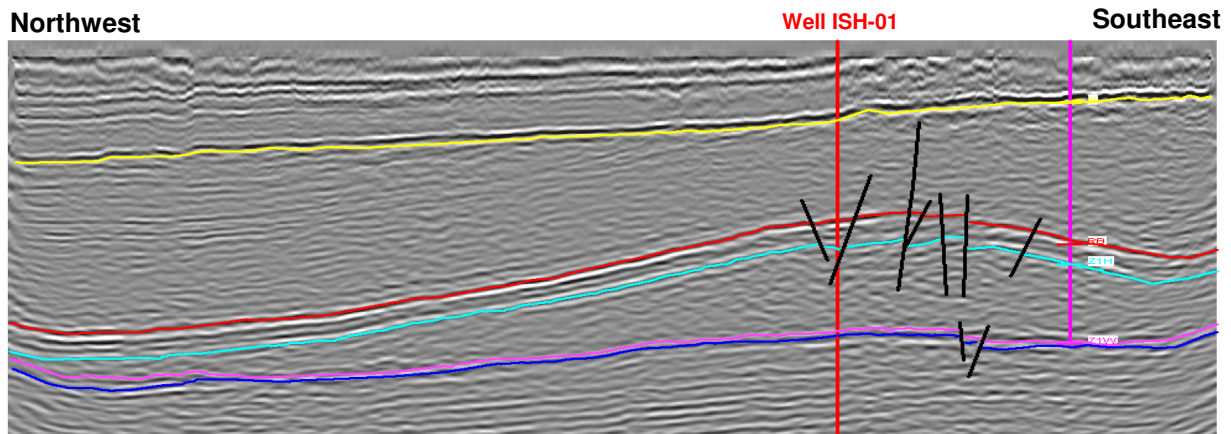


Figure 2: Seismic time profile with interpreted horizons for seismic line ISH-01.

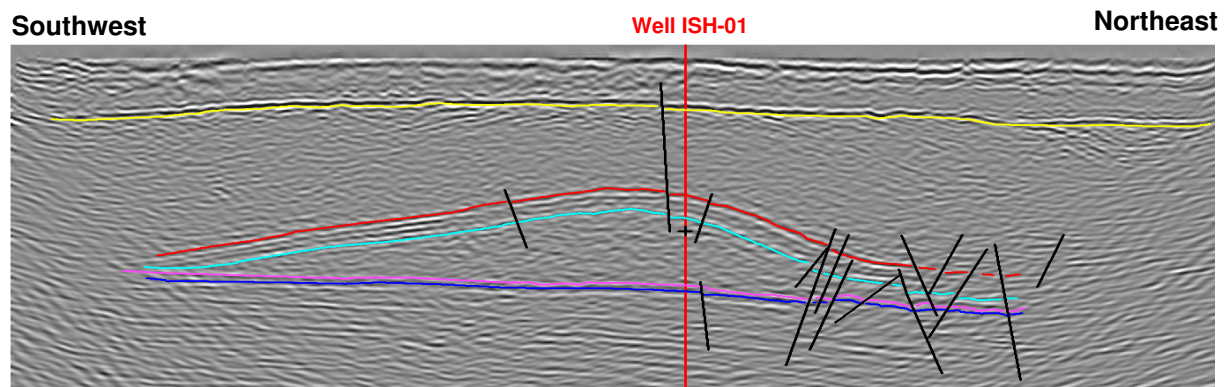
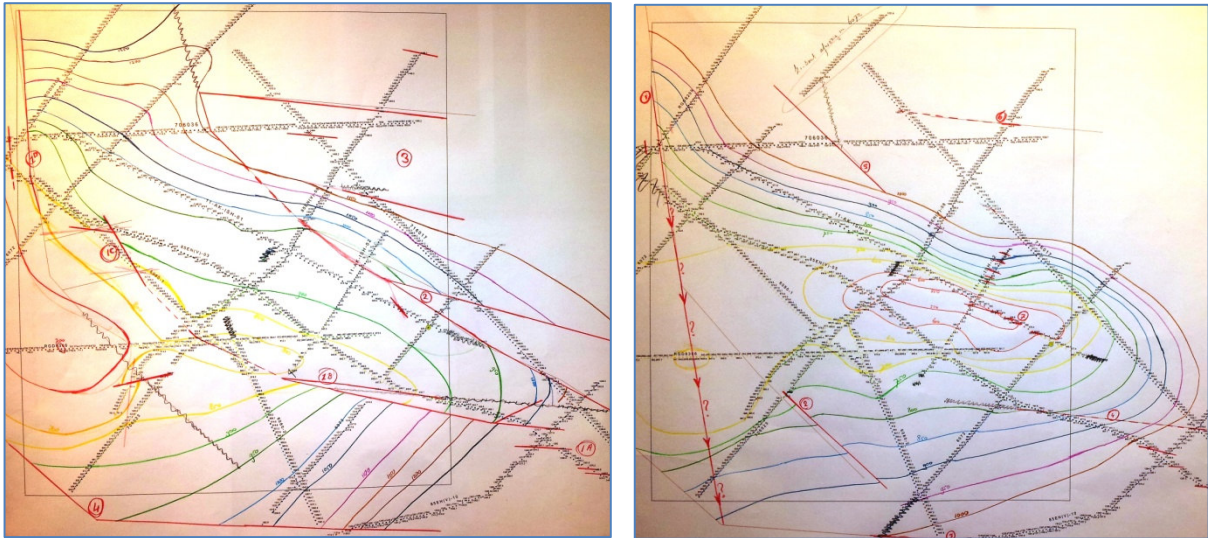


Figure 3: Seismic time profile with interpreted horizons for seismic line ISH-02.

From the seismic interpretation in the Haaksbergen area of interest, depth data for boundaries between six geological formations are obtained to be used to model the depth and thickness of the salt layer of the Zechstein Z1 Halite and other important geological horizons. Interpreted faults are evaluated, especially those that affect the top of the salt layer, for the purpose of evaluating the potential for presence of trapped hydrocarbons. Furthermore, additional insight was gained in the geological setting in the Haaksbergen area of interest that led to a better understanding of how the salt pillow structure was formed. Final data delivery from T&A Survey consisted of the location and depth of the interpreted geological boundaries in digital (i.e. ASCII) and hardcopy format.

### Geological modeling method and results

Updating of the previous geological model of the salt pillow focused on the Zechstein Z1 Halite deposits (primary target) and was done in two consecutive steps. First, manual interpretation of the depth of the top and base of the Zechstein Z1 Halite was done in order to get a good feeling for the geology in the area, to trace important geological faults running through the area, and to find outliers within the used depth data. Results of the manual interpretation are presented in Figure 4.



**Figure 4: Manually interpreted depth of the base (left) and the top (right) of the Zechstein Z1 Halite.**

Following further analysis of the orientation of the faults, several adjustments were made to the data in order to optimize the results from computer modeling, without compromising the integrity of the data, like removal of outliers. Several data interpolation techniques were tested to optimize the fit with the interpreted seismic data for each of the geological horizons, focusing on the area with the thickest salt deposits as this area is most promising for future salt mining. Using state-of-the-art methods the most important geological horizons were then reconstructed in the form of surfaces at different depths in the subsurface, thus obtaining a geological model in three dimensions of the subsurface in the Haaksbergen area of interest.

As a result of the two newly acquired seismic lines data coverage increased significantly, especially in the center of the salt pillow where data coverage was too low to make accurate predictions. Consequently, the modeled depth, geometry and thickness of the formations in the subsurface have become more reliable, particularly in the area where salt deposits are thickest (over 150 m). The new geological model indicates that the base of the Zechstein Z1 Halite is generally located deeper than predicted by the previous model (MWH, 2008b), especially in areas where it was predicted to occur at relatively large depths already (due to the new seismic velocity model used; see Figure 5). Essentially, the same is true for the top of the Zechstein Z1 Halite. However, in-between the two highs of the salt pillow, the depth of the top of the Zechstein Z1 Halite is now predicted to lie shallower as a result of the interpretation of the newly acquired seismic data. The two individual highs that were present in the modeled top of the Z1 Halite in the previous model are now “connected” to form one elongated salt ridge instead, with only minor indications for two individual highs (see Figure 6). Furthermore, the presence and inclusion of faults in the model has caused local changes in the modeled depth of the base of the Zechstein Z1 Halite horizon.

Thickness models for the Zechstein Z1 Halite and the overlying Z2-Z4 Zechstein deposits were created by subtracting the overlying horizons from the underlying ones. Compared to the previous geological model, the modeled thickness of the Zechstein Z1 Halite has changed significantly south of the salt pillow, where a major growth fault has led to another, yet smaller, area with thickened salt deposits. More importantly, because the new model predicts one elongated salt ridge instead of two local highs with a low in-between, the predicted amount of salt present in the structure has increased significantly (see Figure 7).

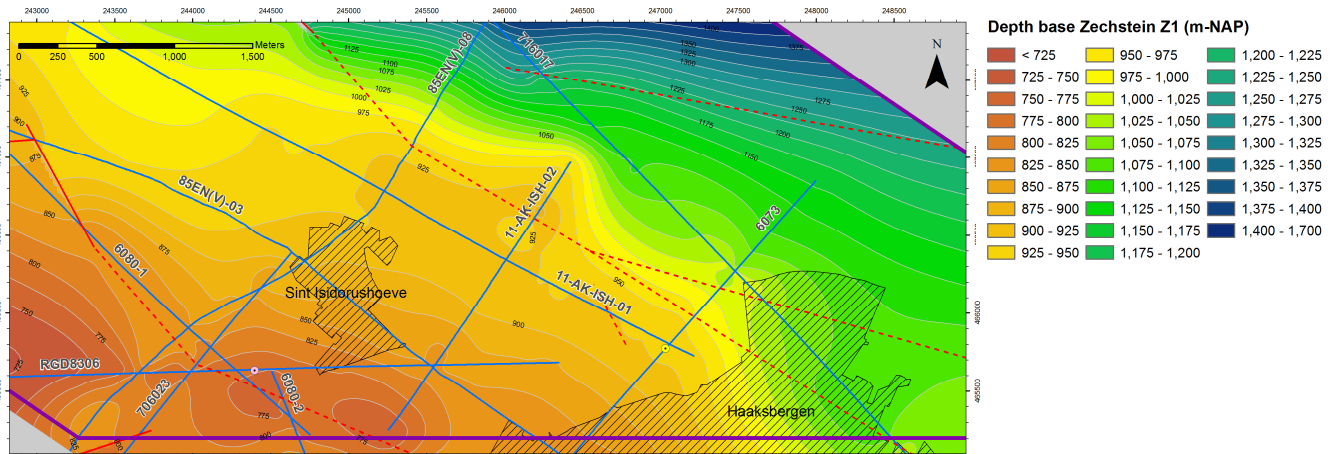


Figure 5: Modeled depth of the base of the Zechstein Z1 Halite in the area with a Z1 Halite thickness of over 150 m.

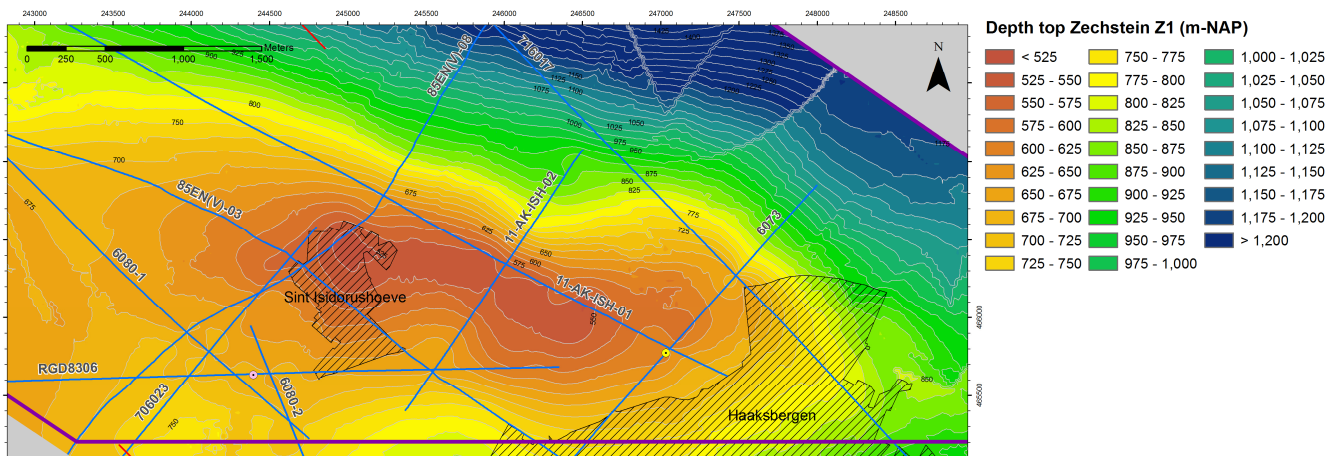


Figure 6: Modeled depth of the top of the Zechstein Z1 Halite in the area with a Z1 Halite thickness of over 150 m.

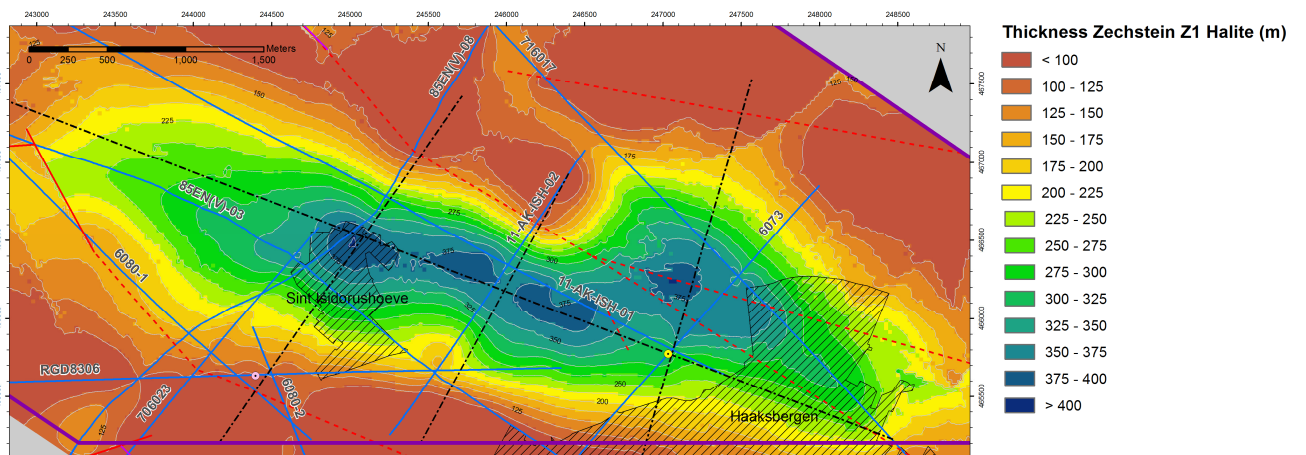
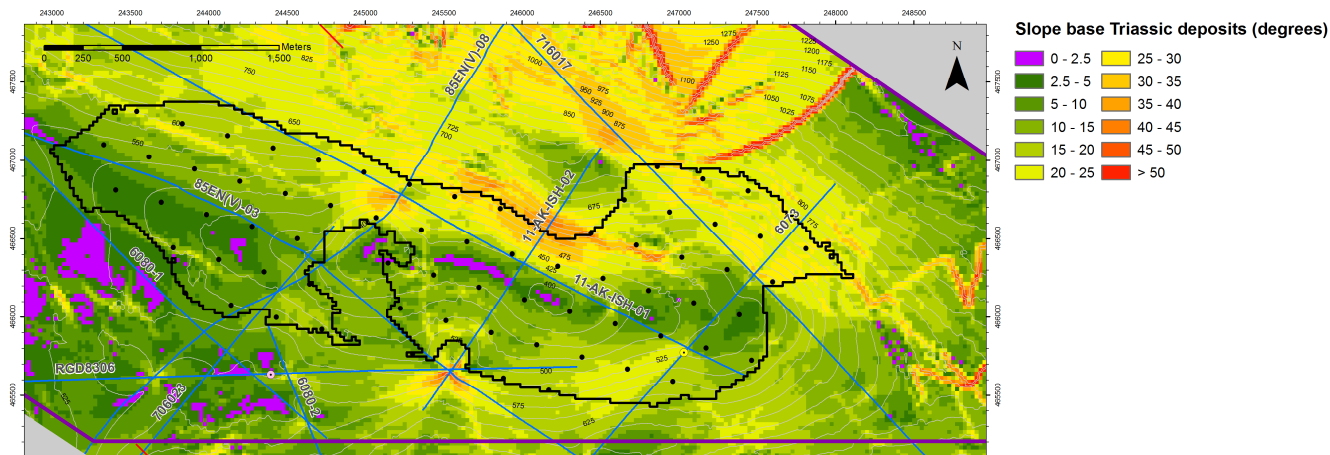


Figure 7: Modeled thickness of the Zechstein Z1 Halite in the area with a Z1 Halite thickness of over 150 m.

## Hydrocarbon risks

As a final investigation step, the new geological model was used to review the risk at encountering hydrocarbons when drilling salt mining wells, which was previously investigated by PanTerra Geoconsultants BV in preparation of drilling of well ISH-01 during the winter of 2010-2011. It can be concluded that there is a very small chance at encountering hydrocarbons (chance  $\approx 1\%$ ) in the upper Zechstein (Z2 and Z3) carbonates, which are located just above the Zechstein Z1 Halite deposits. Risks are considered highest when drilling in local Z2 and Z3 highs, which are located in approximately the same places as the highs in the top of the overall Zechstein formation. These highs are located above the thickest parts of the salt pillow in a narrow band that runs east to southeast of the village of Sint Isidorushoeve (see the purple-colored areas in Figure 8). Other areas with local highs in the upper Zechstein (Z2 and Z3) carbonates might be located just north and south of the salt ridge, where small size local faults may have led to local highs in the top Zechstein (see Figure 9).



**Figure 8:** Map of the slope of the top of the Zechstein and isopachs for the depth of the top of the Zechstein. Combined purple areas and shallowest depths indicate local highs with relatively high potential hydrocarbon risks.

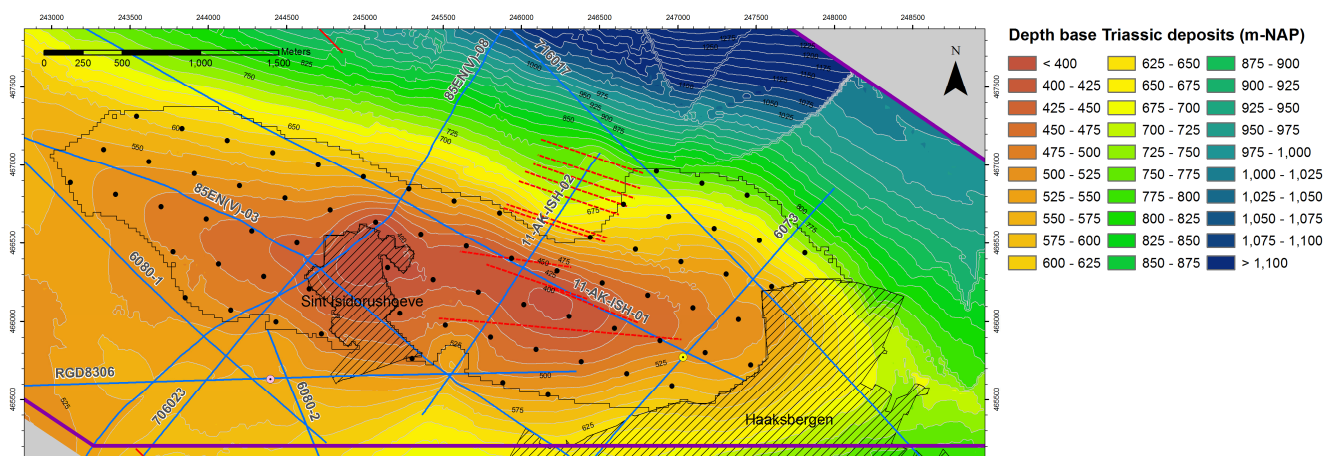


**Figure 9:** Map of the depth of the top of the Zechstein with possible top Zechstein faults. Both areas with shallowest depths as areas with local faults may lead to local highs with relatively high potential hydrocarbon risks.



# 1 Introduction

## 1.1 Background

In the eastern Netherlands, salt mining first started in 1918 near Boekelo from the so-called Buurse concession area. Since 1933, with the opening of the Twente canal, AkzoNobel has been mining salt in concession areas near the cities of Hengelo and Enschede. Using solution mining, Triassic Röt salt is being mined from caverns at depths ranging from 300 to 500 meters. The present mining locations all are situated within the Twenthe-Rijn, Uitbreiding Twenthe-Rijn and Twenthe-Rijn Helmerzijde concession areas.

As possibilities for salt mining are being depleted in these locations, AkzoNobel has been investigating salt mining possibilities in new areas in the eastern Netherlands and from other formation layers, like the deeper, Permian, Zechstein salt.

Since 2006, AkzoNobel has been investigating the geological situation in the area around Hengelo and Enschede to gain insight in its future salt mining possibilities. This investigation is conducted in several steps, like a first regional geological study by the American company Respec (2006), and a second more thorough modeling study by MWH, using both borehole and seismic data (MWH, 2007b). Using the improved model and the previously gathered information on spatial planning opportunities and obstacles, it was possible to make a first selection of six so-called 'areas of interest' that seemed to offer good opportunities for future salt mining. The evaluation of these areas of interest indicated that the best prospects for future salt mining are located in the Haaksbergen area of interest, just west of the village of Haaksbergen (MWH, 2008a). Within this area salt mining from relatively shallow Zechstein salt resources seemed very well possible.

This conclusion led AkzoNobel to investigate the geological situation in the Haaksbergen area of interest in more detail to be able to make well-considered decisions about expensive further exploratory research (MWH, 2008b). This study, that was based on all available and usable (mainly seismic) data, indicated that Zechstein salt resources in the Haaksbergen area of interest are present in an elongated, pillow-like formation at relatively shallow depths ranging from 600 to 900 meters below NAP. In the thickest parts of the salt pillow the thickness of the Zechstein Z1 Halite salt layers adds up to almost 400 meters. The modeled salt pillow seems to have two summits, a western and an eastern one (see Figure 1.1).

Following the positive results of this study, AkzoNobel applied for an production permit under the Dutch Mining Law in April 2009. The permit was granted in March 2010. In early 2011 an exploration well was drilled near Haaksbergen (borehole ISH-01), located just south of the eastern summit on seismic line 6073. The top of the Zechstein Z1 Halite deposits was found at a depth of just over 600 meters and the thickness of the Zechstein Z1 Halite deposits measured approximately 335 meters. These results matched extremely well with the modeled depth and thickness.

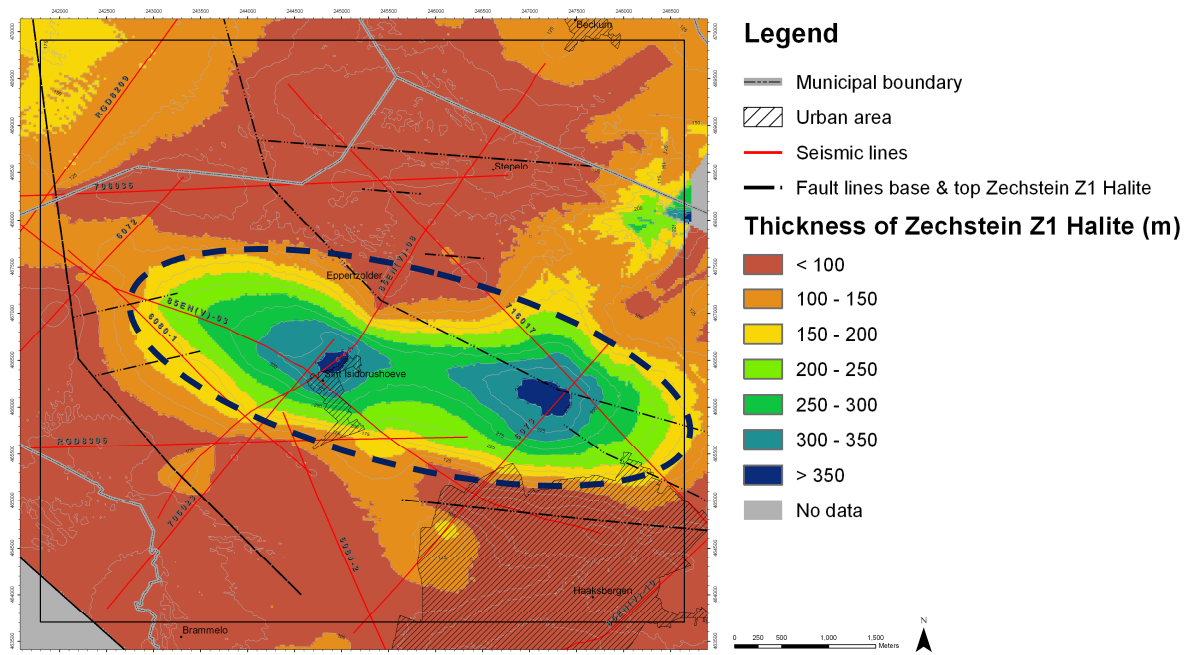


**Figure 1.1: The Haaksbergen salt pillow (dashed line). Map showing the modeled thickness of the Zechstein Z1 Halite, according to the 2008 geological study (MWH, 2008b).**

The exploration well was also meant to get more information on the salt pillow, the overlying deposits and the salt characteristics. Therefore, several well logs, cuttings and cores from the borehole were made, offering a lot of additional insight in the salt pillow, such as information regarding the quality of the Zechstein salt and the geological and geophysical characteristics of the different deposits. Following the again positive results of the exploratory well, AkzoNobel applied for an exploitation permit for concession area 'Isidorushoeve' under the Dutch Mining Law in 2011.

## 1.2 Seismic study and subsequent geological model update

Following the positive results from the exploration well, AkzoNobel decided to conduct a seismic survey in the salt pillow area to gather additional insight into the Zechstein salt deposits as needed for future mining permits and plans.

The objective of the planned seismic survey and geological model update for the Haaksbergen area of interest is to gather sufficiently detailed insight in the Zechstein Z1 Formation (Werra Formation) salt pillow as is necessary for future mining permits and plans. Therefore, three steps are taken:

1. Seismic data acquisition along two seismic lines of approximately 6.2 and 2.8 kilometers length and data processing;
2. Interpretation of the new seismic data and integration within the present (previously interpreted) seismic framework, followed by time-to-depth conversion using a new seismic velocity model;
3. Update of the present geological model of the salt pillow, focusing on the Zechstein Z1-salt deposits (Chapter 5). This model is then used to assess salt reserves within the area and to give extra insight in the risks of encountering hydrocarbons when drilling the wells.

### **1.3 This report**

In Chapter 2 we describe the study area and the geological setting, and we summarize the results of previous studies on the Haaksbergen area of interest as this is the starting point for the present study.

Chapter 3 describes the seismic data acquisition in the Haaksbergen area of interest as well as seismic data processing.

Chapter 4 describes the interpretation of geological horizons within the newly acquired seismic lines, the integration within the seismic framework and the time-to-depth conversion using the updated seismic velocity model.

Chapter 5 forms the major study part of this report for gathering additional insight into the Zechstein salt deposits, as it describes the geological modeling activities and results.

Determination of the resources and reserves is presented in Chapter 6 and hydrocarbon risks are assessed in Chapter 7.





## 2 Description of the study area

### 2.1 Introduction

In 2008 MWH investigated the geological situation in the Haaksbergen area of interest, using all available and usable (mainly seismic) data (MWH, 2008b). In this chapter we give a short overview of the geological setting within the prospect area, mainly based on earlier geological studies like the Thesis of Mark Geluk (Geluk, 2005). Furthermore we summarize the results of the previous study on the Haaksbergen area of interest (MWH, 2008b), including important gaps in knowledge and reliability, as this forms the starting point for the present study.

### 2.2 Location

The Haaksbergen area of interest is located just northwest of the village of Haaksbergen, more or less around the small village of Sint Isidorushoeve. The provincial road N347 runs through the area in a northwest-southeast direction.

### 2.3 Geological setting of the Zechstein salt deposits

#### 2.3.1 General description

Within the different deposits of the Zechstein group, salt is found within four different formations, numbered from the oldest formation (Z1 or Werra formation) to the youngest formation (Z4 or Aller formation). The youngest salt formation is overlain by the Zechstein upper claystone.

For salt mining purposes all Zechstein formations may be of interest, although the Z1 or Werra formation is of most interest as in this area it has the largest thickness and contains salt of the highest quality with hardly any impurities.

The Z1 formation can be further subdivided into five layers, which are named (from oldest to youngest): the Copper Shale layer, the Z1 Carbonate layer, the Z1 Lower Anhydrite layer, the Z1 Salt layer and the Z1 Upper-Anhydrite layer. The Z1 Salt layer is of interest for salt mining. Table 2.1 shows the division of the Zechstein group in various formations and layers.

**Table 2.1: Division of the Permian in Zechstein and Rotliegendes group and in Zechstein formations and Z1 layers.**

System	Group	Formation	Layers	
Permian	Zechstein	Zechstein Upper Claystone		
		Z4 Formation (Aller)		
		Z3 Formation (Leine)		
		Z2 Formation (Stassfurt)		
	Rotliegendes	Z1 Formation (Werra)	Z1 Upper Anhydrite	
			Z1 Salt (Halite)	
			Z1 Basal Anhydrite	
			Z1 Carbonate	
			Copper Shale (Kupferschiefer)	

### 2.3.2 Geological history

As most other salt resources, the Zechstein salt layers were deposited in a shallow marine environment at the bottom of a large shallow sea that formed along the southern edge of the so-called Southern Permian basin during the late Permian (see Figure 2.1). In the eastern Netherlands, a small sea formed that was sometimes land-locked (see Figure 2.2; left window).

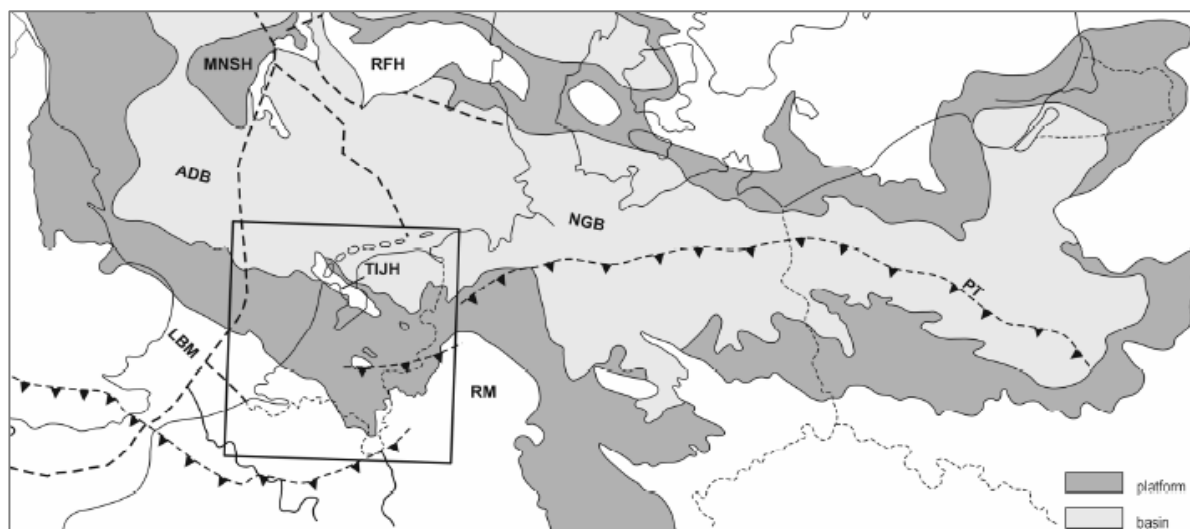


Figure 2.1: Sketch map of the Southern Permian basin during the Late Permian (after Geluk, 2005). ADB: Anglo-Dutch Basin; LBM: London-Brabant Massif; MNSH: Mid North Sea High; NGB: North German Basin; PT: Polish Trough; RFH: Ringkøbing-Fyn High; RM: Rhenish Massif; TIJH: Texel-IJsselmeer High.

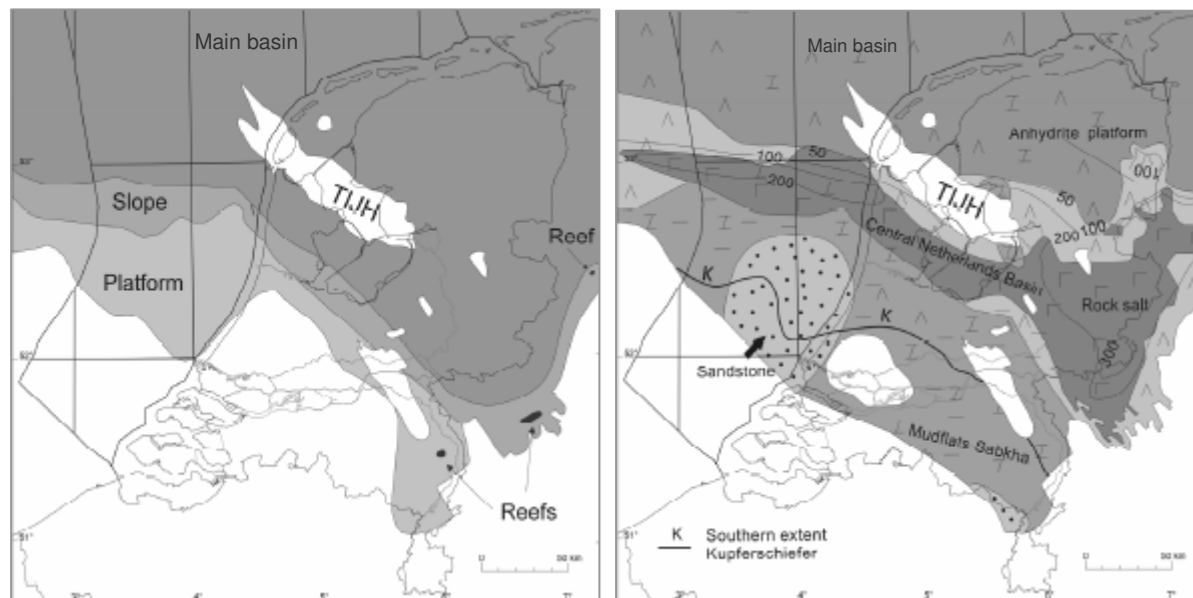


Figure 2.2: Facies (left window) and isopach (right window) maps of the Z1 (Werra) Formation. The greatest thickness, over 400 m, occurs in the anhydrite platform on the southern edge of the main basin in the eastern Netherlands in conjunction with syndepositional faulting. Rock salt deposition occurred in the area of the Central Netherlands Basin. In the main basin a condensed succession of layers of carbonates and evaporates was deposited under starved conditions (after Geluk, 2005). Abbreviations as in Figure 2.1.

### 2.3.3 Geological history of the Haaksbergen area of interest

Based on the general knowledge of the Permian basin and the formation of salt deposits and salt pillows, we can sketch the following geological history of the Haaksbergen salt pillow.

The salt pillow is underlain by a heavily faulted Carboniferous horst block where horsts and adjacent grabens had formed during Permian time. What tectonic regime was present during Late Permian deposition of the Zechstein is unclear. The different faults were probably reactivated during the Variscan Orogeny, as the northernmost occurrence of Variscan thrusts, the so-called Variscan Front, was situated just south of the area of interest. During Late Permian times a more extensional tectonic regime was present during which expansion of the Central Netherlands Basin and rifting of the Variscan front occurred.

According to Geluk (2005) tectonics during the early Zechstein (Tubantian I) along the southeastern margin of the Central Netherlands Basin was extensional too, causing halfgrabens, grabens and graben shoulders to form. During this time, deposition of rock salt took place in tectonically-controlled intra-platform depressions, like the blue colored WNW-ESE trending area in the Netherlands, on the southern edge of the anhydrite platform in Figure 2.3. This WNW-ESE oriented lineament in the Netherlands is assumed to have originated from minor transtensional movements. Within the Haaksbergen area of interest, Z1 salt was deposited filling up these grabens and half grabens. Rapid deposition and loading of evaporates like salt and anhydrite amplified fault relief (i.e. synsedimentary faulting; see Figure 2.7, right window, for an example from the area of interest).

Although this type of tectonics may explain the presence of thick Z1 deposits, it does not explain all thick salt deposits, as most of these thick deposits are not present adjacent to major faults. Therefore it is thought that most other thick salt deposits present originate from the process of halokinesis (salt movement).

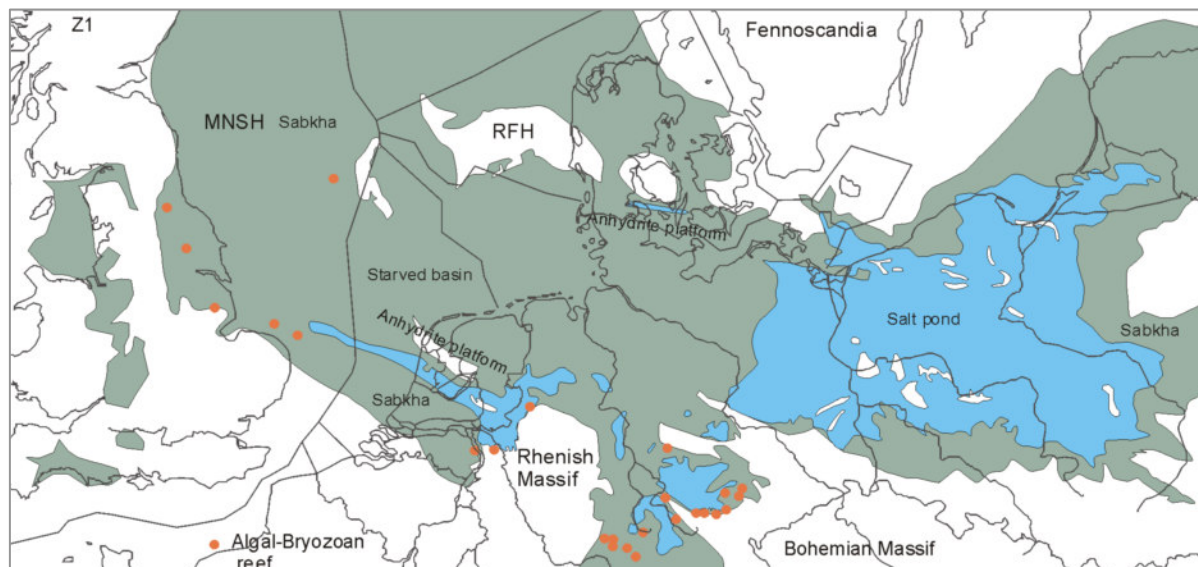


**Figure 2.3: Combined facies and present-day distribution map of the Zechstein Z1 Formation indicating different deposition facies in northwestern Europe. Unpublished map from <http://home.hetnet.nl/~mark.geluk/Z1%20facies.htm> after Cameron et al. (1992), Wagner, (1994), Baldschuhn et al. (2001), Geluk et al. (1996) and Glennie et al. (2003).**

Zechstein and Triassic deposits overlying the salt pillow are seen to show the same folded structure, indicating halokinesis took place after deposition of these younger sediments. From the presence of thickened Röt salt formations in the Beckum synclinal structure (MWH, 2007) we can deduce that halokinesis already started during Triassic times and went on until the end of Triassic times and probably even into Jurassic and Cretaceous times as, except for Tertiary deposits, all salt overlying deposits show the same arched structure.

The Triassic start of halokinesis is assumed to be related to the extensional regime that came into existence during Triassic and Jurassic times. This triggered wide-spread mobilization of Zechstein salt as is shown in Figure 2.4. Nevertheless, it is assumed that extensive salt movement within this area is related to compressional tectonics that did not take place until Late Cretaceous to Early Tertiary times (Subhercynian tectonic phase; Geluk, 2005). During compression deep (Carboniferous) fault zones were re-activated enabling shortening. Salt layers could adapt to this shortening in a different way, causing further halokinesis, especially near WNW-ESE trending faults, like the fault zones cross-cutting this area. Halokinesis is assumed to occur only within thick salt successions over a major fault at the base of the salt. Here, due to its lower density, the salt moves up the northeastern slope of the Carboniferous horst block. Although a thick salt pillow is present, salt movement has not been powerful enough to have caused salt diapirs to break through the overlying layers, probably due to the relatively shallow burial depth. This depth further decreased as Tertiary erosion took away a big part of the sediment load above, causing any further halokinesis to end.

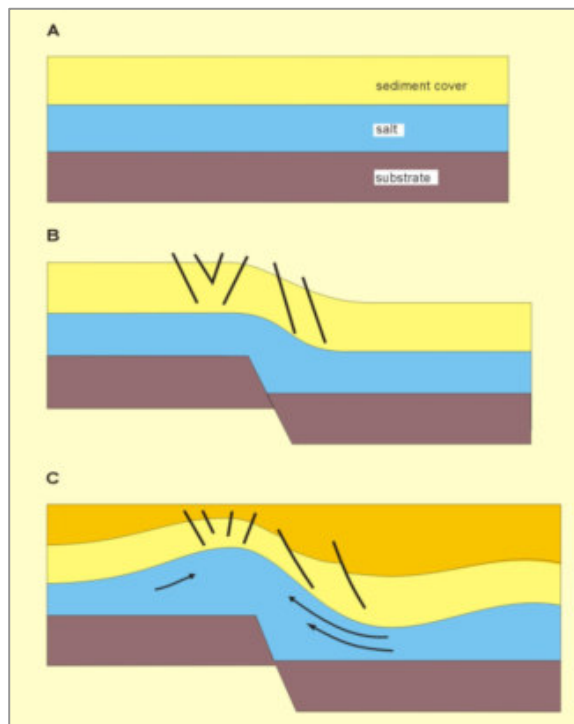


Figure 2.4: Figure from [http://home.hetnet.nl/~mark.geluk/Salt\\_Index.htm](http://home.hetnet.nl/~mark.geluk/Salt_Index.htm) regarding the development of salt structures (after RGD, 1993).

## 2.4 Salt resources and reserves in the Haaksbergen area of interest

### 2.4.1 Salt resources

Previous geological investigations by MWH (2008a & 2008b) indicate the presence of Zechstein salt resources in a pillow-like formation at relatively shallow depths of less than 600 to 900 meters. In the thickest parts of this salt pillow, located exactly below Sint Isidorushoeve and less than 1 km north of Haaksbergen, the thickness of the Zechstein Z1 Halite adds up to over 350 meters (see Figure 2.5). The salt volume within the area where the Z1 Halite deposits are more than 200 meters thick, is indicated to be over 1,700 million m<sup>3</sup> (i.e. 1.7 km<sup>3</sup>). This is the summed volume of the green and blue areas in Figure 2.5. The modeled salt pillow displays a more or less west-east oriented elongated structure. The structure of the salt pillow can best be shown using geological profiles parallel and perpendicular to the elongated structure (see Figures 2.4 and 2.5). The location of the cross section is also shown in Figure 2.5.

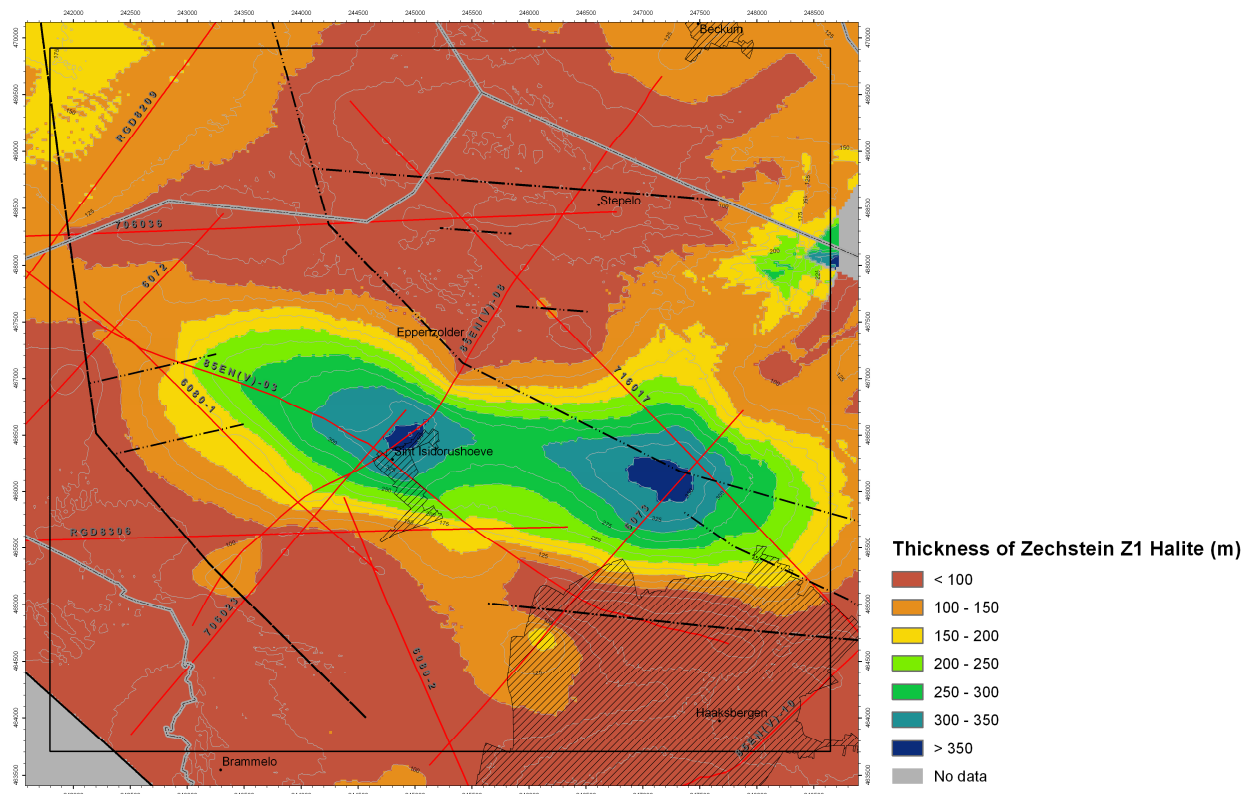


Figure 2.5: Modeled thickness of the Zechstein Z1 Halite (MWH, 2008b).

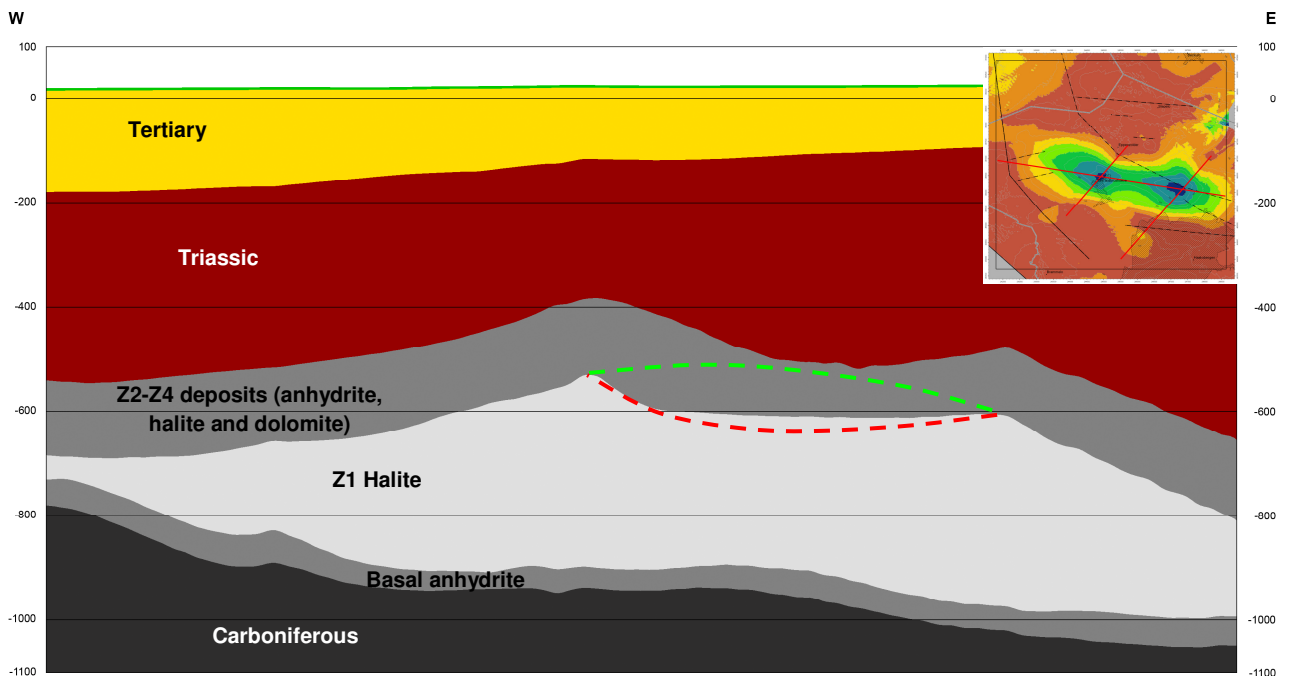


Figure 2.6: Longitudinal WNW-ESE section through the elongated salt pillow (vertical exaggeration three times; MWH, 2008b). Dashed lines indicate a kind of maximum (green) and minimum (red) scenario for the actual top of the Z1 Halite. Top of the Zechstein will be affected in the same way (not drawn in this figure).

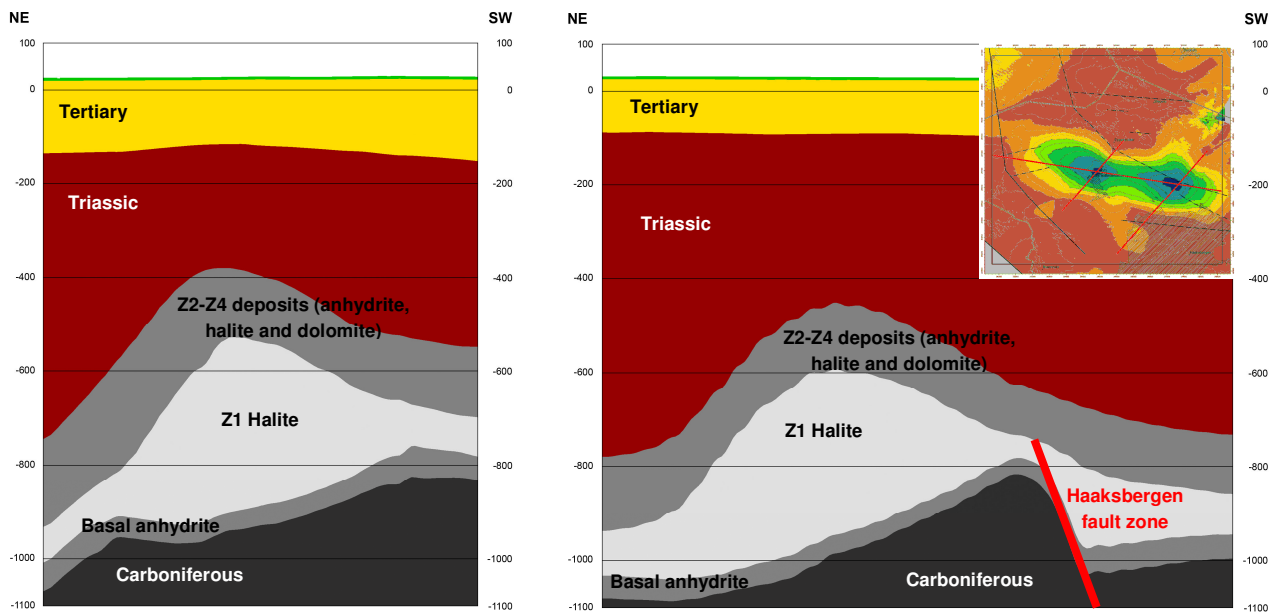


Figure 2.7: SW-NE cross section through both the western (left window) and eastern (right window) areas with the highest salt thickness (vertical exaggeration three times; MWH, 2008b).

#### 2.4.2 Salt reserves

According to the previous 2008-study, extractable salt volumes within the Haaksbergen area of interest, outside areas with severe surface restrictions and using several requirements for the hanging and bedding safety<sup>1</sup> and a complex cavern grid<sup>2</sup>, the total volume of salt reserves amounts to xxx million tonnes that can be mined from xx caverns. Based on an annual production of the Hengelo brine field of x million tonnes, the salt pillow in the Haaksbergen area of interest could provide enough extractable salt for over xx years of production.

#### 2.4.3 Gaps in knowledge and reliability

Gaps in knowledge about the Zechstein salt deposits within the Haaksbergen area of interest and relatively low reliability of the geological model of this area mainly arise from the quality, location, and distribution of the source data. The main area of lower reliability, being located far away from all seismic lines, is the area in between the two salt pillow highs. Here, the lack of nearby source data and the presence of less reliable source data leads to less reliable modeling results. From a geological point of view it can be argued that the actual Zechstein Z1 Halite deposits in this area are very likely thicker than modeled rather than thinner (see Figure 2.6).

Furthermore, the area north and northwest of the village of Sint Isidorushoeve forms an area of relatively low reliability, being located far away from seismic lines.

The present seismic study focuses on these areas and the location of the seismic lines is selected to fill in these gaps.

<sup>1</sup> a 20 m bedding safety to the base of the Zechstein Z1 Halite and a minimum 30 m hanging safety to the top of the Zechstein Z1 Halite as well as a minimum 200 m hanging safety to the top of the Zechstein

<sup>2</sup> grid assuming a hexagonal configuration with hexagonal cavern clusters in which the well to well distance within a cluster of wells is 300 m and the central well to central well distance between clusters is 1200 m

### 3 Seismic survey and data processing (DMT)

#### 3.1 Introduction and location of the seismic lines

The Isidorushoeve survey is focused on gathering detailed seismic information at the most ideal location, to give additional detailed insight in the Zechstein salt deposits in this area, necessary for future mining permits and plans.

The previous study (MWH, 2008b) identified several areas in the Haaksbergen area of interest that seem to offer good possibilities for future salt mining. These areas are, in order of importance:

1. the middle part of the salt pillow, located in-between the two local highs that are visible in the top of the Z1-salt deposits;
2. the area northeast of the eastern local high, north-northeast of Haaksbergen;
3. the area north-northwest of the western local high, northwest of Sint Isidorushoeve.

As the existing geological model already has a high level of detail in those last two areas, the new seismic lines focus on the first area, i.e. the middle part of the salt pillow, where the geological model has limited reliability due to lack of seismic data and salt resources may very well be significantly larger than suggested by the existing model.

AkzoNobel chose the location of the two new seismic lines (see Figure 3.1) to obtain data that are extremely useful in providing insight in the middle of the salt pillow (with both lines intersecting more or less in-between both highs) and in the area north-northwest of the western local high. The area northeast and east of the eastern local high will still remain somewhat of a 'blank spot' in the new model.

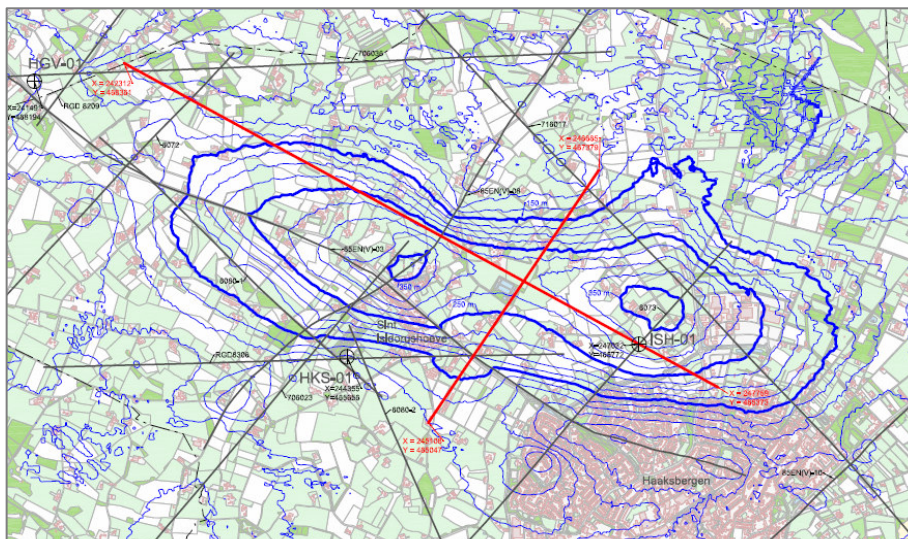


**Figure 3.1: Map with isopachs of the salt pillow with the location of the two seismic lines (red) within the Isidorushoeve seismic survey. Grey lines indicate available seismic lines, used for the existing geological model. Also, the location of exploration well ISH-01 is indicated.**



The acquisition of the two new seismic lines and processing of the acquired data were done by DMT. The remainder of this chapter is comprised by two reports from DMT that describe all data acquisition and processing activities (reproduced with permission from DMT):

- Seismic data acquisition (section 3.2): DMT, 2011. Field report 2D seismic Isidorushoeve 2011. Reflection seismic vibroseis. In the area of Sint Isidorushoeve, The Netherlands. Project number: EG-EI-11-046. By: Swoboda, U., Nowaczek, S., Lukas, W. and Brenner, O.
- Data processing (section 3.3): DMT, 2011. Processing report 2D seismic Isidorushoeve 2011. Reflection seismic vibroseis. In the area of Isidorushoeve and Hengelo, The Netherlands. Project number: EG-EI-11-046. By: Brenner, O. and Rybarczik, G.

All figures referred to in section 3.3 can be found in Appendix II.

## **3.2 Seismic data acquisition**

### **3.2.1 General**

#### **Introduction**

DMT GmbH & Co. KG (DMT), a company based in Essen, Germany, carried out a 2D reflection seismic survey in the Dutch Province Overijssel in the area northwest of the town of Haaksbergen using Mini Vibrator MHV 03 as energy source. The survey started on July 28, 2011 with topographical surveying and the survey was completed on August 4, 2011.

#### **Location of the survey area**

The survey area is located at the northwestern edge of the town of Haaksbergen close to the village of Sint Isidorushoeve and the village of Hengevelde towards the east. The total length of the two seismic lines was 8.975 km. The survey area and all geophone- and source positions are shown in Appendix I.

Most of the survey covered an agricultural area consisting mainly of parcels used as pastures and cropland. Several land owners owned substantial pieces of land in the prospect area. There were also forest areas with access tracks. As the survey was carried out during summer some tourist activities occurred in the survey area.

Following are some milestones of the project:

- The DMT crew started field activities on July 28, 2011 with the surveying activities;
- Field crew arrived and started layout on July 29, 2011;
- Recording started on August 1, 2011 and was completed on August 3, 2011;
- Cable pickup and line clean-up was finished on August 4, 2011.

#### **Objective of the survey**

The primary objective of this 2D seismic survey was to obtain additional structural information regarding the Zechstein-1 (Werra) salt deposit in depths of approximately 600-1000 m below the surface.

### **Working conditions**

The terrain was generally level. Several busy roads and several other small villages were present within the survey area. The weather conditions were very unstable, sunny days alternated with rainy days. The temperature ranged between 24°C and 27°C.

### **Survey design**

Each line was recorded with the roll along method with 192 active channels.

### **Operational issues**

The execution of the survey was conducted in a one shift recording mode. Vibrator lines followed roads and tracks as close to the theoretical grid as possible. The recording parameters were estimated and tested at the preceding Hengelo survey.

### **Technical issues**

Recording was performed with a Summit II<sup>plus</sup> instrument, software version Acquirer 3.11. For the vibroseis operation a MHV 03 Mini Vibrator was used with a peak force of 31,000 N.

## **3.2.2 Preparation of the survey**

### **Survey program**

Total number of lines:	2
Total length of lines:	8.975 km
Number of receiver points:	720 GP
Number of source points:	181 VP
Source point interval:	50 m
Receiver point interval:	12.5 m

### **Scouting**

The survey area was scouted by an experienced person using information provided by the client.

### **Permitting**

The permitting work was carried out by Rossingh Drilling B.V. by order and on behalf of DMT.

### **PPV Monitoring**

During the seismic survey vibration monitoring was carried out in vicinity of sensitive buildings and industrial installations. The levels of vibration allowed were determined using the DIN 4150-3 standard, which satisfies the requirements set by the German Mining Act (BBergG) and the German Immission Control Act (BImSchG).

## **3.2.3 Topographical survey**

The topographical surveying work for the seismic source and receiver stations was performed using real-time differential GPS. The LEICA GPS is a satellite-based radio navigation system that provides precise three dimensional position, navigation, and time information.

Sub-meter accuracies are achievable when differential corrections are applied. For this purpose two or more GPS receivers are necessary to be able to observe the same satellites simultaneously. One GPS receiver is placed at a known point (reference station). Based on the information from the reference station, the other roving stations receive relevant correction values. The accuracy for the corrected coordinates amounts to about 0.03 m in positioning and 0.05 m in elevation. These differential corrections can be applied either in real time, using radios, or by post-processing the data from the receivers afterwards. Differential GPS (DGPS) or Real Time Differential GPS (RTDGPS), also called RTK (Real Time Kinetic) uses the C/A-code information of the GPS signal.

Before starting with RTK measurements, the geodetic parameters and the coordinates of the reference station must be known. Altogether 6 trigonometric points were used to set up the transformation parameters for the project "2D Seismic Isidorushoeve 2011" with details shown below.

### Geodetic reference

EPSG-Code:	28992 (Amersfoort / RD New)
Projection:	Rijksdriehoekstelsel (RD)
Datum:	D_Amersfoort
Projection Type:	Double Stereographic
Origin Latitude:	52.15616056°
Origin Longitude:	5.38763889°
False Northing:	463000.0
False Easting:	155000.0
Scale Factor:	0.99990790
Ellipsoid:	Bessel 1841
Semimajor Axis:	6377397.155 m
Semiminor Axis:	6356078.9628181886
Inverse flattening:	299.1528128
Height reference point:	NAP

### Transformation parameters

#### WGS84 to RD Nieuw Amersfoort (Ellips to Normal-height)

Rotation x	0.80587"
Rotation y	-0.40283"
Rotation z	-3.17229"
Transaltion x	-577.7137 m
Transaltion y	-103.7570 m
Transaltion z	-444.9067 m
Scale factor	-4.9036 ppm

### Surveying operations

Preparation of the project, such as calculating the transformation parameters for the local coordinate system and creating the pre-plot for the survey took place in the DMT office in Essen.

The whole survey consists two lines:

- **11-AK-ISH-01** with 490 receiver and 123 source positions;
- **11-AK-ISH-02** with 230 receiver and 58 source positions;
- In total 720 receiver and 181 source positions.

Field work started on July 28, 2011 with one survey crew. First, pegs were staked out on Line 11-AK-ISH-02. All necessary permit information was compiled and handed over by Rossingh B.V. The Source Point Surveyor was equipped with a safety distance list for vibroseis and shot operations, which had been confirmed by the client representative. Basically these distances followed the German DIN 4150.

Quality checks were carried out on a daily basis first in the field and later also in the office. In addition each surveyor was instructed to measure at least one checkpoint in the morning to ensure proper functioning of his GPS device.

From the database the crew's source pilots were generated for the vibrator and recording crew. The pilots contained information on the actual source position offset and other points of interest e.g. surface, PPV measurements, and other remarks. Cross-sectional daily meetings chaired by the Party Chief ensured that all section heads were informed on the survey progress and operational changes.

### **3.2.4 Execution of seismic survey**

#### **Survey geometry**

The source points were located between the receiver stations. The receiver stations consisted in 1 string of 6 geophones, which were laid out bunched.

#### Template configuration

Method: roll along 192 active receivers

#### Source side

Source lines: 2  
Source point interval: 50 m

#### Receiver side

Receiver lines: 2  
Receiver points per record: 192 roll along  
Receiver point interval: 12.5 m

#### **Energy source**

One MHV 03 mini vibrator was used as seismic vibroseis source.

#### Source specification Vibrator

Type: MHV 03  
Peak force: 31,000 N per vibrator  
Drive Level: High Force 80%  
Low Force 40%  
Base plate area: 0.7 m<sup>2</sup>  
No: 1  
Control: Pelton advanced III VibPro

#### Vibrator source array configuration

Number of vibrators: 1  
Sweeps per position: 6

## **Receiver**

### Receiver specification

Type: Geophone  
Model: JF-20DX  
Nat frequency: 10 Hz  
Shunt: 1.000 Ohm  
Attenuation: 70 %  
Polarity: SEG standard

### Electrical connection

Receivers per string: 6  
Connection: 1 x 6 parallel  
Strings per group: 1

### Pattern configuration normal G1

Pattern G1: normal in line  
Receivers per group: 6  
Receiver rows: 1

## **Recording instrument and parameters**

Recording was performed using a SUMMIT II PLUS version central recording system.

### Parameters

Record length: 3072 ms  
Sample rate: 1 ms  
Correlation: post-stack  
Sweep: 12-200 Hz  
Sweep length: 10 s  
Vertical stack: 6  
Move on: standing  
Spread: 192 active  
Polarity: SEG  
Tape format: SEG-2

## **Recording operations**

The program consisted of approximately 8.975 km 2D divided over 2 lines.

Recording crews started laying out geophones and cables on July 26, 2011. Recording started on August 1, 2011 after recording of the Hengelo survey was finished.

Last vibro points were recorded on August 3, 2011 and final pick-up was completed on August 4, 2011. The crew started its production on line 11-AK-ISH-02 followed by line 11-AK-ISH-01.

### **Daily recording operation**

The daily operation started at 7:00 am with powering up the recording system, including a system self-check procedure. Next, the linecheck personnel would fix all faults on the spread (linebreaks, faulty geophone stations and batteries). Once linecheck activities were completed the daily test procedure was run and written to hard disk to prove good recording conditions of the spread. Daily production usually ended around 4:30 to 6:30 pm depending on the daily production progress.

### **3.2.5 Quality Control (QC)**

#### **Quality Control of the Vibro source**

At the startup of the seismic campaign the vibro source parameters were set up according to general specifications. Then the tests for the sweep parameters were performed. A Pelton Co. Vibroseis source control system consisting of the Adv. III VibPro encoder installed in the recording truck and the Adv. III VibPro decoder installed in the vibrator were used during the survey. These units controlled the ground force, the signal phase, the signal distortion and the synchronicity of the vibro source.

A radio similarity test was done to ensure the synchronicity between the vibro source and the telemetry system. During data acquisition the synchronicity was observed at every vibro position and graphically displayed.

#### **Quality Control of the telemetric data acquisition system**

The recording system and line equipment was tested using manufacturer specifications every morning prior to start of daily production. Components that not conformed to these specifications were eliminated before start of recording. All test results were inspected by the observer and stored on the hard drive.

#### Recording System Channel tests

- DC offset in nV, full band EIN (3 Hz to Nyquist frequency) in  $\mu\text{V}$
- Equivalent input noise (5 Hz to 130 Hz) in  $\mu\text{V}$
- Impulse response at high cut frequency including maximum pass band
- variance from a model in dB, percent variation of roll-off in transition region
- and percent variation of gain accuracy
- Total harmonic distortion in %, with internal source at 11 Hz including
- combined accuracy of LDO & RAM clocks in ppm
- Common mode rejection ratio in dB
- Cross feed rejection ratio in dB

#### Geophone tests

- Percent variation of geophone pulse from pulse average
- Geophone array resistance in Ohm
- Geophone array leakage resistance to ground in MOhm

### Quality control of the seismic data and the geometry data (In-field QC)

The following information formed the basis for the in-field QC:

1. The coordinate tables of the surveyor (Excel format);
2. The observers report (Excel format);
3. The raw seismic data (SEG2 format).

For the main procedures regarding field data management (seismic and corresponding non-seismic data) two software packages were used (ReflexW Version 6.0 (Sandmeier Scientific Software) and Surfer 9 (Golden Software). The ReflexW software was primarily used to check the match between seismic data and the geometry information and for in-field data processing. The mapping and the check of the position of the vibro truck were done with the Surfer 9 software.

Prior to the start-up of each line project files were set up that defined the spread of active receiver stations for each vibration point. These project files contained the source point coordinates for in-field checks of correct vibrator positioning. The tables were delivered by the senior surveyor in Excel-format.

Due to safety distances, developed areas, buildings, pipelines, etc. relocating source points away from the theoretical position was unavoidable. All offsets from the theoretical positions were checked visually using the background image (topographical map). In cases where source stations had to be skipped spread compensation was conducted to guarantee a constant coverage. A source point was compensated at the next free location between receiver stations.

### Geometry control

First of all a cross-check of the records listed in the recording sheets, the seismic data and the files with the geometry information was done to check whether all sets were complete and consistent.

The seismic data were transferred into the seismic processing software.

To check the source positions the geometry information (source and receiver positions) was imported into the processing software. Then the trace of the closest geophone to the vibro source was picked in the seismic data set. The position of this geophone was displayed as a point on the topographic map near the planned vibro positions (displayed as circle). For a correct position the points must lie inside the circle or (for source points with lateral offset) very close to it. Every record was checked according to this procedure.

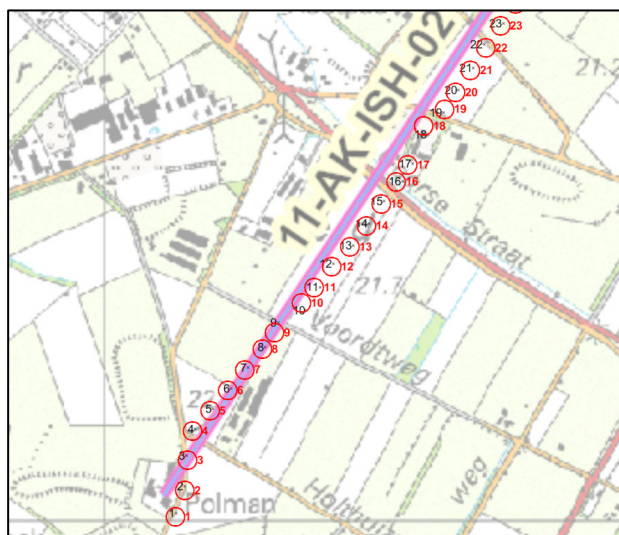


Figure 3.2: Geometry control by comparison of the geophone (black) and vibro position (red).

Irregularities in the offset distribution were checked for correctness with the observers report and the surveyors coordinate tables. Then they were replaced with the true coordinate points.

### Quality control of the seismic data

The raw seismic data were checked for correctness with respect to the following aspects:

- Correct format (SEG-2);
- Total number of recordings and traces;
- Number of missed or damaged traces;
- True allocated position of every station on the line;
- Reversed polarity of the data trace.

This check was done visually at every single record. Geometry changes were corrected to ensure a consistent dataset with an accurate geometry description. Finally, three additional files were created which contain the true geometry information for the vibro positions, the geophone positions and the source-receiver relations separately. The structure of these files follows SPS regulations (SEG field tape standards, Rev. 2.1, Jan. 2006).

### Brute stacks

Concurrent with seismic data acquisition a brute stack was produced for line 11-AK-ISH-02 (see Figure 3.3). This brute stack typically uses only a few parameters for the entire data volume to give a first impression of the reflector sequence.

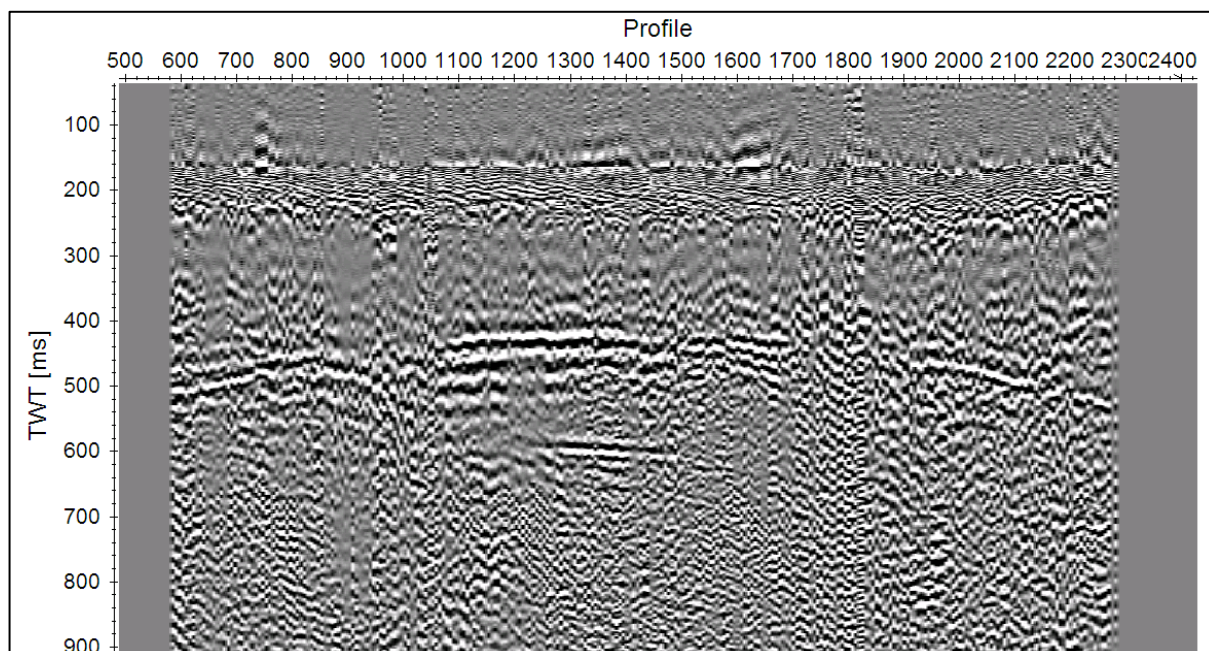


Figure 3.3: Brute stack of line 11-AK-ISH-02.



### 3.2.6 Quality, Health, Safety and Environment (QHSE)

The crew conducted the operations with regard to quality of our services, the health and safety of our employees, their families, our customers, contractors and the protection of the environment according to DMT QHSE Management principles.

The QHSE Management System (MS) is a “living system”, which is checked and verified against standards and procedures through daily controls. Deficiencies in this system are instantly corrected to improve it continuously. The MS covers the following interrelated subjects:

1. Leadership & Commitment;
2. Policies & Objectives;
3. Organisation & Resources;
4. Risk Management;
5. Planning;
6. Implementation & Monitoring;
7. Audit & Review.

The parties associated with the business, the employees, the clients, contractors and third parties were actively involved in this QHSE Management System. The Project HSE Plan described the execution of the survey including the improvement and control measures of potential risks associated with the crew’s and people’s individual tasks. A project specific risk assessment including the appropriate risk management measures was also included in the HSE Plan. The Party Chief carried out the duties of the QHSE Advisor and reported to the head-office in Essen. Crew performance was measured against the objectives set using the YTD LTI Rate:

$$\frac{\text{YTD}^3 \text{LTI}^4}{\text{YTD average headcount}} \times \frac{6.0}{\text{number of months YTD}} = \frac{0}{22} \times \frac{6}{1} = 0.00$$

Due to the short duration of the project no audits were performed by the client.

## 3.3 Data processing

### 3.3.1 General

The line 11-AK-ISH-01 was selected as a primary testline. The processing was carried out in August – September 2011.

All figures referred to in section 3.3 can be found in Appendix II.

### 3.3.2 Survey parameters

#### General

SPS format version num.	SPS2.1_2006
Description of survey area	Sint Isidorushoeve, NL

<sup>3</sup> YTD: **Year-to-date** is a period, starting from the beginning of the current year, and continuing up to the present day. The year usually starts on January 1 (calendar year), but depending on the purpose, may also start on July 1, April 1 (UK corporation tax and government financial statements), or April 6 (UK fiscal year for personal tax and benefits). Year-to-date is used in many contexts, mainly to record results of an activity in the time between two dates.

<sup>4</sup> LTI: lost time injury means an **occupational injury** is bodily damage resulting from working.

Date of survey	July 2011
Client	MWH B.V. / AkzoNobel
Geophysical contractor	DMT GmbH & Co. KG
Positioning contractor	DMT GmbH & Co. KG
Pos. proc. contractor	DMT GmbH & Co. KG
Field computer system	summit RU
Coordinate location	Centre of source and receiver pattern
Offset from coord. location	No offset
Clock Time w.r.t.	GMT -1:00
Geodetic datum, -spheroid	Bessel 1841 6377397.155 299.15281280

### Geodetic datum parameters

Vertical datum description	Amersfoort/RD New
Projection type	RD New
Description of grid units	METERS
Factor to meter	0.9999079

### Lat. of standard parallel(s)

Long. of central meridian	0155000.000E
Grid origin	52 - 9'22.1780"N, 5 - 23'15.5"E
Grid coord. at origin	00000000.00, 00000000.00
Scale factor	1.0000000000
Lat., long. scale factor	
Project code and description	2D Isidorushoeve 2011

### Instrument

Type, model, polarity	DMT Summit2plus,SEG;
Sample int., Record length	1 MSEC, 3072MSEC
Number of Channels	490
Tape type, format, density	harddisk,SEG2
Receiver (Bunched Geophone)	
Type, model, polarity	Land SM-4,NON-SEG
Damp coeff, natural freq	0.25,10Hz
Nunits len(X),width(Y)	6
Unit spacing X,Y	12.5 Meters, 0.000 Meters

### Source

Type, model, polarity	MiniVIB MHV3,SEG
Vert. stack fold	6
Units spacing Isidorushoeve	50.00 m, 0.0 m

### 3.3.3 Prestack processing and time imaging

#### Data input

The raw field seismograms were provided on harddisk in SEG2 and SEGY format. All raw data were read without problems and were imported into the processing software SEISSPACE (Landmark). In addition to the raw data SPS files (r, s and x) and observer logs were provided.

The acquisition sample rate of 1ms sample rate was kept throughout the processing. The trace length of the data was 3 sec.

#### Trace editing and geometry

The geometry information was taken from the sps-files and imported into the database.

Straight line geometry setup was carried out to bin the two lines in the Isidorushoeve survey.

All seismograms were interactively checked after the geometry merge using a trace mute plotted over the first arrivals (**Figure 1a**). The bad traces were edited at the same time.

The raw seismograms were exported in SEGY format, 32-bit floating point. Geometry as well as basic static corrections and final static corrections were written to the trace headers.

#### Minimum delay transformation and polarity

A minimum delay transformation operator was calculated for the vibroseis data (**Figure 2a**) using the autocorrelation of the filtersweep. The autocorrelation (maximum amplitude at 50 ms) of the filtersweep was obtained from an auxiliary channel of the raw seismograms. The minimum phase equivalent of the autocorrelated sweep was computed and the minimum delay operator determined. Different tests concerning the pre-whitening were done, resulting in an operator calculated with 1% of additive noise.

In **Figure 3a** the following sequence is displayed (from top to bottom):

- correlated filter sweep;
- correlated filter sweep transformed to minimum delay;
- correlated filter sweep transformed to minimum delay plus deconvolution;
- correlated filter sweep transformed to minimum delay, deconvolution and zerophasing.

The effect of the minimum delay transformation applied to the seismic data is obvious and as expected as can be seen by comparing **Figure 4a** (raw seismogram before minimum delay transformation) and **Figure 5a** (raw seismogram after minimum delay transformation).

The polarity of the data was reversed at the same time, therefore the polarity definition of the data is as follows: an increase of acoustic impedance is represented as a negative number on tape.

#### True amplitude recovery

Corrections were made for energy loss due to spherical divergence and inelastic attenuation using a function proportional to the  $TWT^{0.7}$ . This was applied to a time of 2.0 seconds.

**Figure 6a**: seismograms before spherical divergence correction

**Figure 7a**: seismograms after spherical divergence correction

The amplitudes of the reflections outside the noise cone and below the refraction events are well balanced in time direction as well as in offset direction.

### Air blast attenuation

Investigation of noise was carried out on shot gathers. The process “Air Blast Attenuation” (ABA) best fulfilled the requirements to suppress directed noise. ABA automatically searches anomalous energy within a shot-gather along a predefined velocity. High amplitudes within the corridor are automatically attenuated.

**Figures 8a and 9a** show a testshot before and after Air Blast Attenuation, which was applied with 330m/s target velocity.

### Deconvolution

The goal of the deconvolution was to increase the resolution in the target area. Several tests regarding operator length, prediction interval and deconvolution types were carried out for the testline. Stacks using the design gate as shown in **Figure 10a** were produced using different deconvolution parameters:

Figure	Operator length (ms)	Prediction interval (ms)	Type
11 a	without deconvolution		
12 a	40	8	Single Trace
13 a	60	8	Single Trace
14 a	80	8	Single Trace
15 a	120	8	Single Trace
16 a	160	8	Single Trace
17 a	60	spike	Single Trace
18 a	60	8	Single Trace
19 a	60	12	Single Trace
20 a	60	16	Single Trace
21 a	60	12	Surface consistent

The deconvolution that best fulfilled the objectives was a surface-consistent single gate predictive deconvolution with the following specification:

Type	Surface consistent predictive
Prediction interval	12 ms
Length	60 ms
Prewhitening	1 %
1 gate	70 – 1200 ms on near offset trace

Single seismograms are displayed before and after the selected deconvolution:

**Figure 22a** Seismograms before deconvolution

**Figure 23a** Seismograms after deconvolution

### Surface consistent amplitudes

Surface consistent amplitude correction was carried out for the components shot and receiver.

### Basic static corrections and residual static corrections

First breaks were picked and refraction statics computed. The following values were used:

Vzero	1150 m/sec
Replacement velocity	1700 m/sec
One layer	Offset range 50 m – 350 m

Datum was 0 m above sea-level.

Stacks with refraction static corrections were computed and compared with stacks based on elevation statics. For all lines the refraction statics was more continuous.

Residual static corrections and velocity analyses were iterated until a satisfactory solution was obtained. Three passes of residual statics were required and two velocity interpretations. In general, strong markers at different travel-times are needed to provide good control for both velocity and statics.

Two methods of residual static computation were used, maximum power autostatics, and external model cross correlations. The Maximum-Power method computes an internal pilot trace using a specified number of neighbouring traces which is then correlated with the single traces for a particular CDP. The External-Model Method uses an appropriately prepared Reference-Model for the correlation with the single traces. The reference model used was the input stack with FXY-deconvolution applied to the data. The best result is then used for the next processing step.

The maximum allowed time-shift varied between 8 ms for the first iteration and 4ms for the last iteration.

### Dynamic corrections

Velocity analyses were computed and interpreted in geologically required intervals. The velocities were picked from a combination display comprised of velocity spectra, dynamically corrected gathers and constant velocity stacks. 17 successive CDP's with 31 constant velocity stacks varying between 1100 m/s and 5000 m/s were used at each analysis position.

These velocities were used as input for the final velocity analysis after DMO. The velocity field obtained was consistent with the geology.

Velocity analyses were computed and interpreted four times: before the computation of residual static corrections, after first and second iteration of residual static corrections and finally, after generation of DMO corrected gathers. The final DMO stacking velocities (RMS) were delivered as ASCII files.

### Coherent noise attenuation

Directed noise was dominant in the two lines of the Isidorushoeve survey, which could be eliminated using the process "Coherent Noise Attenuation" (CNA). CNA was used to suppress linear coherent noise using a multi-trace filtering in the FX-domain. Contrary to FK filtering the process CNA suppresses narrow-banded noise in shot-domain without smearing effects. That allowed the cascaded application of CNA.

**Figure 24a:** shot before application of CNA

**Figure 25a:** shot after application of CNA

**Figure 26a:** stack before application of CNA

**Figure 27a:** stack after application of CNA

### Top and bottom mute

The final top mute applied was selected based on stack tests and has the following offset/time pairs:

Offset(m)	Time(ms)
70	0
120	20
280	220
480	400
1180	890

The noise cone in the center of the seismograms of the Isidorushoeve lines contaminated the stack result. Suppression of the noise was not possible using noise cancellation processes. Therefore, a bottom mute was tested and applied:

Offset(m)	Time(ms)
40	100
55	175
230	620
430	1150
660	1720

A comparison of a stack with and without bottom mute is given in **Figure 28a** (without bottom mute) and **Figure 29a** (with bottom mute).

#### **DMO and final DMO stack**

DMO processing was carried out in shot domain followed by DMO stack.

An Automatic Gain Control (AGC) of 800ms gate length was applied before stack.

#### **Poststack migration**

A poststack time migration (type FD steep dip) was finally applied to the DMO stack with the maximum frequency 150 Hz and 50 degree operator. The migration velocities were the smoothed RMS-velocities after DMO, converted to interval velocities. The final migration velocities (interval) were delivered as ASCII files.

#### **Poststack parameters**

All final filtered and scaled results in time were delivered with the following poststack processing applied:

- zerophase transformation (the zerophasing operator was designed based on a wavelet which was extracted from a stacked section without DMO). The operator length was 81ms, time zero of the zerophasing operators was in the centre at sample 41 = 41 ms.  
The zerophasing operator was delivered as SEG Y file and in ASCII format.
- FX Deconvolution with 50% addback of original data, 400 ms window length with 160 ms overlap, 1% prewhitening, 7 filter samples, frequency range 20 - 150 Hz.
- Bandpass frequency filter, type Butterworth:  
Lowcut 20 Hz, 48 dB/oct;  
Highcut 130 Hz, 96dB/oct;
- AGC with 500ms gate length.

### **3.3.4 Prestack time migration**

The data preparation before prestack time migration included the processing up to muting (section 3.3.3: Top and bottom mute). DMO corrections were not applied before PSTM.

Prestack time migration was performed using a Kirchhoff algorithm in common offset domain by applying a Green's function to each CDP location using an analytic RMS-velocity NMO curve.

The first run was performed using the RMS stacking velocities picked on CDP gathers after DMO.

The prestack time migrated gathers were then inverse NMO corrected such that velocity analyses could be computed and interpreted followed by the next iteration of prestack time migration. The velocity analyses were calculated close to each other in order to have full control along the whole section. This procedure was repeated 2 times resulting in the final RMS prestack time migration velocity field which was delivered in ASCII format (picks only).

The maximum frequency was 130 Hz.

The migration aperture was calculated automatically.

### **3.3.5 Prestack depth migration**

#### **Generation of an initial depth model**

The RMS-velocities from prestack time migration were used to create a velocity starting model. First step was the calculation of interval velocities which were converted to depth in a second step.

The velocity information of well ISH-01 was taken into consideration for the velocity starting model of the two lines of the Isidorushoeve survey. Velocity values were available for the depth range of 115 m to 930 m. Analog sonic information was available for wells TWR-081 and TWR-254. Digital information was available for well TWR-399. A prestack depth migration was carried out for every line using the starting model.

#### **Velocity Model Update**

MVA (Migration Velocity Analysis) is basically a data-driven suite of programs which assumes that migrating common-offset sections with the correct velocity model produces images with reflectors at the same locations. Therefore, reflected events will be flat after sorting these common-offset sections into common reflection point (CRP) gathers if the velocity model was correct. If events are not flat on the CRP gathers the velocity field needs to be changed. The method basically involves performing a Kirchhoff common offset migration using a velocity model, picking the residual moveout and calculating the raypaths for each horizon and then performing a tomographic inversion that modifies the velocity field to eliminate the residual moveout using the raypaths.

The velocity field was iteratively improved until the migrated CRP gathers were flat. For the first iteration the starting model as described above was used. The first step involved examining the CRP gathers. If the gathers were flat then the velocity model could be regarded as final. If not, the data had to be prepared for the horizon based residual moveout analysis. This included the following steps:

- Pick a mute (either CRP or common-offset domain);
- Signal-noise enhancement on CRP image gathers.

Residual moveout was then picked at various positions along a horizon, thus leading eventually to local changes in the model. A plot of the section together with the velocity model used for the migration and display of selected CRP gathers were always being monitored at the same time.

After the residual moveout was picked, the raypaths were traced for each horizon and several tomo-

graphic inversions using different parameters were done. The changes were examined together with the ray density display in order to judge their geological plausibility, and if necessary, they were edited. The inversion itself could be influenced to produce large or small changes with different amounts of smoothing by choosing appropriate parameters. It is also possible to apply constraints, such as directing the program to produce a layer with a linear gradient or constant velocity or to instruct the program to leave a part of the section untouched, for instance in the vicinity of a well. This procedure was repeated until a geologically plausible model with flattened CRP gathers was achieved. The final velocity field attained after the edited inversions was represented as a series of space and depth pairs, in this case with a depth sampling rate of 2 meters.

### **Kirchhoff Common Offset Section Migration**

This method was used to produce the depth migrated common-offset sections that were necessary for refining the velocity model. It had the advantage of being relatively fast, accurate and able to handle steep dips. The input model was a vertically and spatially varying interval velocity field specified according to the CDP position and depth. The algorithm used applied traveltime functions mapping the time and amplitude from each surface location to a region in the subsurface.

The input data were the gathers processed up to muting (see section 3.3.3: Top and bottom mute) with the zerophasing operator and TV-filter applied (see section 3.3.3: Poststack parameters).

## **3.4 Data delivery**

Raw shots with geometry, basic and final static corrections in trace header, SEG-Y, 32 bit floating point, sample rate and trace length as recorded.

Utilities:

- Report (pdf-document), also as printout;
- Presentation (pdf-document), also as printout;
- CDP Coordinates;
- Minimum delay transformation operator (ASCII and SEG-Y);
- Zerophasing operator (ASCII and SEG-Y);
- RMS stacking velocities after DMO;
- Interval migration velocities;
- RMS prestack time migration velocities;
- Final SEG-Y deliverables (32 bit floating point):
  - Raw stack, unfiltered and unscaled, minimum phase;
  - Raw migration, unfiltered and unscaled, minimum phase;
  - Final filtered and scaled stack, zero phase;
  - Final filtered and scaled migration, zero phase;
  - Raw stacked prestack time migration, minimum phase;
  - Filtered and scaled stacked prestack time migration, zero phase;
  - Filtered and scaled stacked prestack depth migration, zero phase;
  - Depth to time conversion of PSDM-stack, zero phase;
  - Velocity model of prestack depth migration.





## 4 Seismic data interpretation (T&A Survey)

The seismic interpretation of the new seismic lines 11-AK-ISH-01 (ISH-01) and 11-AK-ISH-02 (ISH-02) was done by T&A Survey. This chapter is a reproduction of the report from T&A Survey that describes all data interpretation activities (reproduced with permission from T&A Survey):

- T&A Survey BV, 2011. Seismic interpretation of the subsurface salt deposits in the concession Isidorushoeve. Project number: 0911-OEM2510. By: Stegers, D.

All figures referred to in sections 4.1 - 4.7 can be found in Appendix III.

### 4.1 Introduction

MWH carries out a study on subsurface salt for AkzoNobel in the region of Hengelo-Enschede. For this study MWH has assigned T&A Survey for the seismic interpretation of new seismic lines. T&A Survey has performed previous studies on the subsurface salt deposits in this region in 2008, 2009 and 2011. The results of this report are related to these studies.



Figure 4.1: Location of the newly acquired seismic lines near Haaksbergen

The results of the seismic interpretation near Haaksbergen are five geological boundaries in depth that will be used to estimate the depth and thickness of the salt layer of the Zechstein Z1 Salt Halite (ZEZ1H). Interpreted faults are evaluated, focusing on faults that affect the top of the salt layer. Maximum depth in this interpretation study is approximately 1 second Two-Way-Traveltime (TWT), corresponding to depths of 1700-1800 m below sea level. The Zechstein Z1 Halite reaches a maximum depth of 1700 m. The location and depth of the interpreted geological boundaries are available in digital (i.e. ASCII) and hardcopy format, included in this report.

## 4.2 Data

The seismic data that is used for the seismic interpretation near Sint Isidorushoeve has been provided by DMT GmbH & Co. KG (DMT; see chapter 3) and consists of two seismic lines that reach a total length of almost nine kilometers. The trace distance is 50 meters. The processing services for the 2D seismic data were carried out by DMT as well (see chapter 3). The processed seismic data provided are located in the folder 'dtconv\_stack\_prestack\_depth\_migration' and are named:

- 11-AK-ISH-01\_zph\_dtconv\_stack\_prestack\_depth\_migration.sgy
- 11-AK-ISH-02\_zph\_dtconv\_stack\_prestack\_depth\_migration.sgy

Seismic data is available as digital SEG-Y files with header and navigation information. RD Nieuw Amersfoort is used as surface coordinate system.

The coverage of nearby seismic lines is irregular and the distance between neighbouring lines can be more than two kilometers. The seismic acquisition dates from 1960 to 1987. The reflection time of the different seismic lines is within the range of four seconds TWT, depending on the vintage.

The datum plane for the 85EN(V) survey is sea level. For a number of lines the datum plane is unknown. Explosives or Vibroseis are used as a source. The coverage is 6 to 60 times, the trace distance is 15 or 25 meters and the sample rate is 2 to 4 milliseconds. The type of processed wavelet (i.e. minimum phase or zero phase) has not been documented. Lines made in 1971 and older are non-migrated, whereby only NMO (Normal Move Out) and stack is applied.

The two wells HKS-01 and HGV-01 reach depths of about 850 and 1000 meters below sea level and were respectively drilled in 1950 and 1985. Well ISH-01 reaches a depth of 950 meters below sea level. As ISH-01 is the only well within the study area that contains new sonic data in respect to the earlier performed studies within this area, well velocities have mainly been obtained from a study performed by T&A Survey in 2011 in which a new seismic velocity model was developed after evaluation of the sonic log of well ISH-01 (T&A Survey, 2008 & 2011a).

## 4.3 Methods

For evaluation of seismic and well data a dual screen geological workstation is used. Hardware consists of a High-End Intel-based PC system. The software is the Kingdom suite, seismic interpretation software of Seismic Micro Technology (SMT). Available are EarthPAK, 2D/3DPAK, VuPAK and VelPAK modules.

### 4.3.1 Data loading

Data of 14 vectorised lines with navigation information are loaded in the Kingdom seismic interpretation software. Two new lines are used directly for this project, 12 lines are available from earlier MHW projects. All data are displayed with 4 milliseconds interval.

Only a few wells are present in the studied area: HGV-01, HKS-01 and ISH-01. The proper data of these wells has been imported manually as the digital data was not in a usable format.

### 4.3.2 Evaluation well data

For the seismic interpretation of the different geological boundaries, both seismic and well data are used interactively. Wells HGV-01 and HKS-01 reach maximum depths that penetrate strata of Carboniferous age. Well ISH-01 penetrates the salt layer of the Zechstein Z1 Halite and reaches its maximum depth in the anhydrites at the base of the Zechstein interval.

As these wells mainly contain data in depth, they cannot be used directly to estimate the reflectors in the seismic sections. Only well ISH-01 contains sonic data, which is mainly used for the velocity model. As soon as a reliable velocity model is ready, depths of the formation tops in wells are compared with depth converted horizons. This is applied for all three wells in the vicinity of seismic lines.

### 4.3.3 Quality Check and Normalizing seismic lines

After loading the seismic data, the quality of the lines has been checked. Remarkable are the rather 'blurry' seismic edges of line ISH-02 (see Figure 4.2). There are no clear reflectors at the sides of the seismic line that can be continued. It looks like these areas have not been migrated.

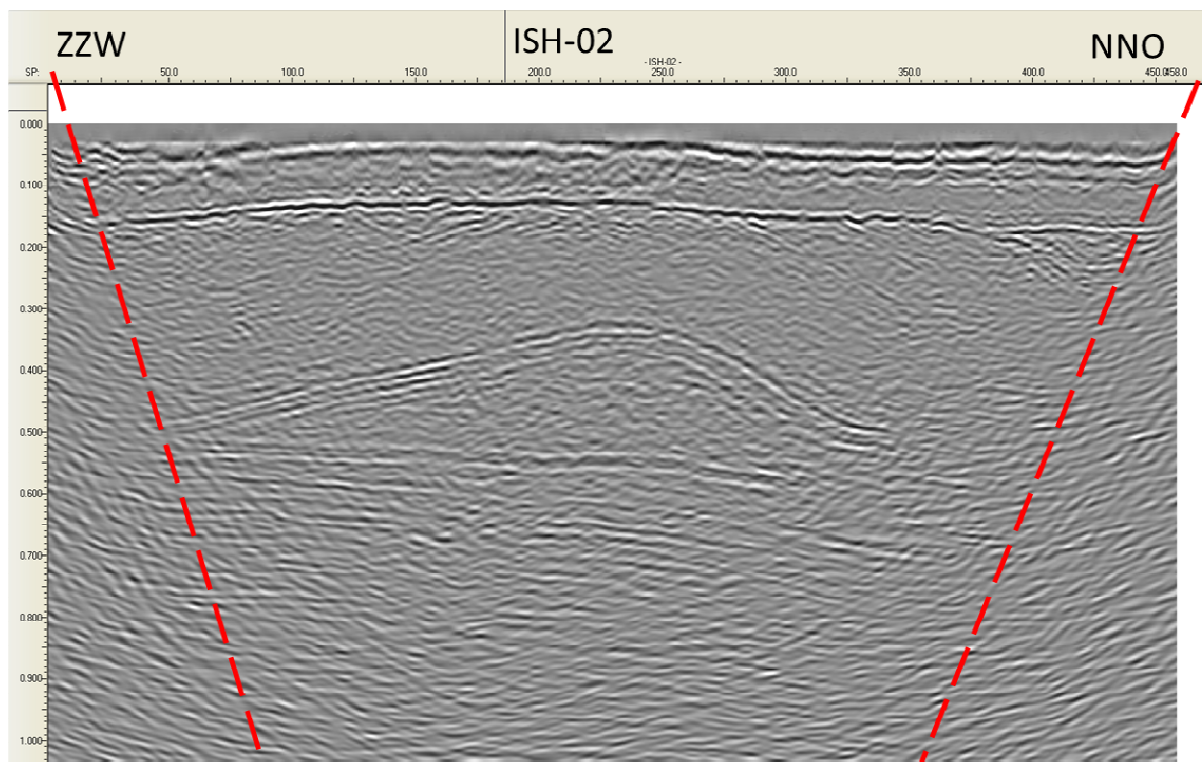


Figure 4.2: Seismic section of line ISH-02. The seismic data below the dashed line is not reliable.

After the acquisition of seismic lines, the reflectors on the lines are migrated to move them to their proper position in the subsurface. This might cause strong lateral movement of reflections. This is especially the case when the geology is not flat, for example at the dipping flanks of salt structures. The flank of the salt structure migrates upwards towards the top of the salt pillow. The strength of this effect depends on the velocity difference between the salt and the overlaying sediments. In order to properly migrate the flanks of a salt structure, the data acquisition needs to start at a proper horizontal distance from the salt structure.

In the case of the Haaksbergen salt structure this has to be at least one to two kilometers away from the edge of the salt pillow. The acquired lines lack this distance and as a consequence the edges of seismic line ISH-02 are not properly visualized. Therefore this data is not reliable. Consequently, these parts of the section have not been interpreted.

The other seismic lines in the study area have different trace characters since they are part of several seismic surveys, shot by different contractors in different times and with different targets. This often results in different datum planes. Within a 2D migrated survey there are strike and dip lines, which are processed in the direction of each specific line. For these reasons, more or less comparable reflectors in crossing seismic lines often do not match.

The best possible fit is made by time-shifting and normalizing with help of fairly good interpretable and rather flat reflectors. The Base Tertiary and Base Lower Germanic Triassic are good seismic references for normalizing. The 85EN(V)-surveys are used as reference set because of its coverage and quality. Datum plane of this survey is sea level (i.e. NAP).

#### **4.3.4 Interpreting seismic data**

Seismic interpretation of previous performed projects (T&A Survey, 2008) is used as a base for the interpretation of the new ISH-lines. The chosen geological boundaries in that project are based on data of nearby wells from the Stratigraphic Nomenclature of the Netherlands that are representative for the subsurface of the region of Hengelo-Enschede. These boundaries correspond with fair to good continuous seismic reflectors and make it possible to interpret the new seismic lines.

Since the seismic surveys are from different vintages, the seismic character of the other seismic lines is slightly different. Investigation shows that all surveys have the same normal polarity and all signals show predominantly a minimum phase character. This means that reflection on a layer with high acoustic impedance an acoustic wave shows a sinusoid reflection and starts with a black peak. The to-be-interpreted horizons are picked in a peak or a trough, depending on the well data fit and the type of geological boundary (regarding velocity and density changes).

The reflectors chosen for interpretation are fair to good in continuity but only in non-disturbed regions. They are generated by lithological transitions representing mostly significant geologic boundaries. The following geologic boundaries are used for horizon interpretation in the new seismic sections of the Isidorushoeve survey:

- Base North Sea (N)
- Base Lower Germanic Trias (RB)
- Top Z1 Salt Member (ZEZ1H)
- Top Z1 Lower Anhydrite (ZEZ1A)
- Base Zechstein (ZE).

The geological boundaries of the Intra Muschelkalk Formation (RNMU) and the Base Röt Evaporite Member (RNRO) that were interpreted in previous studies in the adjacent seismic lines are not or just barely present in the ISH-lines and are therefore not interpreted in these lines. The seismic characterization of the different stratigraphic units is described below.

### **Base North Sea Supergroup (N)**

This interface is chosen by its velocity characteristics and the type of boundary. As it lies unconformably on the Niedersachsen Group (SK), the Altena Group (AT) and the Upper Germanic Trias Group (RN) in this region, the interfaces show angular unconformities. Very often the reflector shows an alternating character as result of acoustic impedance changes. This interface is present in the whole region. Predominantly the reflector is a trough.

### **Intra Muschelkalk Formation (RNMU)**

Velocity calculations give a rather strong black peak in the vicinity of the base of this formation. The reflector is fairly good continuous on the post-1970's surveys only and is not present throughout the entire area because it is truncated by later erosion. Due to this erosion it is almost entirely absent in seismic lines ISH-01 and ISH-02. This reflector represents a layer near the base of the Muschelkalk.

### **Base Röt Evaporite Member (RNRO)**

The Base Röt Evaporite Member is picked on a reflector that is caused by the acoustic impedance change of high-to-low velocity at the base of this formation. The Main Röt Evaporite Member (RNRO1) is truncated by later erosion. Due to this erosion it is almost entirely absent in seismic lines ISH-01 and ISH-02. Only on the outer edges it might be present. However, as the formation is very thin at these locations, it is not interpreted.

### **Base Lower Germanic Trias Group (RB)**

This reflector also represents the top of the Zechstein, which forms the transition of the sands and clays of the Triassic to the dolomites and anhydrites of the upper Zechstein. It is displayed as the first strong black peak at the base of the Germanic Triassic. The strong reflectivity is caused by salt clay, which lies on top of the Zechstein formation.

### **Top Z1 Salt Member (ZEZ1H)**

The reflector lies at the base of an interval with strong reflectors that are caused by the claystones and anhydrites in the upper Zechstein. The salt layer appears as a 'fuzzy' layer, with no clear reflectors in it.

The Haaksbergen salt structure is a result of the movement of this salt.

### **Top Z1 Lower Anhydrite (ZEZ1A)**

The Z1 Lower Anhydrite, or Basal Anhydrite, forms the base of the Z1 Salt Member. As the velocity increases from the salt to the anhydrite, the reflector is picked on a trough.

### **Base Zechstein Group (ZE)**

Where the Rotliegend formation is absent, this interface is the top of the Limburg Group of Carboniferous age. The interface shows an angular unconformity and is therefore recognizable at some locations. Mostly it lies at a constant vertical distance of the Basal Anhydrite reflector.

The selected reflectors are mainly interpreted manually in Kingdom, because the quality and character of their traces do not justify automatic horizon picking. In case of inclined surfaces since seismic data is 2D-migrated, the seismic image does not fully represent the geology. Where this is the case, interpretation is done above or under the respectively non- or over-migrated reflector.

#### 4.3.5 Time to depth conversion

For time-depth conversion the stratigraphy above the Base Zechstein is divided into five layers with each a specific seismic velocity (Table 4.1). Layer velocities are defined by the lower boundary of the interpreted layer. Velocities are obtained from previous executed studies (T&A Survey B.V., 2008 & 2011a). The sonic data of well ISH-01 justifies the use of constant velocities for the different stratigraphic intervals. Only the Triassic interval contains a depth-dependent variable velocity. The depth-dependency is necessary because the mean depth of the Triassic is strongly variable over the area. It has been obtained from the sonic log data of well ISH-01.

The time-depth conversion is applied within the seismic sections. As only 2D seismic data is depth converted and no 3D depth modeling is done, well depths may not fit exactly with horizon depths.

Layer	Interval Velocity (m/s)	Datum Velocity (m/s)	Depth dependence (m/s/m)
North Sea Supergroup	1808		
Triassic		2600	1,9447
Zechstein Z2/Z3/Z4	5524		
Zechstein Z1 Halite	4552		
Zechstein Lower Anhydrite	6000		

Table 4.1: Velocity model for time to depth conversion

## 4.4 Evaluation study

In this section a brief explanation of the geology is given as was used for the interpretation of the data. The emphasis is placed on the results of the interpretation.

### 4.4.1 Geology

The geology of the nearby region has been described in several studies and a brief description is given below (T&A Survey BV, 2007, 2008, 2009; TNO, 1998; TNO, 2004; Geluk, 2005; Wong et al., 2007). The region is characterized by northwest-southeast trending faults. Initiation of these faults dates back to pre-Permian (Van Buggenum & Den Hartog Jager, 2007; De Jager, 2007). During the Cretaceous inversion, formations younger than Zechstein age were torn apart by lateral horizontal movement of fault blocks, at which old faults in the pre-Permian might have been reactivated. The tectonic processes also resulted in flexure and deformation of these formations. During this process, the Zechstein salt acted as a sliding layer and at some locations the salt intruded into the faults.

The Base North Sea Super Group is an erosion surface, representing the Alpine orogeny tectonism. In several areas in the Hengelo Enschede region the boundary truncates the Jurassic layers and even the upper Triassic.

#### 4.4.2 Haaksbergen Structure

The Haaksbergen salt structure is an WNW-ESE trending elongated small dome, with a steep northern flank in respect to the southern flank (see Appendix III.5) . It is located right next to a NW-SE trending fault zone in the Carboniferous (see Appendix III.3). To the north and the south of the structure, sediments of the Jurassic and the Upper Triassic (Muschelkalk and Röt formations), are truncated by the base of the Tertiary. As a result the sediments of the Quaternary and Tertiary lie discordant directly on top of the Triassic sediments of the Main Buntsandstein Subgroup (RBM).

Along the seismic lines of ISH-01 and ISH-02 the salt pillow, composed of salts of the Z1 Salt Member, reaches a maximum thickness of 390 meters just east of the crossings of these lines. The top of the Zechstein salt at the top of the structure is estimated at approximately 520 meters below sea level. The faulting on top of the salt structure is discussed in section 4.4.3. The anhydrites at the base of the salt pillow appear to be more or less horizontal with a slight dip towards the northwest. However, the reflectors below the center of the salt pillow are artificially 'pulled' up, due to the high seismic velocities of the salts. Once converted in depth, the base of the salt pillow lies deeper, than might be expected initially (see Appendix III.4 and Appendix III.5).

The northeastern edge of the salt pillow appears to be strongly faulted at the base, with vertical throws up to fifty meters (see Appendix III.5). However, as mentioned before (section 4.3), this part of the seismic line is located near the point where the seismic line is not processed accurately. The actual amount of faulting in this part of the seismic section may be less than currently interpreted. The western flank shows a relative steady dip, with almost no interruptions that indicate the presence of faults (see Appendix III.2).

The southeastern edge of the salt structure is located outside of seismic line ISH-01. Extrapolation to this edge of the salt pillow is not part of this study, but may be done with help of the interpretations of lines 716017, 85EN(V)-03, 85EN(V)-10 and 6073.

#### 4.4.3 Faults on top of the Haaksbergen salt structure

On top of the salt pillow small faults are detected, with maximum throws of 25-30 meters (see Appendix III.4 and Appendix III.5). These single faults cannot be correlated in between two seismic sections. The faults are most probably the result of the upward movement of the salt. The layers directly on top of the salt are pressed upwards. Through this upward motion, the top layer suffers extensional stresses (see Figure 4.3). The observed normal faults are the result of this extension.

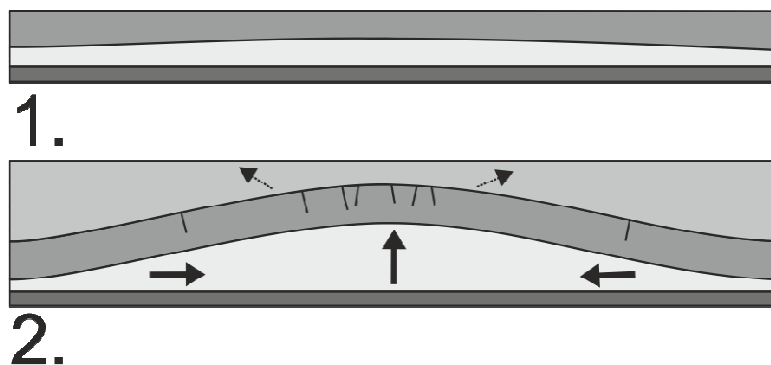
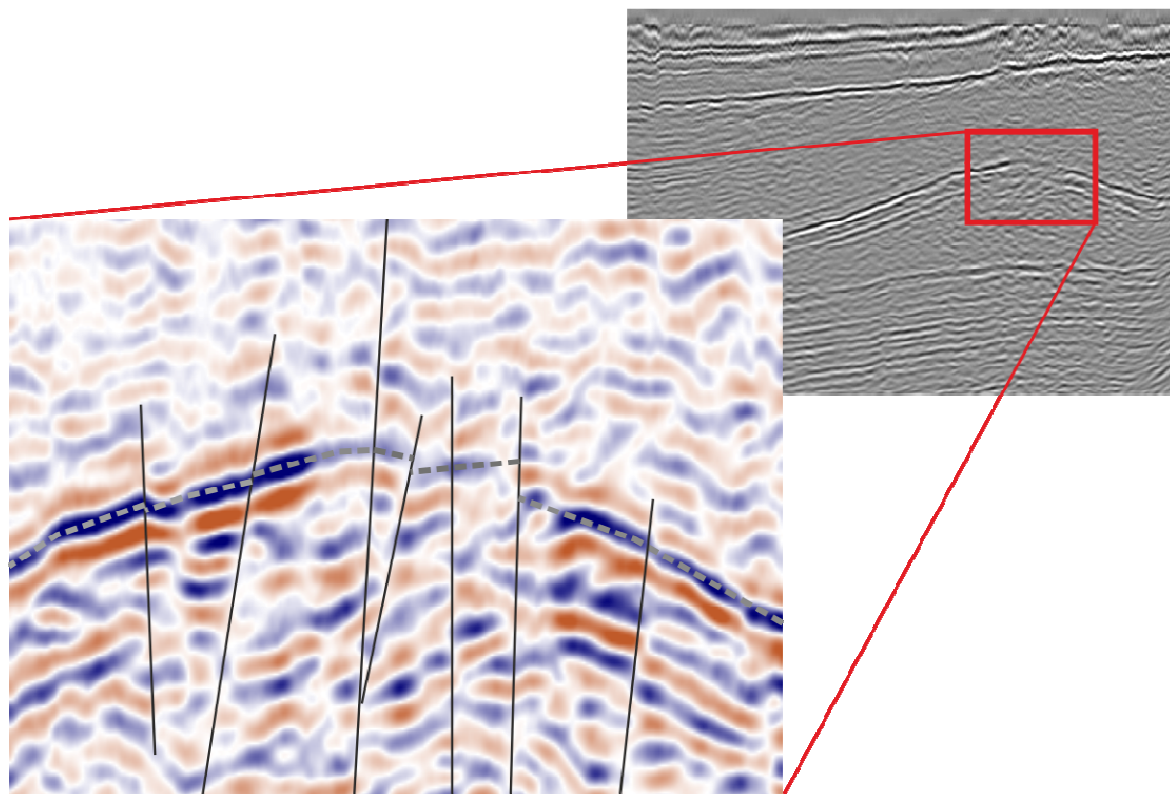


Figure 4.3: Schematic overview showing faulting as a result of salt movement.



The faults can cause a diffuse image in the seismic data. This is also observed in line ISH-01 where the top of the salt appears to be absent. However, a different color view reveals that the reflector that represents the top of the salt continues (see Figure 4.4). The diffuse image of the reflector is probably caused by a fault that lies sub-parallel to the seismic section. Consequently, the interpreted faults in this part of the section should be considered as one fault or as parallel branches within one fault zone.



**Figure 4.4: Diffuse imaging as a result of faulting. The close-up reveals that the interpreted reflector continues in the diffuse section. See appendix 2 for a complete interpretation of seismic section ISH-01.**

#### 4.4.4 Quality check time-to-depth conversion

After time-to-depth conversion the seismic interpretation of the newly acquired seismics is compared with well data in ISH-01 for three horizons. For the base North Sea Group there is a difference of approximately thirteen meters. The Base Lower Germanic Trias Group differs ten meters. The top Z1 Salt Member is nearly spot on.

The cause of the mismatch of the base North Sea Group is probably the result of the chosen constant velocity for this interval. As there is no sonic (logging) data of this stratigraphic interval in well ISH-01, no extra data is available to validate adjustments to the chosen velocity. Due to the decrease in thickness of the Tertiary towards the east, especially in the area near well ISH-01, the velocity is probably slightly too high at this location. Towards the northwest the fit will be better, as the horizon deepens. Besides that, the seismic reflectors become more stable due to the increase in thickness of the Tertiary sediments.

The ten meter offset of the base of the Triassic lies within expected accuracy ranges. However, the composite well log of well ISH-01 shows the transition from claystone to the first substantial dolomite/anhydrite layer at a depth of 530 meters. The sonic log also reveals a significant change at this point. It is very probable that the picked reflector marks this transition.

As the overall fit of the horizons matches quite well with depth data from ISH-01, no further adjustments are made to the velocity model.

#### 4.4.5 Adaptation into the current framework

The interpretation of the new seismic lines is incorporated into the current framework. Small adjustments are made to compensate for small misfits between crossings of the different seismic lines.

Further analysis has shown significant misfits of line 716017. Closer inspection indicates that this seismic line has to be moved along the section. In a previous study (T&A Survey B.V., 2009) a line of the same '71 survey also had to be moved 500 meters, due to incorrect numbering during vectorization. Therefore it has been decided to transfer this line 500 meters to the southeast along the seismic section, resulting in a considerable improvement of fits of the horizons.

After adjustments were made, a new time-to-depth conversion of the previously interpreted seismic lines in the nearby area has been applied, using the same, new velocity model. The depth converted lines are summarized in Table 4.2. The interpreted time sections and converted depth sections of these lines are included in Appendix III.6 to III.29.

**Table 4.2: Depth converted seismic lines neighboring lines ISH-01 and ISH-02**

Line ID	Survey	Line ID	Survey
706023	L2NAM1970B	RGD8209	L2RGD1982A
706036	L2NAM1970B	RGD8306	L2RGD1983B
6072	L2NAM1965D	85EN(V)-03	L2PET1985E
6073	L2NAM1965D	85EN(V)-08	L2PET1985E
6080 I&II	L2NAM1965D	85EN(V)-10	L2PET1985E
716017	L2NAM1971C		

## 4.5 Recommendations

The northern slope of the Haaksbergen salt structure is quite steep. As migration processes are performed in the direction of the seismic line, this can cause misfits in the processed image. A 3D-survey would give the most accurate result of the geometry of the salt structure.

The velocity model is mainly based on a previous performed study (T&A Survey, 2011a), with some adaptation from the well data of ISH-01. To obtain a more secure depth prognosis, additional velocity data is needed to improve the velocity model.

## **4.6 Reliability**

This study is done by experienced and up to date geoscientists who have knowledge of the Dutch subsurface in the concerning region. All data and information is evaluated to generate the best result. The used software and hardware are up-to-date and state of the art and are generally applied by oil, gas and mining companies all over the world. Only data quality and coverage are limitations for an ultimate product.

T&A Survey does not accept responsibility for damage that could result from using this report, as an evaluation of seismic data has limitations.

## **5 Geological modeling**

### **5.1 Introduction and objectives**

MWH used the depth data received from T&A Survey to model the following geological horizons (from deep to shallow):

- base of the Zechstein Z1 Halite,
- top of the Zechstein Z1 Halite,
- base of the Triassic deposits and
- base of the Tertiary deposits.

From these modeled horizons the thickness of the Zechstein Z1 Halite and the thickness of the Z2 to Z4 Zechstein deposits were calculated.

The objective was to create the best possible and most reliable geological model of the Haaksbergen area of interest using all available seismic data in an optimal way. Special emphasis was placed on modeling the base and the top of the Zechstein Z1 Halite as these together determine the thickness of the Zechstein Z1 Halite deposits in which AkzoNobel is interested for salt mining purposes.

### **5.2 Results of the manual interpolation**

First a manual interpolation was performed to bring in geological expertise during the computer modeling of the depth data and to find out more about the faults running through the area.

For the manual interpolation shot points and fault lines, as derived during the previous geological study of the area (MWH, 2008b) were plotted on two large-scale maps, one for the base and one for the top of the Zechstein Z1 Halite horizons. Then isohypses connecting shot points with the same depth values were drawn by hand by a senior geologist using both seismic information as well as geological expertise and knowledge of the area. Figure 5.1 shows the results of the manual interpolation of the base of the Zechstein Z1 Halite. Figure 5.2 shows the results of the manual interpolation of the top of the Zechstein Z1 Halite. Both maps can be found in A3-size in Appendices IV and V. The results of the manual interpolation are used to verify and improve the computer modeling results during the next stage.

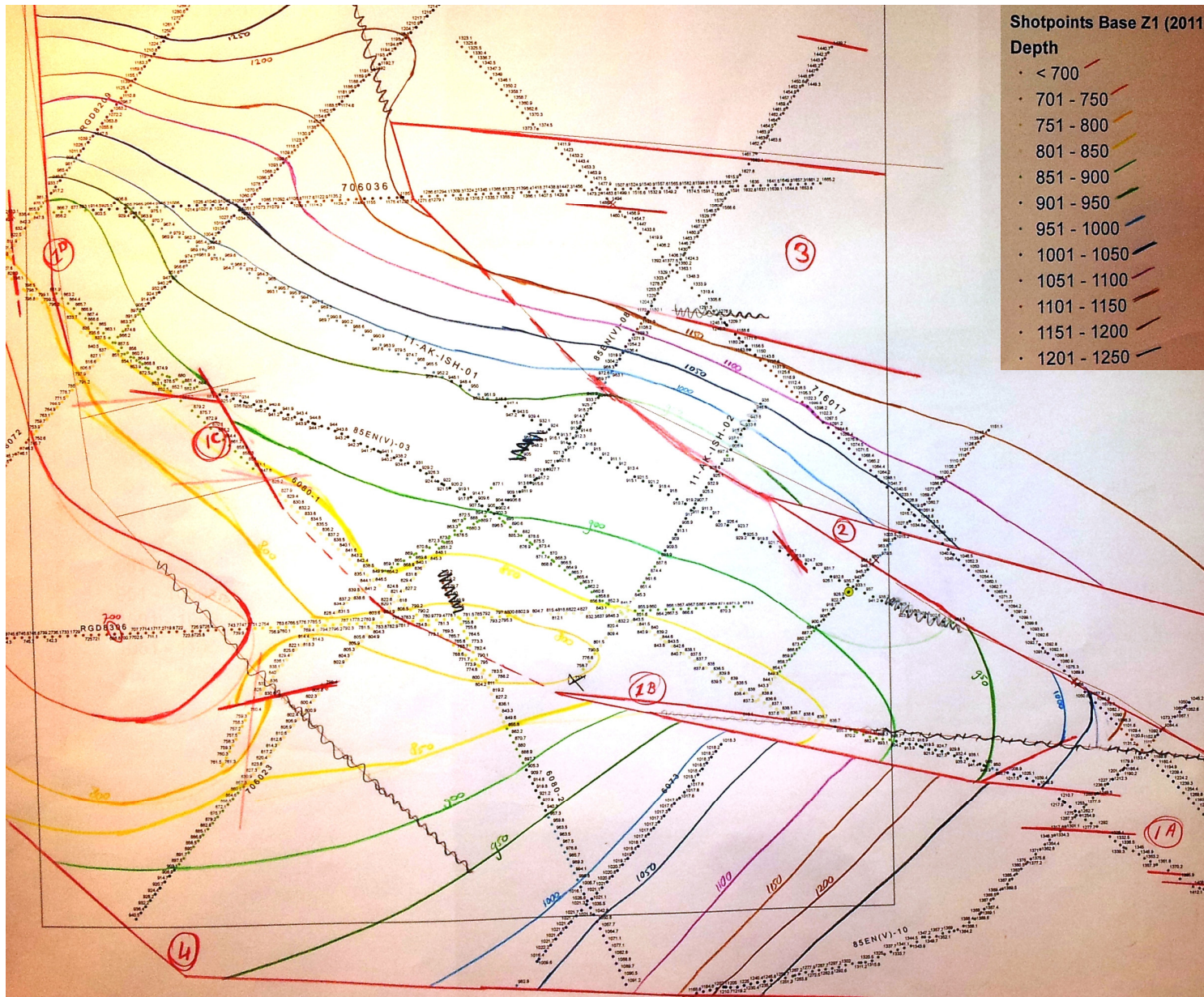


Figure 5.1: Results of the manual interpolation of the depth of the base of the Zechstein Z1 Halite.

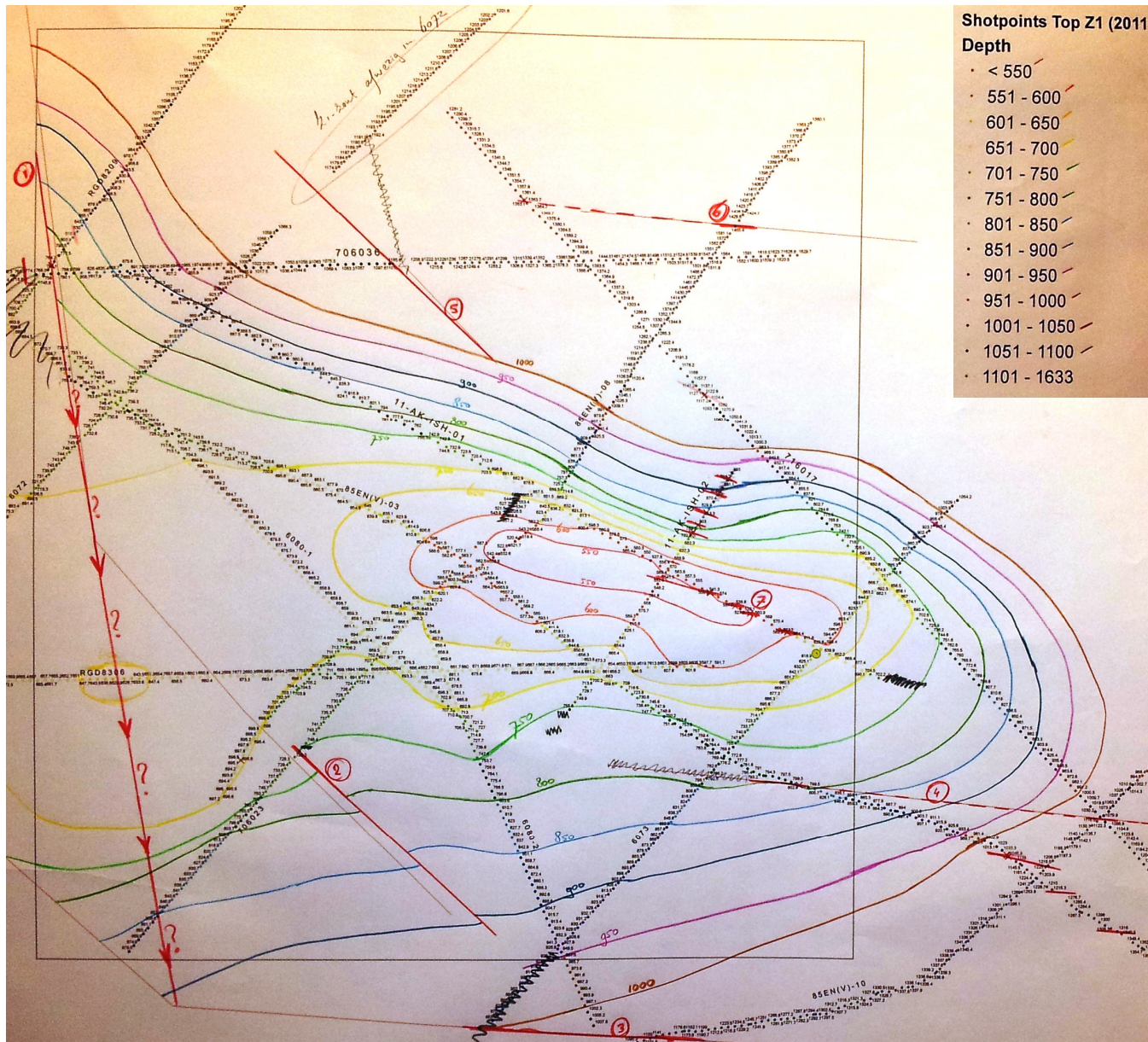


Figure 5.2: Results of the manual interpolation of the depth of the top of the Zechstein Z1 Halite.

## 5.3 Fault orientation analysis

Following the manual interpolation, the fault line orientation, as was available from the previous geological study of this area, was updated using the re-interpreted seismic lines and the new depth data. Main problem with identifying faults in seismic lines is the fact that the orientation of fault lines that cross-cut a seismic line is unknown. Furthermore, faults that are clearly visible in one seismic line and have a huge offset of tens or even over hundred meters may have disappeared in another nearby seismic line. This makes fault line interpretation very difficult. The general orientation of all fault lines, trending from WNW to ESE (i.e. parallel to the main orientation of the Central Netherlands Basin) helps a little when identifying the orientation of major fault zones.

### 5.3.1 Base Zechstein Faults

As was described in chapter 2, based on the previous geological study, the salt pillow is underlain by a heavily faulted Carboniferous horst block where horsts and adjacent grabens had formed during Permian time. Many of these faults were probably reactivated during later compressional phases (like the Variscan Orogeny and the Late Cretaceous to Early Tertiary Subhercynian tectonic phase) as well as extensional phases (like during Late Permian times and Tertiary extension).

Three different fault zones can be distinguished in the fault zone map for the base Zechstein Z1 Halite horizon (see Figure 5.1 and Appendix IV). The base Zechstein Z1 Halite horizon is intersected by the Langelo fault zone in the far southwestern corner of the study area (seismic line 706023). This fault is also clearly visible in several lines just southeast of the area (lines 6080-2, 6073 and 85EN(V)-10). Although due to limited seismic information the exact position of this fault remains somewhat unclear.

A second fault zone is seen to run through the entire study area, from the southeastern corner to the northwestern corner, but seems to be discontinuous. This zone combines both the Haaksbergen fault zone and the Hengevelde fault zone, mentioned in the previous geological study of the salt pillow. Although this zone shows some major offsets at several places, it is not a continuous fault zone, but seems to consist of a northwestern more north-south oriented branch (about 2 km northwest of Sint Isidorushoeve; formerly known as the Hengevelde fault zone) and a south-eastern more west-east oriented branch (more or less underneath the village of Haaksbergen; formerly known as the Haaksbergen fault zone). In the middle part, just south of Sint Isidorushoeve, it is difficult to trace this fault as no clear offset is visible in the seismic lines over there. In the extreme southeastern part of the study area, east of Haaksbergen, this fault seems to consist of many parallel fault branches, as can be seen in seismic line 85EN(V)-03.

The third fault zone is the so-called Eppenzolder fault zone, which runs through the northern half of the area, from just northeast of Haaksbergen to the north-northwest. Also this zone seems to be discontinuous, with a more pronounced offset in the north-northwest and in the northeast, but with hardly any offset north of the Haaksbergen salt pillow. Furthermore this zone is seen to have several more or less west-east oriented branches. It is supposed to be associated with the northeastern flank of the Carboniferous horst block and the adjacent graben.

All fault zones exhibit a bending shape – starting with an almost N-S orientation in the northeastern part of the area of interest and slowly bending towards a NW-SE or even E-W orientation in the southern part of the area of interest. Within the ‘bend’ the fault zones seem to lose their influence and are not clearly visible in the seismic lines.

All fault zones are thought to have been part of the structures related to the carboniferous horst and graben system, which has been reactivated during later compressional and extensional phases.

Within the study area there are only some smaller faults that are seen to have a different orientation, like the small fault in the southwestern part of the area, intersecting seismic lines 85EN(V)-08 and 706023.

### **5.3.2 Top Zechstein Z1 Halite faults**

Due to the plastic behavior of thick salt deposits, many of the carboniferous and base Zechstein faults disappear within the Zechstein Z1 Halite deposits, especially where these salts are seen to be extremely thick. Therefore the Top Zechstein Z1 Halite fault map shows much less faults than the Base Zechstein fault map and faults which are visible show less offset. The major Base Zechstein fault zones, described above, are hardly visible, leaving only some short parts.

Only in the northwestern part of study area a major fault, intersecting the top Zechstein Z1 Halite horizon is visible within seismic lines RGD8209, 706036 and 85EN(V)-03, where it was formerly known as the Hengevelde fault zone. It is unclear how this fault continues in a southern or southeastern direction. In the southern half of the area two other faults are visible, but it remains unclear how these are related to this fault zone.

All other faults are only traceable within one or two seismic lines and show relatively little offset.

What becomes clear from the fault orientation analysis of the top Zechstein Z1 Halite faults is that the well studied area of the salt pillow, which is being cross-cut by six or seven seismic lines, has hardly any faults. Only within seismic lines 11-AK-ISH-01 and 11-AK-ISH-02 some small normal faults are seen in the northern flank of the salt pillow and exactly on the highest point of the salt pillow. These probably originate from extension due to the uplift of the salt pillow due to halokinesis (see section 4.4). As these are only seen in the newly shot seismic lines and are not traceable in neighboring seismic lines, these faults were not dealt with during modeling. Nevertheless these faults do impact the top Z1 Halite horizon as well as the top Zechstein (base Triassic) horizon. Consequences of this are discussed later on.

## **5.4 Data preparation**

The depth data resulting from the seismic interpretation by T&A Survey were used as source data to develop digital models of the important geological horizons. As the two deep boreholes present in the modeling area (ISH-01 and HKS-01) are located on seismic lines and were in fact used to verify the seismic interpretations, these boreholes were not used as source data for modeling purposes (data redundancy).



Previous to the computer-based modeling phase some data preparation occurred. First, the results of the interpretation of all seismic lines were imported into a format that can be used for modeling. Next the original seismic source data were modified to optimize the quality of the source data for modeling in order to produce the best possible modeling results.

The distance between shots in the depth data files (ASCII) received from T&A Survey varies considerably between the various seismic lines. Shot points on the seismic lines RGD8306 and RGD8209 are separated by approximately 5 m and the shot points on the newly acquired seismic lines 11-AK-ISH-01 and 11-AK-ISH-02 are separated by approximately 6 m. The distance between shot points on other seismic lines varies from approximately 15 m on the lines from the 85EN(V)-series to approximately 25 m on the remaining seismic lines.

Also, the shot points are not evenly distributed over the modeling area as in a gridded pattern, but rather all shot points are located on lines crossing the modeling area. Consequently, on each seismic line shot points are separated by a short distance, while the distance between shot points on different seismic lines is much larger (except where seismic lines cross each other).

Most interpolation techniques (e.g. natural neighbor, IDW, kriging) calculate a weighted average of surrounding data values to assign values to unsampled locations. Other interpolation techniques (e.g. splines) try to fit curving planes through the data points. Seismic lines with an extremely high data density would therefore have a relatively large influence during modeling as more shot points on these lines would be included in the calculations. Also, two data points close to each other are likely to have very similar values (data redundancy). Therefore, the data density on all lines was reduced before modeling in order to produce the best possible modeling results. This reduces data redundancy and helps to include points from various lines/directions for interpolation. Data density was reduced on every line in such a manner that the distance between shot points on each line was approximately 45 m to 50 m (except near fault zones where the seismic data could not be interpreted and the distance between shot points in the original depth data file exceeded 50 m).

Based on experience gained during both the manual interpolation of the base and the top of the Zechstein Z1 Halite horizons and during the testing phase of various digital interpolations some more modifications were made to the seismic input data before final testing of various computer-based interpolations. The following modifications were made to ensure the best possible final modeling results:

- Shot points at the northwestern end of seismic line 6080-2 (north of seismic line RGD8306) were removed before modeling the base of the Zechstein Z1 Halite horizon. The depth values at these shot points deviate significantly from depth values at nearby shot points located on seismic lines of higher quality (RGD8306 & 706023). Removing these shot points (shot points 3294.5-3297.75) before modeling will improve model quality;
- Shot points at the northeastern end of seismic line 706023 were removed before modeling the base and the top of the Zechstein Z1 Halite horizon. The depth values at these shot points (shot points 1141-1154) are unreliable and would have an adverse effect on the model of the top of the Zechstein Z1 Halite horizon. Also, sufficient shot points located on other seismic lines are available in this area for proper modeling, so these low quality shot points can be removed without concern;

- Shot points at the southeastern end of seismic line 11-AK-ISH-01 were removed from the point where depths start decreasing before modeling the base and top of the Zechstein Z1 Halite horizon. As decreasing depth values at this end of the line are almost certainly due to distortions in the seismic data rather than actual decreases in the depths of both horizons, removing these shot points (shot points 889-977 in base Zechstein Z1 Halite and shot points 926-977 in top Zechstein Z1 Halite) before modeling will improve model quality. Shot points at the northeastern end of seismic line 11-AK-ISH-02 were removed before modeling the base of the Zechstein Z1 Halite horizon (shot points 378-397.64191) and shot points at the southwestern end of seismic line 11-AK-ISH-02 were removed before modeling the top of the Zechstein Z1 Halite horizon for the same reason (shot points 36-72).
- Shot points at the southwestern end of seismic line 6073 were removed before modeling the top of the Zechstein Z1 Halite horizon. The depth values at these shot points (shot points 2654.5-2668.75) appeared unreliable during manual interpolation. Moreover, these shot points are located at a large distance from the salt pillow, so these shot points can be removed without concern;
- Shot points at the western ends of seismic lines 706036, 85EN(V)-03 and RGD8209 (west of the probably fault line) were removed before modeling the top of the Zechstein Z1 Halite horizon. No clear pattern could be observed in the depth values at these shot points during manual interpolation. These shot points are located west of or even within a significant fault zone, at the edge of the modeling area, and at a large distance from the salt pillow. As such removing these shot points will have little impact on the final model of the top Zechstein Z1 Halite.

As the shape of the base of the Triassic deposits (= top Zechstein) is known to resemble the shape of the top of the Zechstein Z1 Halite horizon, the same modifications made to the top Z1 Halite horizon shot points were also applied to the base of the Triassic horizon shot points.

Finally, an important conclusion of the manual interpolation was that the data density in the northeastern corner of the modeling area is relatively low and that it is in fact too low for computer modeling purposes. Therefore, it was decided to eliminate this part of the modeling area from all geological models.

## **5.5 Modeling method**

### **5.5.1 Introduction to modeling**

The base and top of the Zechstein Z1 Halite were modeled manually first followed by computer modeling in order to get the best possible digital representation. The base of the Triassic deposits was modeled by computer only as this horizon more or less follows the top of the Zechstein Z1 Halite horizon and can be modeled using the same modeling techniques. Also the base of the Tertiary deposits was modeled by computer only as this is a more or less flat lying horizon with relatively little differences in depth and little structures. The results of the manual interpolation are used to check and improve computer modeling results.

Several different interpolation techniques and parameters were tested during the computer-based modeling phase to determine which technique and what parameters should be used to create the best possible and most reliable geological models.

### 5.5.2 Available interpolation techniques

Computer-based interpolation was performed using ESRI ArcView software with Spatial Analyst and Geostatistical Analyst extensions. Various automated interpolation techniques were explored and tested.

#### 1. Inverse Distance Weighting (IDW)

IDW is a simple and exact interpolation method. IDW assigns values to unsampled locations by calculating a weighted average of nearby surrounding data values. Weights assigned to nearby data points are based on the inverse distance between the data point and the unsampled location and the power of the IDW function. Using a higher power IDW increases the weight of data points closer to the unsampled location. Interpolated values are strongly dependent on the distance function, which is often a best guess. Clustering of data points and/or the presence of outliers can cause egg-shaped model artifacts.

IDW requires no assumptions of the data and is an exact interpolator. Depending on the resolution of the model IDW reproduces the measured value at each data point. IDW does not model values beyond the range of measured values.

IDW offers several different approaches to determine which nearby data points are used for interpolation. The variable search radius approach allows the user to define the number of surrounding data points that should be used to interpolate a value at an unsampled location. Sometimes a maximum search radius is set to limit the distance that source data points may be removed from the interpolation location. Another approach is the fixed search radius in which all data points located within a user-specified radius around the unsampled location are used during IDW interpolation. A minimum number of points may be set to guarantee that a minimum number of data points is used for interpolation. The (maximum) search radius is not derived from the input data and therefore it is not always known whether the surrounding source data and the value at the unsampled location are really correlated. Both search radius approaches allow the definition of barriers, i.e. lines that cannot be crossed when searching for the closest surrounding data points for interpolation.

#### 2. Natural neighbors

The natural neighbor interpolation method is a variant of the IDW interpolation method. Natural neighbors also calculates a weighted average of surrounding data values, but in this case the weights are assigned based on proportionate areas of Thiessen polygons. ESRI warns that this interpolation method requires a high source data density for good results.

#### 3. Splines

The spline interpolation method fits piece-wise mathematical functions through a small number of local data points while at the same time ensuring that the joins between the local functions are as smooth as possible. The resulting model is a smooth surface that fits through the data points (exact interpolator) and minimizes overall curvature of the surface. Splines often produce unrealistically smooth surfaces, although for geological horizons that have been formed or moderated by processes like compression, extension, folding or even halokinesis, smooth surfaces may be an advantage instead. Minimum and maximum interpolated values may be outside the range of measured values, which also can be an advantage when modeling geological horizons. With splining it is possible to define barriers, i.e. lines that cannot be crossed when fitting local functions through data points.

#### 4. Kriging

Kriging is a geostatistical interpolation method that uses a linear combination of surrounding data values to predict values at unsampled locations. Kriging assigns weights to each of the surrounding data points that result in optimal (error variance is minimized) and unbiased estimates (on average the difference between the predicted values and the actual values is zero).

Kriging weights are calculated using a fitted semivariogram model. A semivariogram is a model of the spatial dependence structure of the source data. That is to say, in kriging the assignment of weights is not limited to the inverse distance model (see IDW) and information derived from the source data itself (semivariogram) is used to assign weights to nearby data points. In summary, kriging uses the source data twice: once to estimate the spatial correlation structure of the variable of interest (variogram modeling) in order to assign weights to surrounding data points and once to calculate prediction values at unsampled locations.

Kriging only predicts values within the range of measured values. Furthermore, kriging tends to overestimate low values, while high values tend to be underestimated.

To build a semivariogram it is necessary to assume that the spatial variation of the variable of interest (e.g. depth of base of the Zechstein Z1 Halite) is homogeneous over the study area, i.e. once structural effects are accounted for the pattern of variation of the variable repeats itself in space (second order stationarity). Additionally, some kriging methods assume that the source data values are normally distributed.

Previously discussed interpolation methods have no built-in method for error assessment (unless a separate validation data set is available). With kriging interpolation, not only are values predicted at unsampled locations, but the kriging variance is also calculated at all locations. The kriging variance can be used to identify problems with source data, model parameters, and in the definition of the local neighborhood.

##### 5.5.3 Comparison and selection of interpolation techniques

In the previous modeling study of the Haaksbergen area of interest (MWH, 2008b) various interpolation methods were tested and the IDW interpolation was found to generate the best models for the various geological horizons. As this time more source data are available, particularly in the area of most interest, i.e. the area with the thickest Zechstein Z1 Halite deposits, several interpolation methods were tested again to determine the best interpolation method and parameters for the most important geological horizons. As our objective was to optimize modeling results in the most important area (i.e. the area where the salt pillow is located and salt deposits are thicker than 150 m), the best interpolation method and parameters were selected with this goal in mind. However, it is important to note that parameters selected to optimize the models in this area may have adverse effects on model quality and reliability elsewhere. This will be discussed further in section 5.9.

The natural neighbors interpolation method was deemed unsuitable for modeling the geological layers in the Haaksbergen area of interest because of limited data density in areas located in between seismic lines.

Kriging interpolation offers certain advantages, such as the fact that weights are assigned using a spatial correlation model derived from the input data itself and the calculation of kriging variances. However, in this case kriging was found to be an unsuitable interpolation method. It was not possible to build proper semivariograms of the seismic source data. Likely, too many different geological processes (deposition, erosion, displacement along faults, folding, salt displacement, etc.) have im-

pacted the different horizons and the Zechstein Z1 Halite itself in the Haaksbergen area of interest and these processes have impacted different subsections of the area of interest in different ways. Therefore, the assumption of second order stationarity no longer holds and no proper variogram model could be built.

In the previous modeling study (MWH, 2008b) IDW interpolation was found to generate the best models for the various geological horizons in the Haaksbergen area of interest. With the addition of the new seismic data IDW interpolation again was found to generate reasonably good models for the various geological horizons. However, as was pointed out in the previous study one drawback of using IDW interpolation is that all modeled depth values lie within the range of measured depth values. Also, as IDW assigns values to unsampled locations by calculating a weighted average of nearby surrounding data values, this interpolation method may lead to an underestimation of the highest depth values (deepest points) in each layer and an overestimation of the lowest depth values (shallowest points). This is particularly likely in this case when the IDW interpolation is forced to include data from different directions which is recommended as the nearest data points in most cases are all located on the same line (unidirectional). As noted in the previous study the likely overestimation of the lowest depth values is problematic, particularly in the models of the base and the top of the Zechstein Z1 Halite horizons, as the areas where the base and top Zechstein Z1 Halite horizons are located closest to the surface are located right in the middle of the area with the thickest salt deposits. Here modeled depths are by sure deeper than actual depths.

Meanwhile, in the previous modeling study splines were found to create unrealistically smooth models of the various geological horizons. However, with the addition of the data along the two newly acquired seismic lines the data density in the area of most interest has increased significantly. Focusing on the area of most interest, i.e. the area where the salt pillow is located and salt deposits are thicker than 150 m, spline models, specifically tension splines, were now found to generate the best models for the various geological horizons in the Haaksbergen area of interest.

Tension splines minimize the first and second derivatives of the spline function which results in a surface that is more closely constrained by the source data range than some other types of splines. This prevents problems with extreme interpolated minimum and maximum values that (may) occur in regions with rapidly changing gradients in the modeled phenomenon.

Different spline model parameters were tested to create the best final model for each horizon: several different search neighborhoods, several kernel (smoothing) parameters, inclusion/exclusion of fault zones as barriers, etc. Due to some important differences in the base and top Zechstein Z1 halite horizons that were observed during manual interpolation different parameters were selected to model these two horizons.

During manual interpolation no significant faults (with major offset) were observed in the area of most interest, i.e. area with thickest deposits, in the top Zechstein Z1 Halite horizon. Therefore, we opted to model this horizon without faults (barriers). The best model of the top Zechstein Z1 Halite horizon was created using a tension spline model with a search neighborhood with 8 sections at an angle of 22.5 degrees, a maximum search radius of 1,500 m, a maximum of 8 neighbors per section, a minimum of 0 neighbors per section and an optimized kernel parameter of 0.000685 (very little smoothing).

The definition of multiple sections within the search neighborhood forces the spline function to be fitted for shot points located in various directions (i.e. on different seismic lines). The same parameters were used to model the base Triassic horizon as the shape of the base of the Triassic deposits is known to resemble the shape of the top of the Zechstein Z1 Halite horizon.

During manual interpolation of the base Zechstein Halite Z1 horizon we noted that the structure of this horizon is fairly complex with several significant faults (with major offsets) near the area of most interest, i.e. area with thickest deposits, in the base Zechstein Z1 Halite horizon. Therefore, we opted to model this horizon with faults (barriers). Including fault lines as barriers during modeling essentially breaks up the modeling area into smaller parts that are modeled separately. This means that during interpolation near a fault line barrier nearby shot points across that fault line are not used during modeling. The best model of the base Zechstein Z1 Halite horizon was created using a spline model where the most important faults were included as barriers and with no smoothing factor. Unfortunately, the modeling software allows little flexibility in defining the search neighborhood when including barriers in the interpolation. Consequently, it was not possible to define multiple sections within the search neighborhood. This probably caused the final model of the base Zechstein Z1 Halite horizon to appear a little too smooth. However, these parameters still resulted in the best possible model of a horizon with a complex structure.

## **5.6 Modeling results**

### **5.6.1 Base Zechstein Z1 Halite**

Figure 5.3 shows the final model of the depth of the base of the Zechstein Z1 Halite. This map is also provided in Appendix VI. Appendix VII contains the depth of the base of the Zechstein Z1 Halite for the concession area Isidorushoeve.

This horizon shows a local high ('horst'), located in the western part of the area, in between the Langelo and Hengevelde fault zones, with the highest point at approximately 700 m below sea level. Although data density in this western area is relatively low, the horst seems to have a more or less northwest-southeast orientation. Further east the orientation of this high seems to change towards a more west-east orientation. So the high follows the bending shape which is similar to the change in fault line orientation that was observed earlier.

From this local high, the base of the Zechstein Z1 Halite in the Haaksbergen area of interest first gradually and then more steeply deepens in a northeasterly direction. A local low ('graben') with a lowest point of over 1,600 m below sea level occurs in-between two faults.

In a southeasterly direction, a steep deepening is visible, south of the Haaksbergen fault zone, of which the offset consequently increases to over 150 m.

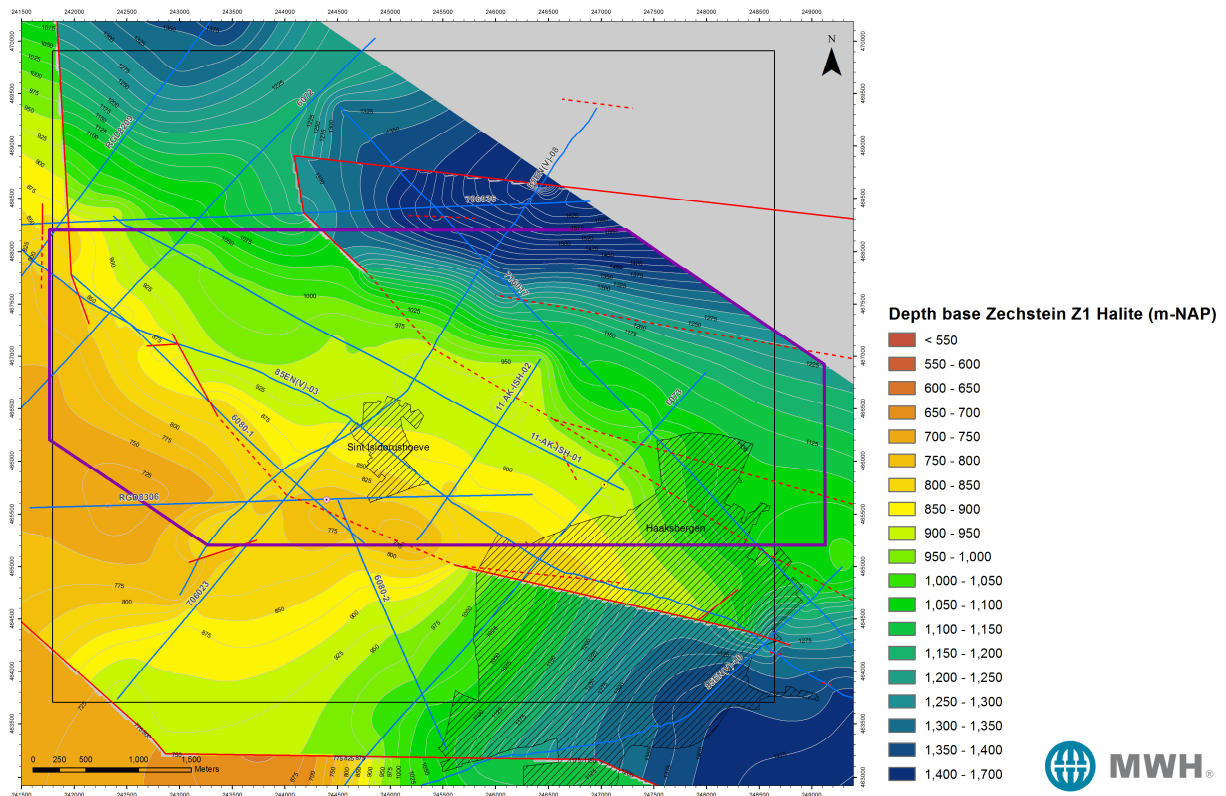


Figure 5.3: Modeled depth of the base of the Zechstein Z1 Halite.

### 5.6.2 Top Zechstein Z1 Halite

Figure 5.4 shows the final model of the top of the Zechstein Z1 Halite. This map is also provided in Appendix VIII. Appendix IX contains the depth of the top of the Zechstein Z1 Halite for the concession area Isidorushoeve. It clearly shows the Haaksbergen salt pillow, located just northwest of Haaksbergen, stretching from the village of Haaksbergen to the village of Sint Isidorushoeve and even a little further. The area where the top lies at a depth of less than 600 meters has a length of about 3 kilometers.

The highest point of the top of the Zechstein Z1 Halite (approximately 520 m below sea level) occurs in the center of AkzoNobels Zuidoost Twente concession area, just underneath the northern part of the village of Sint Isidorushoeve.

Especially towards the north-northeast the top of the Zechstein Z1 Halite steeply deepens into the basin, known as the Stepelo depression (MWH, 2010). A dip of over 40° can be inferred from the isopachs. The deepest part of the area has a depth of over 1,600 near the eastern tip of seismic line 706036, about 2 km north of the Haaksbergen salt pillow. This depression is more or less located at the same place where the local low in the base of the Zechstein Z1 Halite occurs. As seismic data density decreases in this area, mainly towards the east, modeling results should be dealt with cautiously.

Also towards the southeast, the top of the Zechstein Z1 Halite seems to steeply deepen into another basin, which also is located at the same place where a basin is observed in the base of the Zechstein Z1 Halite.

Towards the west a very smooth deepening can be seen to approximately 675 m below sea level, followed by a slight shallowing to 600 meters again in the extreme west of the area.

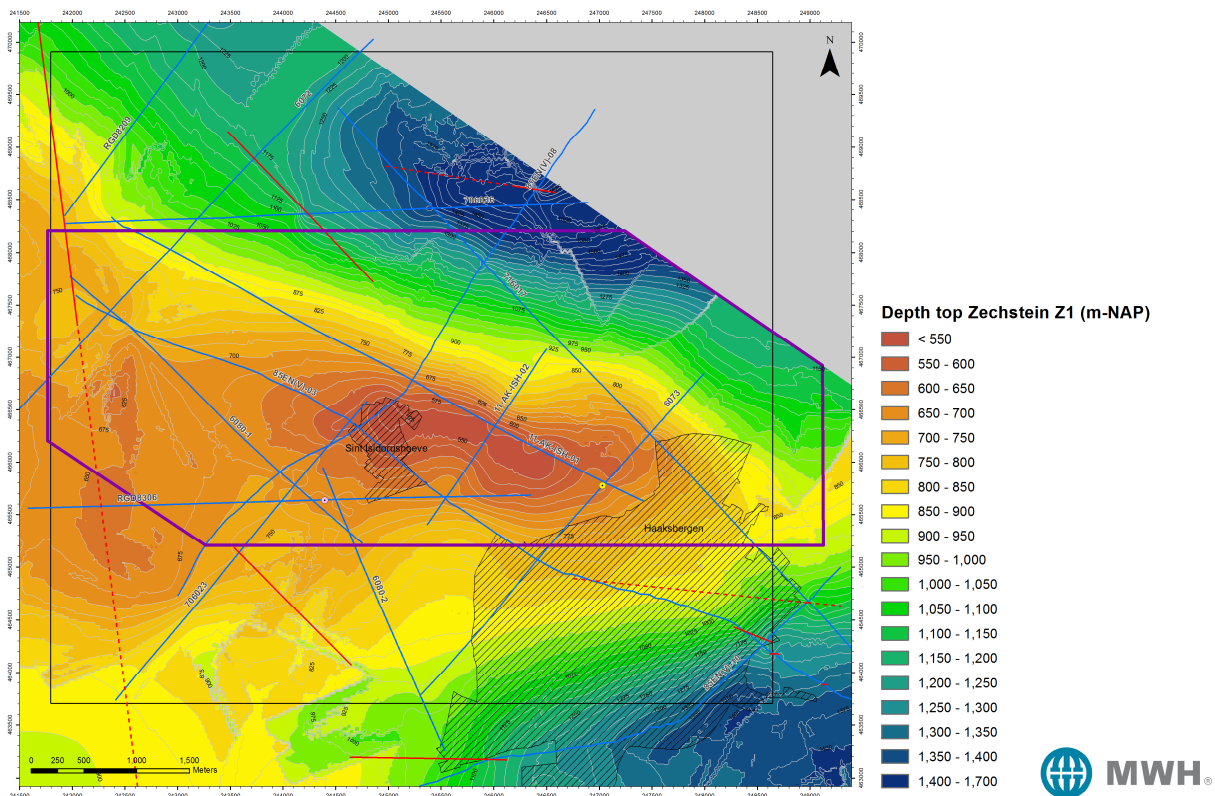


**Figure 5.4: Modeled depth of the top of the Zechstein Z1 Halite.**

Comparing the models of the base and top of the Zechstein Z1 Halite shows that the area with the shallowest depth of the base is located just south of the shallowest depth of the top of the Z1 Halite. In other words, the salt pillow is not located on top of the underlying Carboniferous horst block structure, but more or less on the flat part of the northern slope of the horst block

### 5.6.3 Thickness of the Zechstein Z1 Halite

Figure 5.5 shows the final model of the thickness of the Zechstein Z1 Halite. This map is also provided in Appendix X. Appendix XI contains the thickness of the Zechstein Z1 Halite for the concession area Isidorushoeve. The thickness of the Zechstein Z1 Halite deposits varies from less than 100 meters outside the salt pillow area just over 400 meters at its thickest. The model of the thickness of the Zechstein Z1 Halite clearly shows the elongated salt pillow structure located on the northern slope of the Carboniferous horst block (see Figure 5.3, base of the Zechstein Z1 Halite). Two areas are observed with a thickness just over 400 meters. The first one is located underneath the northern part of Sint Isidorushoeve, exactly where the top of the Zechstein Z1 Halite reaches its shallowest depth. A second one just northwest of Haaksbergen where a relatively shallow top of the Zechstein Z1 Halite is overlying an already steeply dipping part of the base of the Zechstein Z1 Halite.

As the base of the Zechstein Z1 Halite dips towards the northeast, the already elongated shaped top of the Z1 Halite produces an even more elongated salt pillow. The area with a thickness of over 350 meters has a length of almost 3 kilometers and the area with a thickness of over 300 meters has a length of almost 4.5 kilometers.



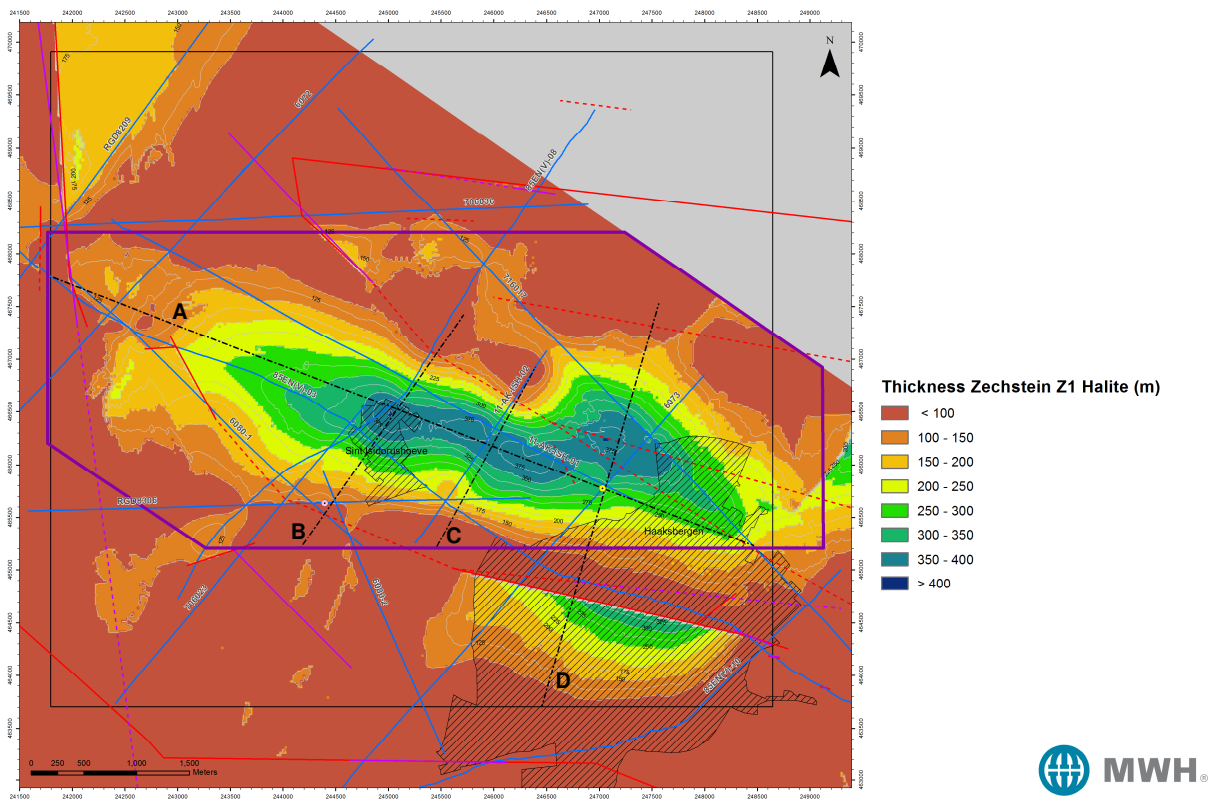


Figure 5.5: Modeled thickness of the Zechstein Z1 Halite with indicated profile lines (see section 5.7).

#### 5.6.4 Base of the Triassic deposits

Figure 5.6 shows the final model of the depth of the base of the Triassic deposits (= top Zechstein). This map is also provided in Appendix XII. Appendix XIII contains the depth of the base of the Triassic deposits for the concession area Isidorushoeve. The depth of the base of the Triassic deposits varies from a high of approximately 380 m below sea level beneath the north of Sint Isidorushoeve to a low of over 1,500 m below sea level in the northeastern part of the area. The high occurs in the same place as the modeled top of the Zechstein Z1 Halite and the low occurs in the same location as the local lows in the base and the top of the Zechstein Z1 Halite.

The shape of the modeled depth of the base of the Triassic deposits very much resembles the shape of the modeled top of the Zechstein Z1 Halite. Consequently, the thickness of the overlying Z2 to Z4 deposits varies little across the Haaksbergen area of interest. This thickness is shown in Figure 5.7. This map is also provided in Appendix XIV. Appendix XV contains the thickness of the overlying Z2 to Z4 deposits for the concession area Isidorushoeve. As this thickness is calculated by extracting two individually modeled horizons, some modeling artifacts may lead to unreliable high or low thicknesses. In general the thickness of the overlying Z2 to Z4 deposits varies from less than 50 m beneath the village of Haaksbergen in the southeastern corner of the area and in the north of the area, to almost 200 m in the center of the area of interest. The thickness of the overlying Z2 to Z4 deposits is more than 100 m in the majority of the area where the salt pillow is located.

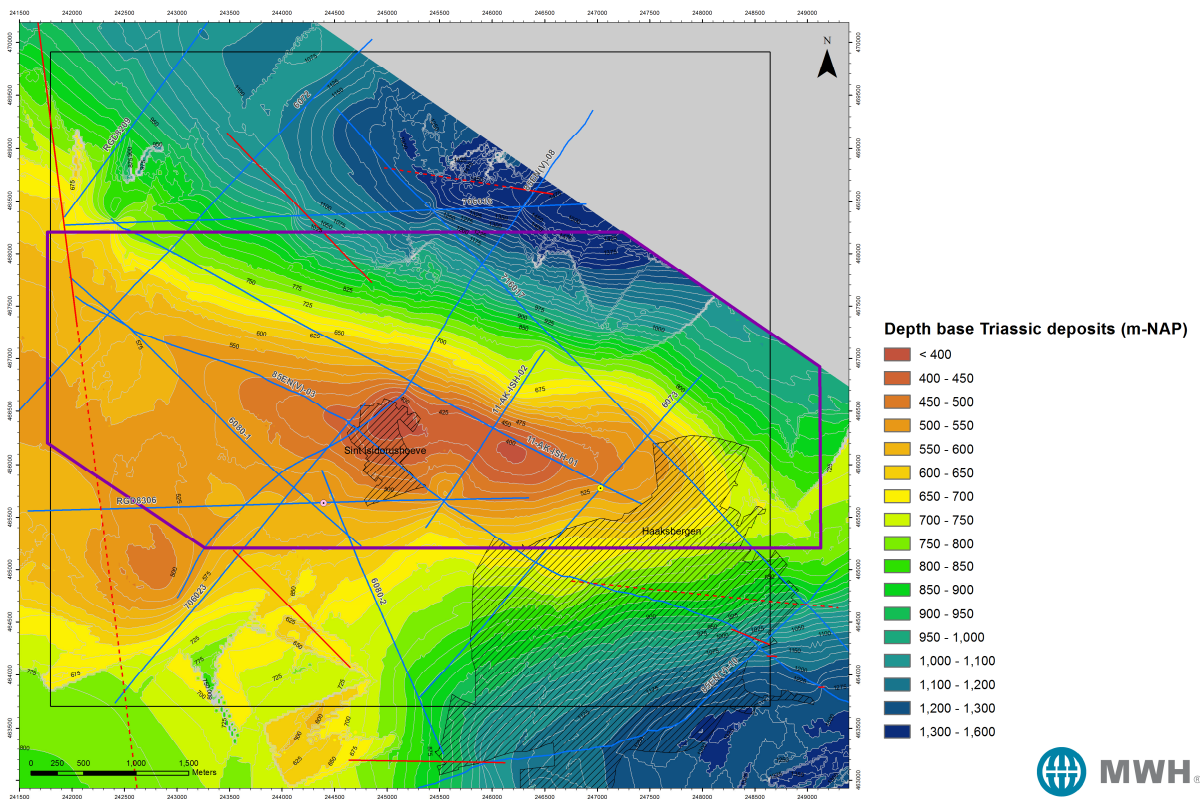


Figure 5.6: Modeled depth of the base of the Triassic deposits.

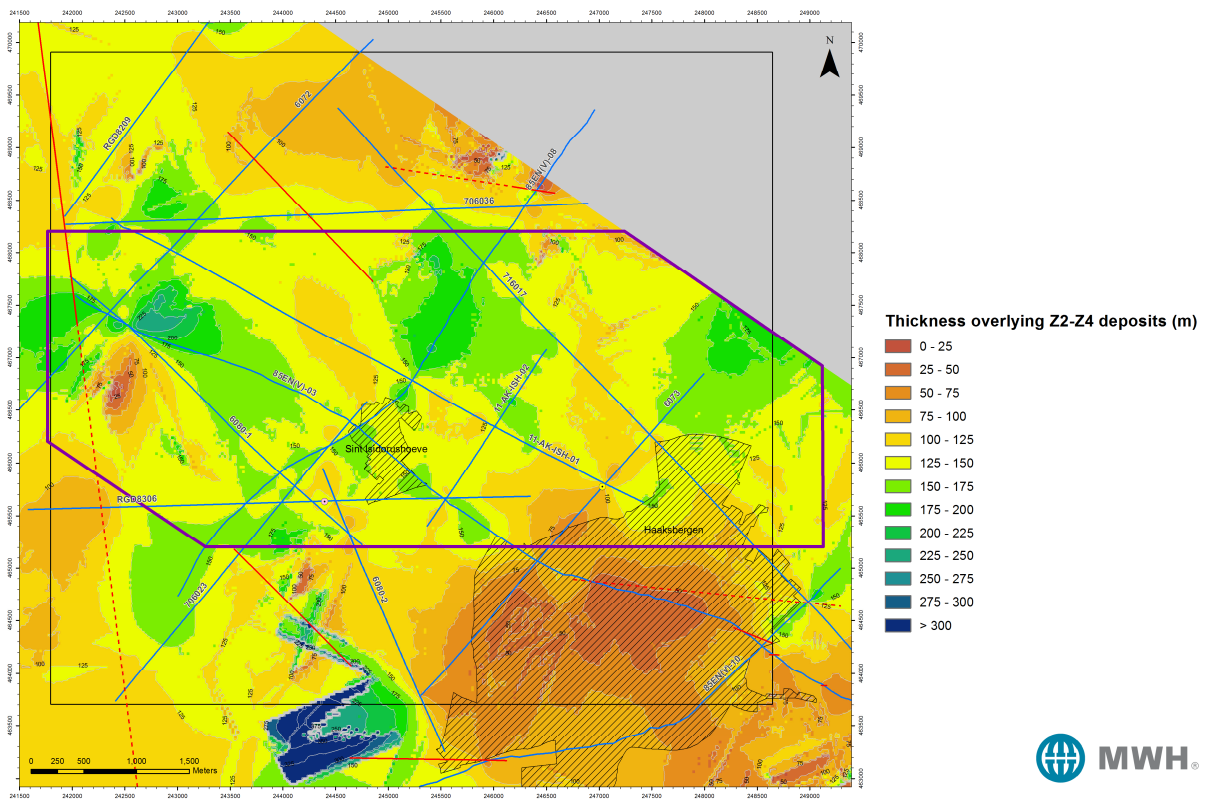


Figure 5.7: Modeled thickness of the Z2 to Z4 deposits.

### 5.6.5 Base Tertiary deposits

Figure 5.8 shows the final model of the depth of the base of the Tertiary deposits in the Haaksbergen area of interest. This map is also provided in Appendix XVI. Appendix XVII contains the depth of the base of the Tertiary deposits for the concession area Isidorushoeve. In general the base of the Tertiary deposits slowly, but gradually, ascends in an eastern direction. The depth varies from about 180 m at the western edge of the Haaksbergen area of interest to about 80 m at the eastern edge.

From the fact that almost all patterns that were visible in the modeled base and top of the Zechstein Z1 Halite and the modeled base of the Triassic deposits, are not visible in the modeled base of the Tertiary we can conclude that this horizon is an erosional unconformity.

Nevertheless, some slight shallowing pattern is visible, exactly above the modeled salt pillow, leading to a local high underneath the northern part of Haaksbergen and a ridge like structure stretching from there in a west-northwestern direction toward the village of Sint Isidorushoeve and from there in a more northwestern direction. The fact that this pattern is visible indicates that some uprising of the salt pillow (and overlying strata) has occurred since erosion took place. From this we can conclude that some halokinesis has occurred since the end of the Laramide orogeny, i.e. during the Tertiary. When looking at the seismic profile of seismic line ISH-02 in depth (see Appendix III) the slight uplift of the base Tertiary of over 25 m is well visible. When looking at the same seismic profile in time it can be seen that even quite shallow layers (0.05 seconds TWT) show some upward bending right above the salt pillow.

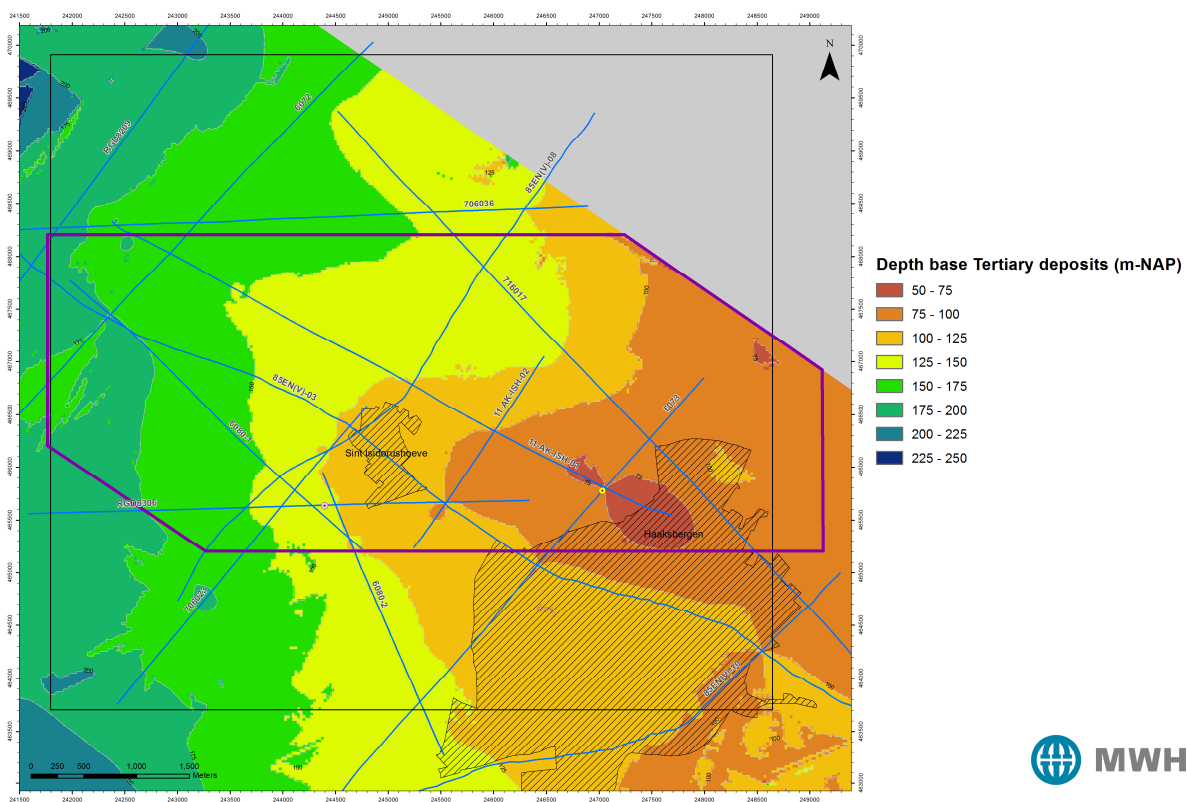


Figure 5.8: Modeled depth of the base of the Tertiary deposits.

## 5.7 Profiles through the salt pillow

To get a better understanding of the structure of the elongated salt pillow that is located northwest of the village of Haaksbergen, we have drawn four profiles through the area, focusing at the salt pillow area, profiles A to D. Profile A is positioned in a west-northwest to east-southeast direction across the elongated salt pillow (longitudinal section). The other three profiles (B, C and D) run more or less perpendicular to the elongated salt pillow (western, middle and eastern cross sections).

The western cross section is located just east of seismic line 85EN(V)-08, the middle cross section is located just east of new seismic line 11-AK-ISH-02 and the eastern cross section is located just west of seismic line 6073. The location of the profiles can be seen in Figure 5.5.

Figure 5.9 shows the WNW-ESE longitudinal section (profile A; see also Appendix XVIII). It clearly shows the high ridge of salt stretching over several kilometers, from a location underneath the north of Sint Isidorushoeve in the west to a location just north of Haaksbergen in the east. Above a more or less flat base, the salt pillow with its maximum thickness of approximately 400 m is clearly visible.

Figure 5.10 shows profile B (left panel), i.e. the western SW-NE cross section (see also Appendix XIX) and profile C (right panel), i.e. the middle SW-NE cross section (see also Appendix XX). Figure 5.11 shows profile D, i.e. the eastern SW-NE cross section (see Appendix XXI).

All cross sections clearly show the salt pillow, located on the northeastern slope of the Carboniferous horst block. In the middle (profile C), the salt pillow seems to be less wide than in the east and west and here the northeastern flank of the pillow seems to be steepest. Furthermore in the eastern cross section (profile D) the Haaksbergen fault zone, located underneath the village of Haaksbergen, with an offset of some 200 m is clearly visible. This fault cannot be traced further northwestward.

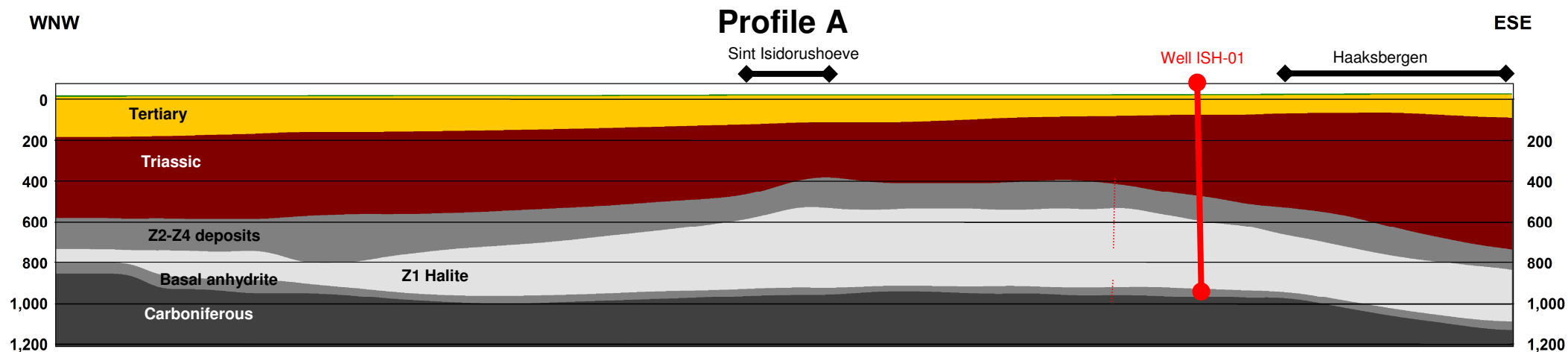


Figure 5.9: Profile A: longitudinal WNW-ESE section through the elongated salt pillow (no vertical exaggeration). See Figure 5.5 for the location of this profile. Dashed red lines indicate small scale faults as visible in nearby seismic lines.

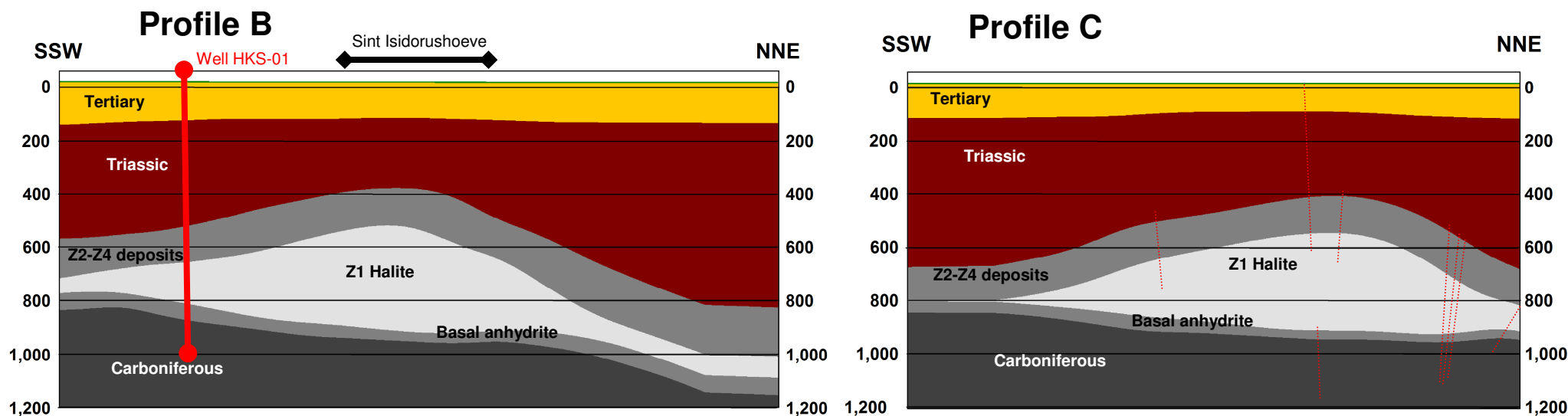


Figure 5.10: SW-NE cross sections through the western (Profile B; left panel) and middle (Profile C; middle panel) part of the elongated salt pillow (no vertical exaggeration). See Figure 5.5 for the location of these profiles. Dashed red lines indicate small scale faults as visible in nearby seismic lines.

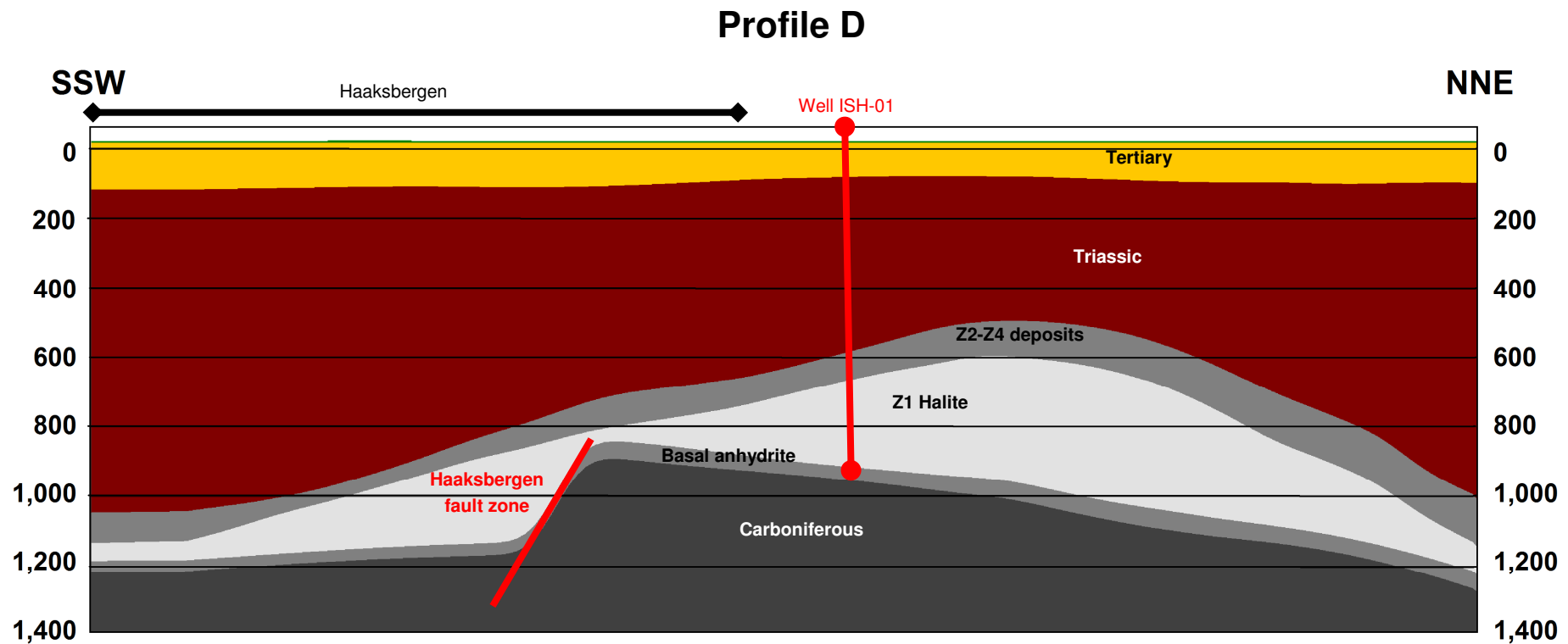


Figure 5.11: Profile D: SW-NE cross sections through the eastern part of the elongated salt pillow (no vertical exaggeration). See Figure 5.5 for the location of this profile.

## **5.8 Discussion of the implications of the geological modeling results**

In this section we discuss the main aspects of the results of the geological modeling, focusing on the most important changes that have been made since the 2008 geological modeling study of this area.

### **5.8.1 Base Zechstein Z1 Halite**

At the base of the Zechstein Z1 Halite most changes have arisen from the introduction of faults into the modeling. These faults act as barriers during modeling, creating some sharp edges in the new model, while more smooth (but very steep) flanks occurred in the 2008-model.

Other differences arise from the different modeling technique used, i.e. the IDW-technique in the 2008-modeling and the spline-technique in the present modeling. This other technique leads to smoother edges and to modeled minimum and maximum values that may be outside the data range and at locations away from the source data.

Especially within the central part of the study area (i.e. the salt pillow area) the new seismic lines ISH-01 and ISH-02 have increased data density and therefore model reliability. The new data points have not changed the model in a major way, although some changes are visible. The most important change can be seen at the northern half of seismic line ISH-02, where a rather flat lying base of the Zechstein Z1 Halite seems to exist. This is not in real good agreement with neighboring seismic lines 85EN(V)-08 and 6073, which show a much steeper base Zechstein Z1 Halite and also seismic line 716017, just north of the northern end of ISH-02, suggests the base lying at a larger depth than observed in seismic line ISH-02. The fact that the base of the Zechstein Z1 Halite might be influenced by faulting in this area may provide a possible explanation for the observed disagreements.

Within areas where the base of the Zechstein Z1 Halite occurs at relatively larger depth, the depth has increased with respect to the 2008-model. This is a consequence of the new seismic velocity model and consequent time-to-depth conversion, as the Triassic has a high depth dependent seismic velocity increase.

### **5.8.2 Top Zechstein Z1 Halite**

Also at the top of the Zechstein Z1 Halite most differences arise from the different modeling technique used, i.e. the IDW-technique in the 2008-modeling and the spline-technique in the present modeling, leading to smoother edges and to modeled minimum and maximum values that may be outside the data range and at locations away from the source data.

Furthermore the new seismic lines ISH-01 and ISH-02 have increased data density and therefore the model reliability within the central area, for example in-between the two modeled highs in the 2008-model. The new model shows a more elongated high ridge instead of two separate summits. During modeling the focus was on the central high thickness area. Therefore the new model gives geologically more reliable results within this area at the expense of the reliability within more distinct areas, with less data density. Consequences of this can be seen in the extreme western part of the area, in the Stepelo depression (northern part of the area) and in the southeastern part of the area.

Within areas where the top of the Zechstein Z1 Halite occurs at relatively larger depth, the depth has increased with respect to the 2008-model as a consequence of the new seismic velocity model and consequent time-to-depth conversion.

### **5.8.3 Zechstein Z1 Halite thickness**

As a consequence of the changes of both the top and base of the Zechstein Z1 Halite, also the modeled thickness has changed. Important changes, mainly in the more distinct parts of the area, arise from the use of fault barriers during modeling of the base. The most pronounced example is visible just south of the salt pillow, where a relatively high thickness is being calculated as a result of a normal fault within the base of the Zechstein Z1 Halite. This might have been an ancient growth fault, leading to increasing accumulation space during salt formation. Most other differences arise from the different modeling technique used, i.e. the IDW-technique in the 2008-modeling and the spline-technique in the present modeling.

Especially within the central part of the study area (i.e. in the salt pillow area) the new seismic lines ISH-01 and ISH-02 have increased data density and therefore the model reliability. Here the effect of the more pronounced high ridge in the new model, instead of the two separated summits, becomes clearly visible, leading to an elongated high thickness area as well.

The newly modeled thickness gives the idea of two instead of one salt ridge: a western one with an almost west-east orientation and an eastern one with a northwest-southeast orientation. The western one is located above the more flat lying part of the Carboniferous horst block, while the eastern one is located above the northeastward dipping flank of the horst block.

Finally the newly modeled salt pillow is about 250 m less wide within western two third, is a little longer and has a higher thickness in the middle part. As a consequence all flanks are steeper, especially the northern one, near seismic line ISH-02.

### **5.8.4 Implications for the geological history**

As described in chapter 2, the salt pillow is located on top of a heavily faulted Carboniferous horst block. Evidence of this faulting has become more clear as many faults have been visualized in both the older as the newly shot seismic lines, like along the northern edge of the salt pillow in line ISH-02 and on both sides of the salt pillow within line 716017. Thickened salt deposits on the southern side of the Haaksbergen fault zone (see the eastern cross section in Figure 5.11), underneath the village of Haaksbergen, seem to point at synsedimentary faulting. This halfgraben, which originated from transtensional movements during the early Zechstein, became filled with rock salt rapidly, probably even amplifying fault relief.

A same phenomenon may have caused the formation of thick salt deposits in the northeastern part of the area. Here a large basin is present, bordered by some normal faults, of which the Stepelo fault zone seems to be the most important one. In contrary to the situation underneath the village of Haaksbergen, at present the thick salt deposits north of Haaksbergen are not located within this basin anymore but have migrated up the northern flank of the Carboniferous horst block, to form the Haaksbergen salt pillow. This halokinesis probably already started during Triassic times, being extension related, and may have continued into the Jurassic and Cretaceous when a compressional regime (Subhercynian tectonic phase) reactivated deep fault zones, causing widespread salt movement (Geluk, 2005).



## 5.9 Quality and reliability

Various factors impact the quality and the reliability of the modeled geological horizons (base of the Zechstein Z1 Halite, top of the Zechstein Z1 Halite, thickness of the Zechstein Z1 Halite deposits, base of the Triassic deposits, and base of the Tertiary deposits), including issues related to the interpolation method and parameters used to create the models, quality of the seismic source data, as well as source data density and distribution.

### 5.9.1 Reliability with respect to the choice of the interpolation method

First, the quality of the models for the various geological layers is affected by the choice of the interpolation method. As our objective was to optimize modeling results in the most important area, i.e. the area where the salt pillow is located and salt deposits are thicker than 150 m, the best interpolation method and parameters were selected with this goal in mind. This also means that the selected interpolation method and parameters not necessarily lead to optimal modeling results outside the area of most interest. In fact, by optimizing modeling results in this particular area modeling results in the rest of the modeling area probably show more anomalies and irregularities and are less reliable than would be the case if interpolation method and parameters were selected to optimize modeling results for the entire modeling area.

One drawback of splines is that they can produce unrealistically smooth surfaces, especially when limited source data are available. This does not appear to be a problem in the models of the top Zechstein Z1 Halite horizon and the base of the Triassic deposits. However, the model of the base of the Zechstein Z1 Halite horizons appears a little too smooth. This may be caused by two different factors. First, the decision to use several faults as barriers during interpolation resulted in the modeling area essentially being broken up into smaller parts that are modeled separately. That means that fewer source data points were available to model each part. Also, as the modeling software does not allow for the definition of multiple sections within the search neighborhood when interpolating with barriers, the local data points through which the spline interpolation method fitted the interpolated surface (base of the Zechstein Z1 Halite horizon) are mostly located on the same seismic line.

Also, spline models produce poor(er) results when significant changes occur in the source data values within short distances. This may occur in areas where a fault line with significant offset that was not included as a barrier during interpolation intersects a seismic line or in areas where multiple seismic lines cross each and are not tied flawlessly. While this does not appear to cause major problems in the final geological models presented here, some modeling anomalies can be observed near some seismic line intersections, e.g. near the intersection of seismic lines 716017 and 6073. In areas with fewer source data this can lead to more significant incongruities further away from the source data on the seismic lines as there are no source data to constrain the interpolated surface. This can be observed in the modeling anomalies that can be observed in the model of the top Zechstein Z1 Halite horizon in the area around the intersection of seismic lines 6080-1 and 85EN(V)-03.

For the final models of the top Zechstein Z1 Halite horizon, base Triassic deposits and base Tertiary deposits we opted to define multiple sections in the search neighborhood. The definition of multiple sections within the search neighborhood forces the interpolated surface to be fitted through shot points located in various directions (i.e. on different seismic lines). This has clear advantages in this particular case as the source data are very unevenly distributed across the modeling area and the

nearest data points are almost always all located on the same seismic line (unidirectional). However, defining multiple sections in the search neighborhood can also cause some modeling anomalies, particularly in areas with little source data and/or at some distance from the source data. The V-shaped irregularity north of Haaksbergen that can be observed in the model of the top Zechstein Z1 Halite horizon is the most pronounced example of such an anomaly.

### 5.9.2 Source data location and distribution

Model reliability is also highly affected by the location and distribution of the source data. Obviously, the reliability of the models decreases with increasing distance from the source data on the seismic lines, i.e. model reliability is high in areas close to the seismic lines and model reliability is low in areas located far away from any seismic lines. While extrapolation (interpolation outside the area where source data are available) or interpolation in areas that are not surrounded by source data in all directions obviously lead to poorer modeling results, this is especially true for spline models as the fitted (splined) surface in those areas is no longer constrained by source data, or at the least is not constrained in all directions.

To get an idea about the source data distribution, Figure 5.12 shows the distance from every location in the Haaksbergen area of interest to the closest shot point (see also appendices XXII-a and b).

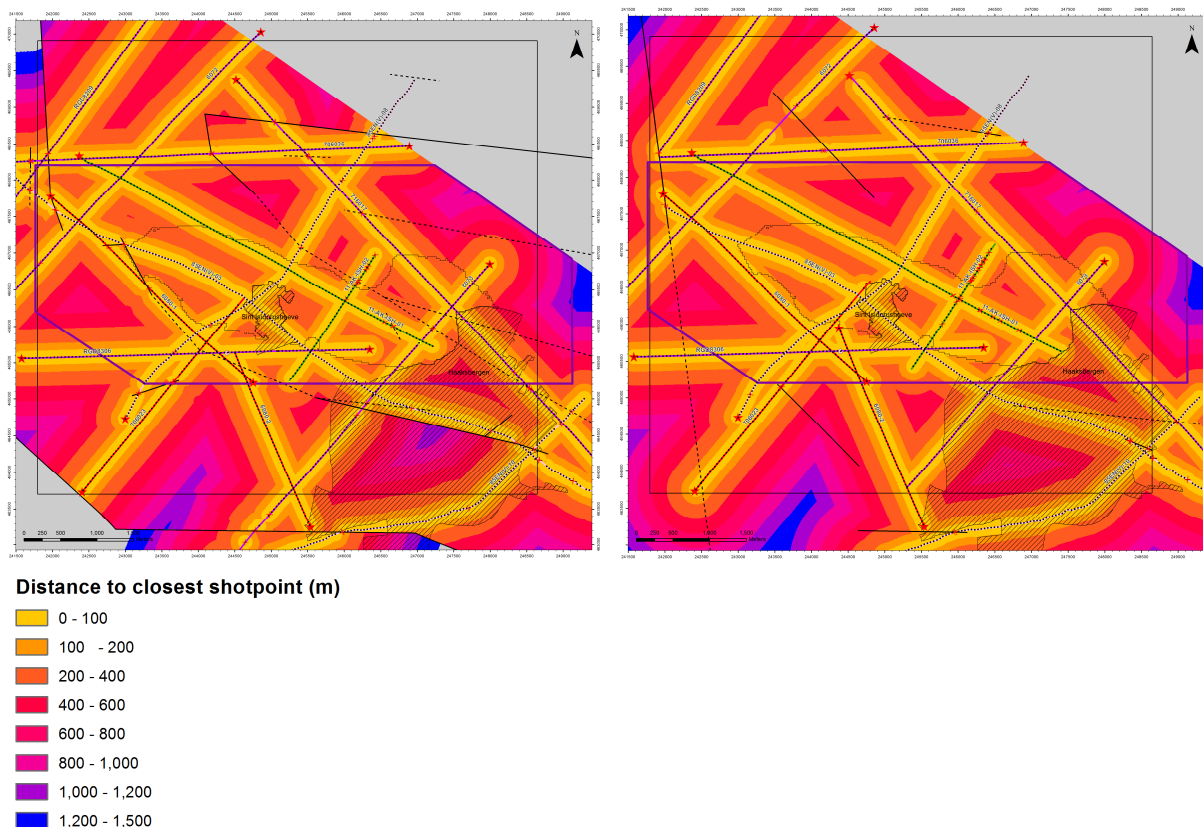


**Figure 5.12: Distance to closest shot point for the base (left window) and the top (right window) of Zechstein Z1 Halite models.**

Figure 5.13 shows the shot point data density for the top Zechstein Z1 Halite. This map shows the number of shot points located within a 1 mile radius in every location of the Haaksbergen area of interest (see also appendix XXIII). Due to the barriers used to interpolate the base Zechstein Z1 Halite horizon is was not possible to create a map of the data density of the source data for this horizon. Generally, modeling results tend to be more reliable in high data density areas as long as the source data quality is high. However, as noted previously, in case of splining, the additional requirement applies that no significant changes occur in the source data values within short distances.

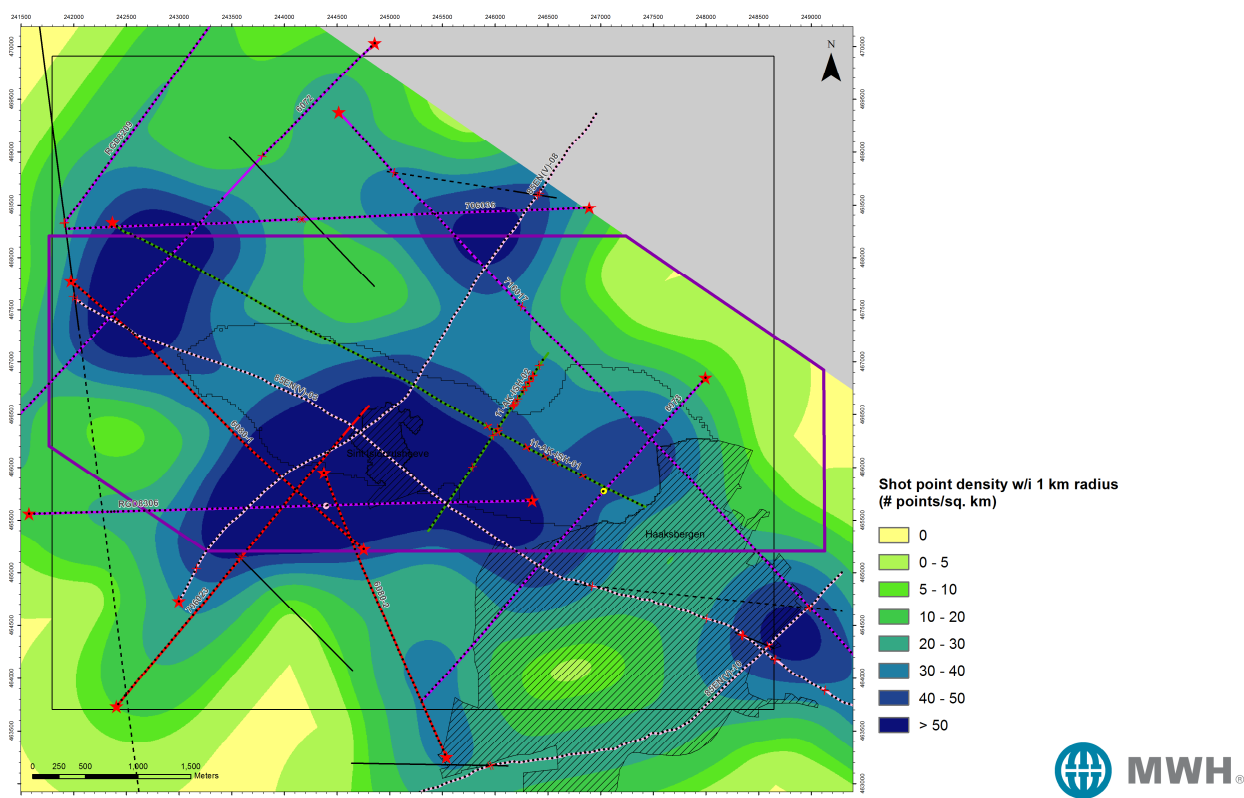


Figure 5.13: Shot point density for the top Zechstein Z1 Halite model.

### 5.9.3 Source data reliability

The reliability of the models also depends on the reliability of the source data. Less reliable source data result in less reliable modeling results. The reliability of the model input data is not uniform.

First, not every seismic line is of the same quality. The newly acquired seismic lines 11-AK-ISH-01 and 11-AK-ISH-02 were specifically acquired to obtain more information about the salt deposits in this area. The quality of these lines are therefore optimal for our purposes and have an average error of approximately 10 m. As discussed in the previous study (MWH, 2008b), seismic lines 85EN(V)-03 and 85EN(V)-08 that diagonally cross the Haaksbergen area of interest are high quality lines, as is line 85EN(V)-10, with an average error of approximately 10 m. Seismic lines 706023, 6080-1 and 6080-2 have poor coverage resulting in low quality source data. All other seismic lines are of average quality (see Figures 5.12 and 5.13 and Appendices XXII and XXIII).

The quality of the source data also varies within a single seismic line. First, seismic interpretations of horizons are less reliable in areas where this (or an overlaying) layer (steeply) slopes as less energy is reflected to the surface. The reliability of seismic data on the highest quality lines (+/- 10 m) can be reduced significantly in steeply sloping areas. Also, the seismic information at the end of seismic lines (loose ends) is less reliable. Note that not each end of a seismic line in the Haaksbergen area of interest is a loose end. Some seismic lines are interpreted partially because only part of the line runs through the area of interest or shot points at the end of a line were removed before modeling as they were deemed not reliable (see section 5.4). Finally, shot point values near fault zones are less reliable.

#### **5.9.4 Calculated thickness**

All factors described above impact the quality and the reliability of the models of the individual geological horizons separately. As the model of the thickness of the Zechstein Z1 Halite was created by subtracting two models (i.e. top and base of the Zechstein Z1 Halite horizons) this model displays the combined modeling anomalies of the two source models and is less reliable than either of the source models. The same is true for the model of the thickness of the overlying Zechstein Z2-Z4 deposits.



## 6 Resources and reserves

### 6.1 Introduction

Mineral deposits can be classified based upon the amount of information available describing these deposits and the economic value of the deposits.

The term *mineral occurrences* is used to signify known occurrences of minerals which are of geological interest but which may or may not be of economic interest.

*Mineral resources* indicate geological deposits of minerals that are potentially of economic interest and that have been examined to some degree to determine their quality. *Indicated mineral resources* are mineral resources of economic interest which have been minimally investigated so a very approximate estimate can be made of the quality and quantity of the mineral resources. *Measured mineral resources*, meanwhile, are indicated resources that have undergone sufficient investigation, as judged by an expert, to establish an acceptable estimate of mineral quality and quantity.

Finally, *mineral reserves* are resources that are known to be both economically and technically feasible for extraction (i.e. minable). The terms *probable reserves* and *proven reserves* are used in a manner similar to indicated and measured resources as discussed above.

Figure 6.1 shows this classification according to the International Reporting Template for the Public Reporting of Exploration Results, Mineral Resources and Mineral Reserves van de Committee for Mineral Reserves International Reporting Standards (CRIRSCO).

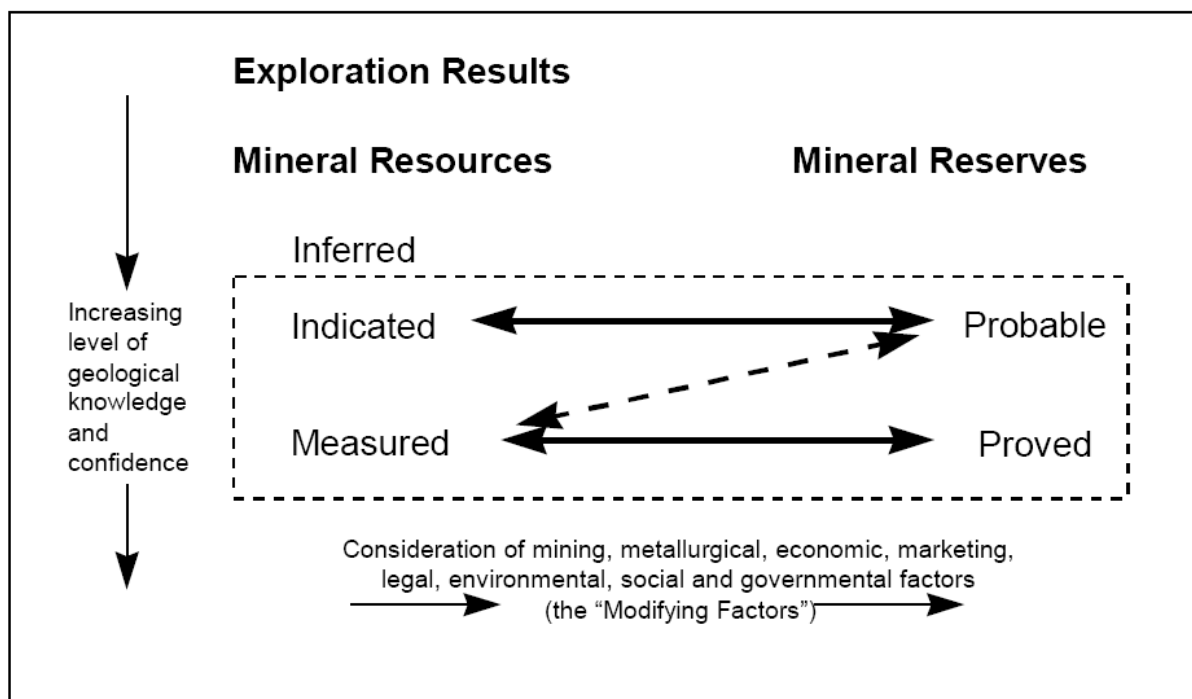


Figure 6.1: Schematic visualization of the relation between mineral resources and mineral reserves according to the International Reporting Template for the Public Reporting of Exploration Results, Mineral Resources and Mineral Reserves van de Committee for Mineral Reserves International Reporting Standards (CRIRSCO).

In this chapter we categorize the modeled salt deposits in the Haaksbergen area of interest according to this classification, using the models of the various geological horizons and the thickness of the Zechstein Z1 Halite deposits.

For determining the reserves, i.e. potentially extractable salt volumes, several technical criteria and safety regulations are being used to calculate the maximum cavern height for each of the caverns within a technically feasible cavern grid. Surface restrictions as known from MWH's 2008 spatial planning study are also considered.

## 6.2 Salt resources

### 6.2.1 Introduction

Zechstein Z1 Halite resources in the Haaksbergen area of interest are defined as the total volume of the modeled Zechstein Z1 Halite deposits within the Concession area Isidorushoeve. No safety regulations are taken into consideration. With respect to the surface situation that may put restrictions on the accessibility of the resources, resources beneath developed areas are excluded from the total amount of salt resources.

The following definitions are being used to determine the measured and indicated resources, based on the distance to seismic surveys and exploration boreholes acquired specifically for the purpose of salt mining:

Distance to seismic data and boreholes	Resources
>60 m	Indicated
<60 m	Measured

The 60 meter boundary is based on the cavern radius of 62.5 m (see further on). By defining this distance for the measured resources, AkzoNobel is assured that caverns placed within this zone will be successful as the continuity of the Zechstein halite has been proved by explorational research focused on salt mining.

Figure 6.2 (Appendix XXIV) shows the boundary (cyan outline) of the concession area for which Zechstein Z1 Halite resources are calculated and shows the developed areas of Sint Isidorushoeve and Haaksbergen within the concession area.

### 6.2.2 Indicated and measured Zechstein Z1 Halite resources

Zechstein Z1 Halite resources are calculated by multiplying the modeled thickness of the Zechstein Z1 Halite within the entire Concession area Isidorushoeve, not taking any minimum thickness criteria or safety regulations into account, but excluding those resources that are located directly underneath developed areas. Measured resources are located within 60 m of seismic surveys and exploration boreholes acquired specifically for the purpose of salt mining, indicated resources are located outside this buffer.

Results of this calculation are presented in Table 6.1.

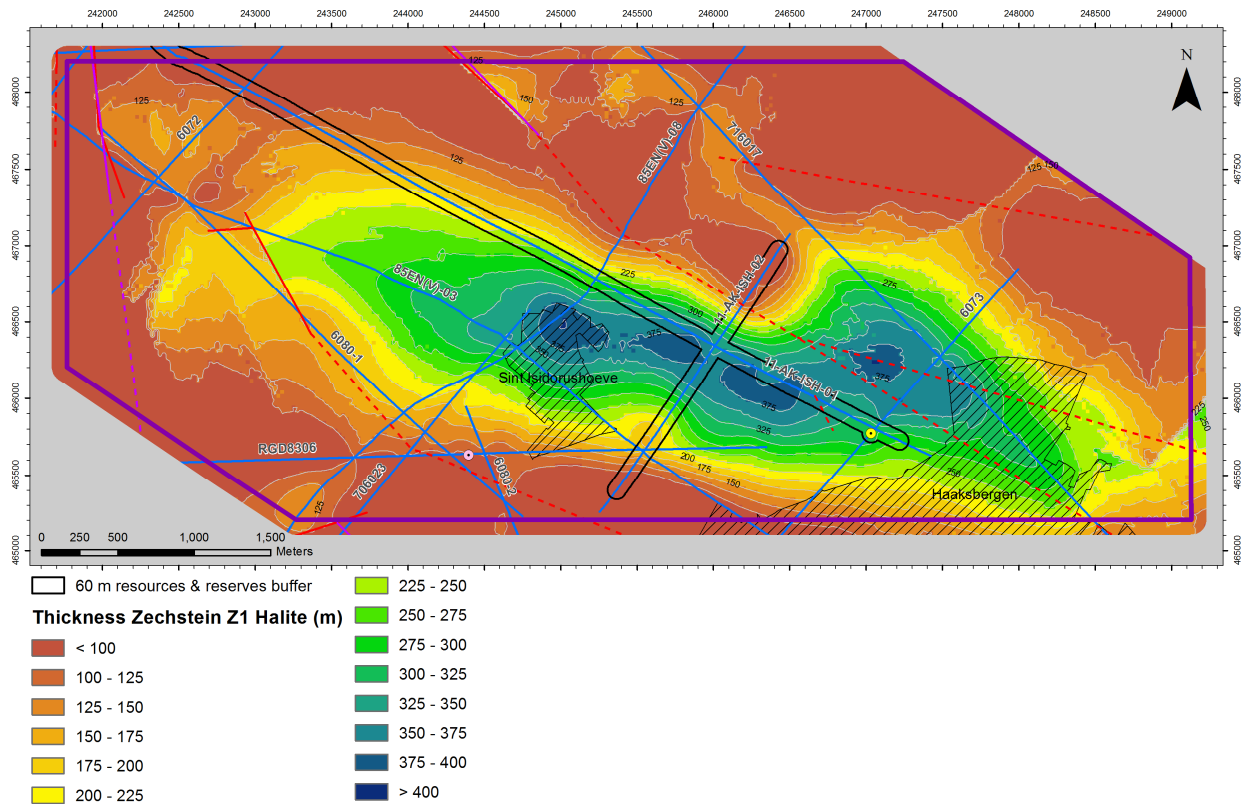


Figure 6.2: Zechstein Z1 salt thickness within the concession area for which Zechstein Z1 Halite resources are calculated, the developed areas of Sint Isidorushoeve and Haaksbergen within the concession area and indication of the 60 m buffer around seismic surveys and exploration boreholes acquired specifically for the purpose of salt mining.

Table 6.1: Indicated and measured Zechstein Z1 Halite resources in the Concession area Isidorushoeve (assuming a salt density of 2.155 tonnes/m<sup>3</sup>).

Zechstein Z1 Halite resources	10 <sup>6</sup> m <sup>3</sup>	10 <sup>6</sup> tonnes
Indicated Zechstein Z1 Halite resources	X,XXX	X,XXX
Measured Zechstein Z1 Halite resources	XXX	XXX
Total (indicated + measured) Zechstein Z1 Halite resources	X,XXX	X,XXX

### 6.2.3 Zechstein Z1 halite resources scenarios

Zechstein Z1 Halite resources can also be calculated for different minimum Z1 halite thickness scenarios. For example, the minimum 200 m thickness resources mean the total amount of salt, located within the area with a minimum salt thickness of 200 meter, excluding developed areas.

When applying the minimum salt thicknesses, isolated salt deposits falling within the thickness limits may arise not located in a contiguous salt pillow. This happens at a minimum thickness of 200 meters and at thicker limits. From a thickness limit of 200 m onwards, isolated thick salt spots have therefore been removed from the resources. Table 6.2 shows the resources (summed total of indicated and measured) for several minimum salt thicknesses.



## 6.3 Salt reserves

Obviously, not all Zechstein Z1 Halite resources within the Concession area Isidorushoeve can be extracted due to safety regulations, technical reasons and economic considerations.

In this section we apply these restrictions to the salt resources within the Concession area Isidorushoeve to determine the reserves. The distinction between proven and probable reserves is based on the distance to seismic surveys and exploration boreholes acquired specifically for the purpose of salt mining again:

Distance to seismic data and boreholes	Reserves
>60 m	Probable
<60 m	Proven

The 60 meter boundary is based on the cavern radius of 62.5 m (see further on). By defining this distance for the proven reserves, AkzoNobel is assured that caverns placed within this zone will be successful as the continuity of the Zechstein halite has been proven by exploratory research focused on salt mining.

### 6.3.1 Mining engineering and safety restrictions

Based on their salt mining engineering experience and safety regulations AkzoNobel has defined the parameters for the most probable future mining scenario, leading to the cavern design in Figure 6.3:

#### Hanging wall safety pillar

The hanging wall of the potential cavern should consist of at least 70 meters of Zechstein Z1 salt to create a thick enough salt roof to assure the stability of the cavern (IfG, 2009). The eventual thickness of the overlying Z2 to Z4 Zechstein deposits, mainly consisting of anhydrites, dolomites and some halite, is not taken into account.

#### Footwall safety pillar

The footwall of the potential cavern should consist of at least 10 meters of Zechstein Z1 salt to create a thick enough bottom to assure the stability of the cavern (IfG, 2009).

#### Minimum salt thickness / minimum cavern height

A minimum Zechstein Z1 salt thickness of 200 meters is assumed. Taking the footwall and hanging wall criteria into account, this means a minimum desired cavern height of 120 meters.

#### Cavern diameter

A cavern diameter of 125 meters is assumed, meaning a cavern radius of 62.5 meters (DEEP, 2010).

#### Cavern grid

The cavern grid is created using the following parameters: hexagonal grid with a 300 m distance between the centers of caverns (IfG, 2009). As a cavern diameter of 125 meters is used, this results in 175 m thick safety pillars between the caverns.

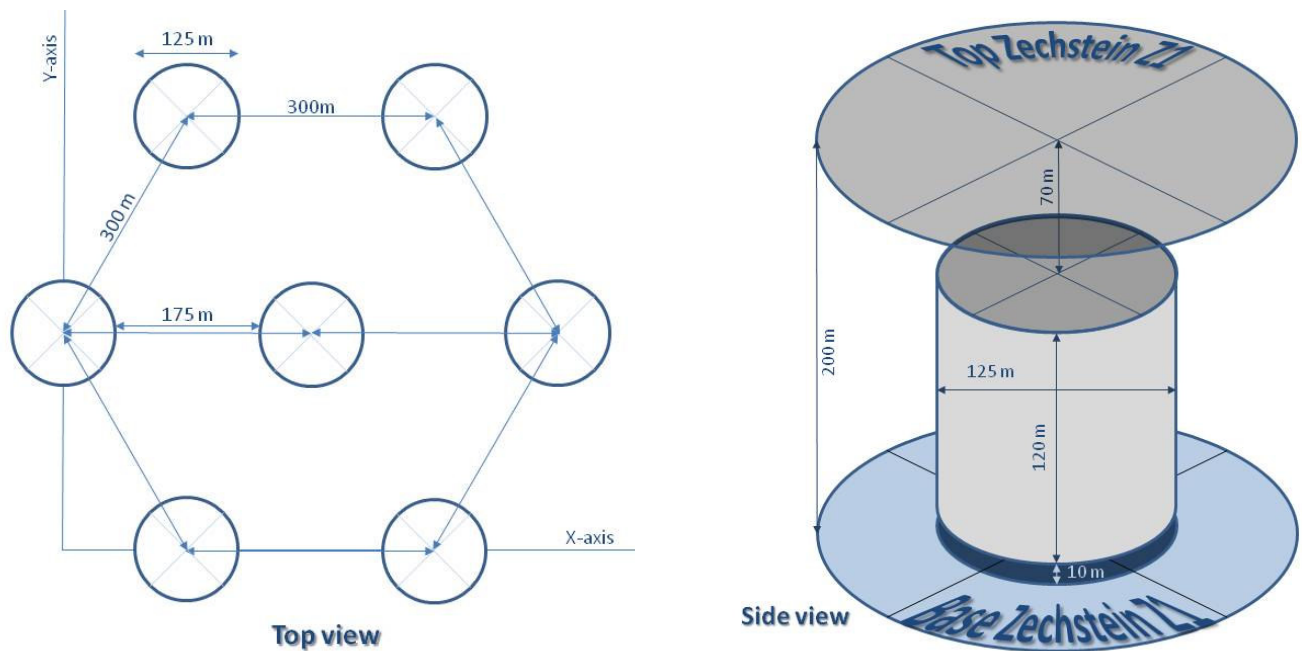


Figure 6.3: Mining engineering and safety restriction cavern parameters, top view and side view (based on IfG, 2009 and DEEP, 2010)

### 6.3.2 Calculation of reserves

The volume of each cavern can be measured by calculating the height of each cavern (being the Zechstein Z1 thickness minus 80 m, so at least 120 meters, but much more within the thicker parts of the salt pillow) and multiplying this by the cavern area:

$$\text{Volume} = \pi \cdot (62,5)^2 \cdot (\text{Zechstein Z1 Halite thickness} - 80 \text{ m})$$

This volume is multiplied with a factor of 0.8 to account for any insoluble material and for non-optimal leaching (DEEP, 2010).

### 6.3.3 Optimal configuration of the cavern grid

The cavern grid described above can be placed on the reserves area (i.e. the area with over 200 m of salt thickness outside the developed areas) in many different ways, each leading to a slightly different volume of minable salt. It has been decided to find an optimal cavern grid configuration based on the geological situation, i.e. a configuration in which as much as possible salt is being mined from the reserves area, not taking into account the location of seismic surveys and exploration boreholes acquired specifically for the purpose of salt mining.

This was done by trial-and-error analysis. It can be proven that it is more efficient to maximize the number of caverns that are placed within the reserves area, than to maximize the volume of individual caverns. This is logical as one extra cavern immediately enlarges the total cavern volume with at least **x.xx** million m<sup>3</sup> (as a cavern located at the 200 m thickness boundary will have a height of 120 meters immediately) while an optimization of a cavern location to assure 10 m of extra cavern height only enlarges the volume of that cavern with 120,000 m<sup>3</sup>. In other words, you need to enlarge the height of **xx** caverns all with 10 meters to compensate for only one extra cavern located at the 200 meters Zechstein Z1 Halite thickness boundary.

Dip angles for the base of the Zechstein Z1 Halite are much less steep and within the salt pillow area steep angles only occur close to the northern tip of seismic line ISH-02. Other steep dip angles are related to fault zones at more distinct parts of the area.

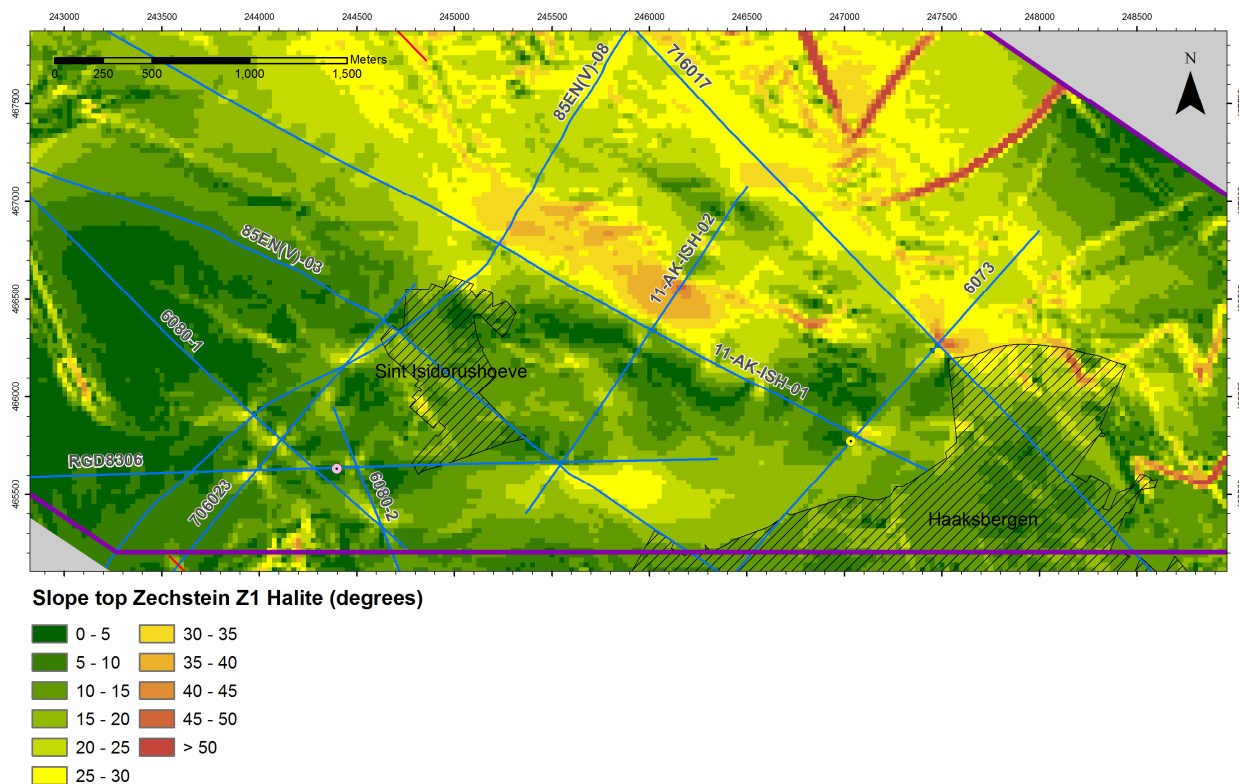


Figure 6.5: Calculated dip angle of the top of the Zechstein Z1 Halite within the concession area.



## 7 Hydrocarbon risks

### 7.1 Introduction

PanTerra Geoconsultants BV has evaluated the hydrocarbon risks of the Haaksbergen Salt Pillow in advance of the planned Isidorushoeve-1 Exploration Well (ISH-01)<sup>5</sup> and has evaluated the blow-out potential of this well in particular<sup>6</sup>. In general the chance of finding hydrocarbons in the salt pillow structure is considered small (less than 5%). Nevertheless, the possibility of encountering hydrocarbons and other gases (H<sub>2</sub>S) during mining activities (especially when drilling new exploitation wells) is a major concern for AkzoNobel as this is an important aspect for the Dutch State Supervision of Mines (SodM) when allowing mining activities.

In this chapter we start with a general discussion about hydrocarbon risks, followed by a summary of the main results of the PanTerra studies. Based on these results we will focus on some critical aspects of the newly gained insight in the salt pillow structure gained during this seismic study and subsequent geological modeling with respect to hydrocarbon risks.

### 7.2 General discussion of hydrocarbon risks within the study area

The chance of encountering hydrocarbons when drilling is determined by the chance of finding a reservoir times the chance of having a trap (i.e. a structure and a seal) times the change of having an active hydrocarbon system.

Within the study area there are two potential hydrocarbon systems: the Zechstein hydrocarbon system and the Carboniferous hydrocarbon system.

#### **The Carboniferous hydrocarbon system**

During the Carboniferous, coals and carbonaceous shales have been formed during the Namurian and the Westphalian. Gas from these source rocks may have been trapped in shallower reservoirs, like the Carboniferous Tubbergen sandstone, which is being exploited near Tubbergen, several kilometers north of the Haaksbergen area of interest, or in the early Permian Upper Rotliegend sandstone, just beneath Zechstein deposits.

#### **The Zechstein hydrocarbon system**

Also within the Zechstein, potential hydrocarbon source rocks may have been formed, being the Z2 and Z3 Carbonates mainly. Within these Zechstein deposits the Z2 Hauptdolomite and the Z3 Plattendolomite are the main potential source rocks, containing potentially bituminous limestone and dolomite. As these are located directly underneath Z2 and Z3 anhydrites and/or salts, these source rocks might act as reservoirs as well with porosities of over 10%.

---

<sup>5</sup> Evaluation of the hydrocarbon risk and associated volumes in the Z1 and Z2 Carbonates over the Haaksbergen Salt Pillow, PanTerra Geoconsultants BV, Report No. G791, February 2010.

<sup>6</sup> Evaluation of the Blow-out Potential of the Z1 and Z2 Carbonates in the Planned Salt Exploration Well Isidorushoeve-1 (ISH-01), PanTerra Geoconsultants BV, Report No. G824, August 2010 & Evaluation of some questions on the drilling program for exploration well Isidoris hoeve - 1 (ISH-01), PanTerra Geoconsultants BV, Report No. G824\_bis, 30 September 2010.

## **7.3 Main results of the PanTerra hydrocarbon and H<sub>2</sub>S risk evaluations**

### **7.3.1 The Zechstein hydrocarbon system**

#### **Source rock potential**

The carbonates of the Plattendolomite and the Hauptdolomite are reported to be bituminous. Because of the interaction of hydrocarbons and anhydrite, which occurs above, within and below the reservoir, H<sub>2</sub>S might be present as well, as is reported in well HKS-01.

Nevertheless, in none of the studied wells (HKS-01, HEN-01 and HGV-01) maturities within the Zechstein carbonates are sufficient to have generated liquid hydrocarbons. Therefore Zechstein source rocks are considered not mature of hydrocarbon generation within the study area and the chance of the source being mature is estimated to be close to zero and the chance of having an active hydrocarbon system is estimated to be close to zero too (about 5%).

#### **Reservoir potential**

From well data (HKS-01 and HGV-01) Panterra concludes that only the lower part of the Z3 Plattendolomite is developed as a porous carbonate (porosity 10-15% within well HGV-01). Both within the HKS-01 and the HGV-01 wells, losses have been observed pointing at either fractures or a vuggy development of the reservoir.

The Z2 Hauptdolomite is developed as dolomite, although in well HKS-01 Carbonates are reported. The chance of having a good Zechstein reservoir is estimated at 90%.

#### **Seal and trap**

Z2 and Z3 anhydrites and salts ensure sealing of the Plattendolomite and Hauptdolomite carbonate intervals, and also the lower part of the Lower-Buntsandstein, being shaly developed, might act as a seal. Tectonical disturbance (faults and fractures) might lower the sealing capacities. As hydrocarbon shows occur in the anhydrites, it is assumed that at least locally the seal is not perfect.

Average thicknesses of the seal are about 53 m for the Z3 Plattendolomite and between 38 and 46 m for the Z2 Hauptdolomite.

The presence of a trap for the Plattendolomite and Hauptdolomite is well defined as Z2 and Z3 anhydrites and salts more or less form a drape over the Haaksbergen salt pillow.

Sealing properties might have been adversely affected by the extensional stress regime within the reservoir and the seal during formation of the salt pillow. Extensive fracturing is expected above the thickest parts of the salt pillow and also over the culmination of the structure some faulting may be observed, that might even place the shallowest parts of the Z3 Plattendolomite against the overlying Lower-Buntsandstein.

The chance of having a good seal for the Zechstein petroleum system is therefore estimated at 25%.

#### **Risk calculation**

The chance of having liquid hydrocarbons in the Haaksbergen salt pillow structure is estimated to be 1.13% ( $0.9 * 0.25 * 0.05$ ).

### **7.3.2 The Carboniferous hydrocarbon system**

#### **Source rock potential**

Coals and carbonaceous shales within the area potentially are good source rocks, mainly for gas. Nevertheless, the Carboniferous is observed to be just about mature enough for the generation of liquid hydrocarbons, but not sufficient to have caused active migration of hydrocarbons. Further northeast near De Lutte gas is being produced from the Carboniferous, but there burial depths have been considerably higher as this area is located on the other side of the Gronau fault zone and towards the center of the Lower Saxony Basin.

Therefore the chance of having an active hydrocarbon system is estimated to be close to zero (less than 5%).

#### **Reservoir potential and seal**

Potential reservoirs may be found within the Zechstein carbonates (see the Zechstein hydrocarbon system) and in sandstones beneath the Zechstein deposits. For reservoir and trap the chances therefore are the same as described above for the Zechstein hydrocarbon system, but seal chances are even smaller as a better seal is required for holding gas.

As thick Zechstein Z1 halite deposits are found in-between the Carboniferous source rocks and the potential Zechstein reservoirs, the chance that hydrocarbons have migrated to these reservoirs is low.

Furthermore no gas related seismic anomalies have been observed in studied seismic lines (excluding lines ISH-01 and ISH-02 which were not yet shot when PanTerra studied the hydrocarbon risk.

#### **Risk calculation**

The chance of having gas (both from the Zechstein and the Carboniferous hydrocarbon systems) in the Haaksbergen salt pillow structure is estimated to be approximately 1%.

## **7.4 Further evaluation of hydrocarbon and H<sub>2</sub>S risks**

### **7.4.1 Introduction**

From the PanTerra studies it can be concluded that mainly the Z2 and Z3 carbonates may offer some, although small, risks of encountering hydrocarbons when drilling for salt. One of AkzoNobels strategies is to have the first wells located where risks are assumed to be highest, meaning that some heavy blow-out measures are necessary. When no hydrocarbons are encountered at these locations it can be assumed that the hydrocarbon risk at other locations is zero and less measures will be necessary for further drillings.

Therefore it is important to identify those areas located within the reserves area that may provide the highest risks of encountering hydrocarbons.

### **7.4.2 Top Zechstein structural highs**

Figure 7.1 shows a geological west-east cross-section drawn by PanTerra, indicating the potential Zechstein Z2 and Z3 reservoirs located in the high above the Haaksbergen salt pillow. From this it becomes clear that highs, both local and regional, play an important role in the chance of encountering hydrocarbons.

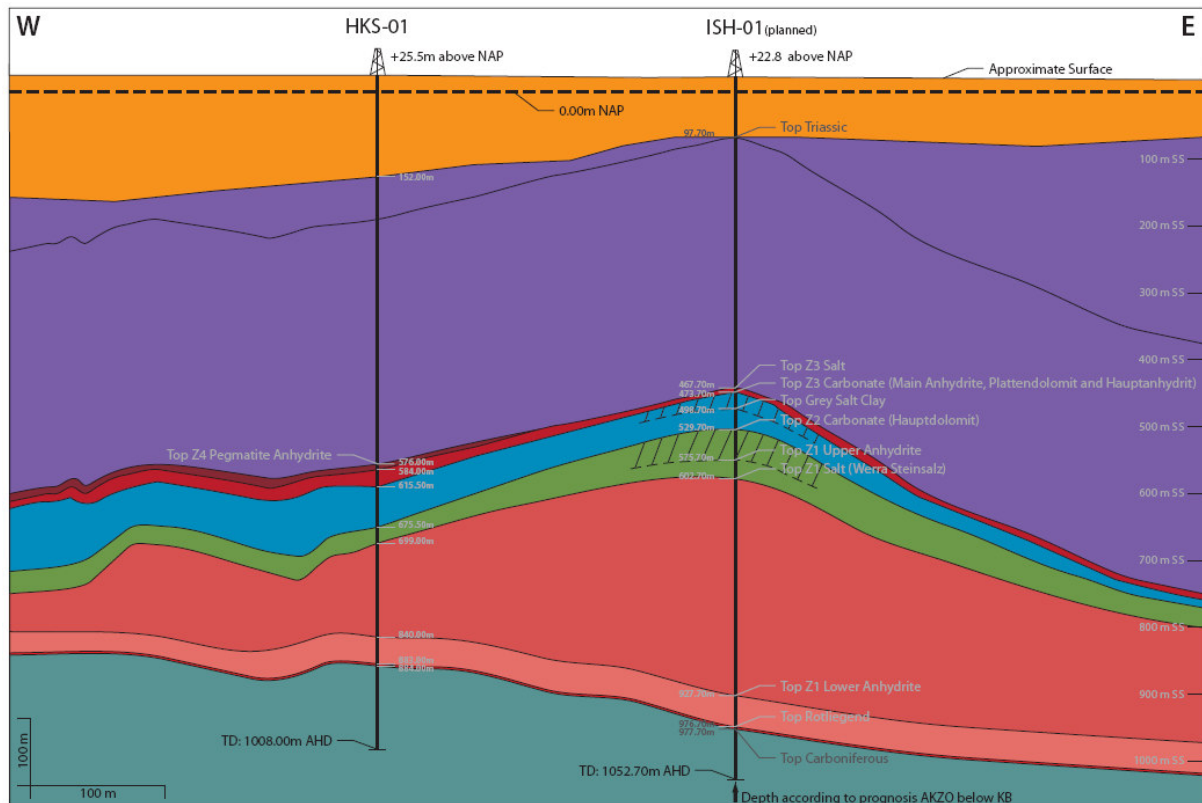


**Figure 7.1: Geological west-east cross-section indicating the potential Zechstein Z2 and Z3 reservoirs located in the high above the Haaksbergen salt pillow (PanTerra, 2010b).**

Local highs in the Zechstein Z2 and Z3 carbonates can be determined by combining the slope of the base of the Triassic (which is more or less indicative for the slope of the Z2 and Z3 deposits) with the depth of the base of the Triassic (which is more or less indicative for the depth of the Z2 and Z3 deposits). Notice that thicknesses of the Z2 and Z3 deposits are assumed to be more or less constant. Figure 7.2 shows a map of the slope of the base of the Triassic, combined with isopachs for the depth of the base of the Triassic. This map can also be found in Appendix XXX. Areas with a slope less than 2.5° are considered (sub)horizontal and are indicated purple. The reliability of this map is much higher within the 200 m Z1 Halite thickness area than outside this area. Figure 7.3 shows the depth of the top of the Zechstein.

Both local base Triassic summits (at depth of less than 400 m), located underneath the village of Sint Isidorushoeve and just southeast of the intersection of seismic lines ISH-01 and ISH-02, coincide with (sub)horizontal areas. Furthermore the area in-between these summits shows a narrow elongated ridge at a depth in-between 400 and 425 m, with a slope near 0° exactly at the crest. Other spots within the 200 m Z1 halite thickness area where the slope is (sub)horizontal are located further west (just west of Sint Isidorushoeve) and further east (northwest of exploratory well ISH-01), but here the depth of the base of the Triassic is between 450 and 475 m.



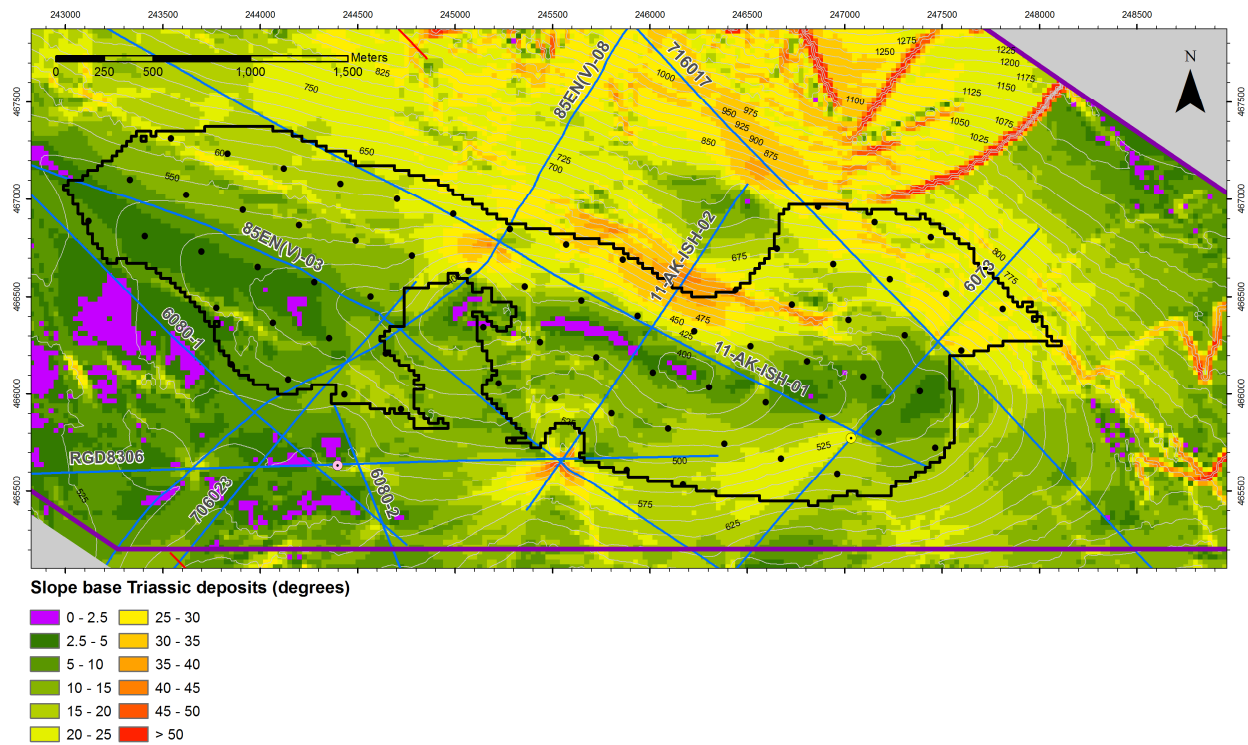


Figure 7.2: Map of the slope of the base of the Triassic, combined with isopachs for the depth of the base of the Triassic and with potential cavern locations as determined in chapter 7.

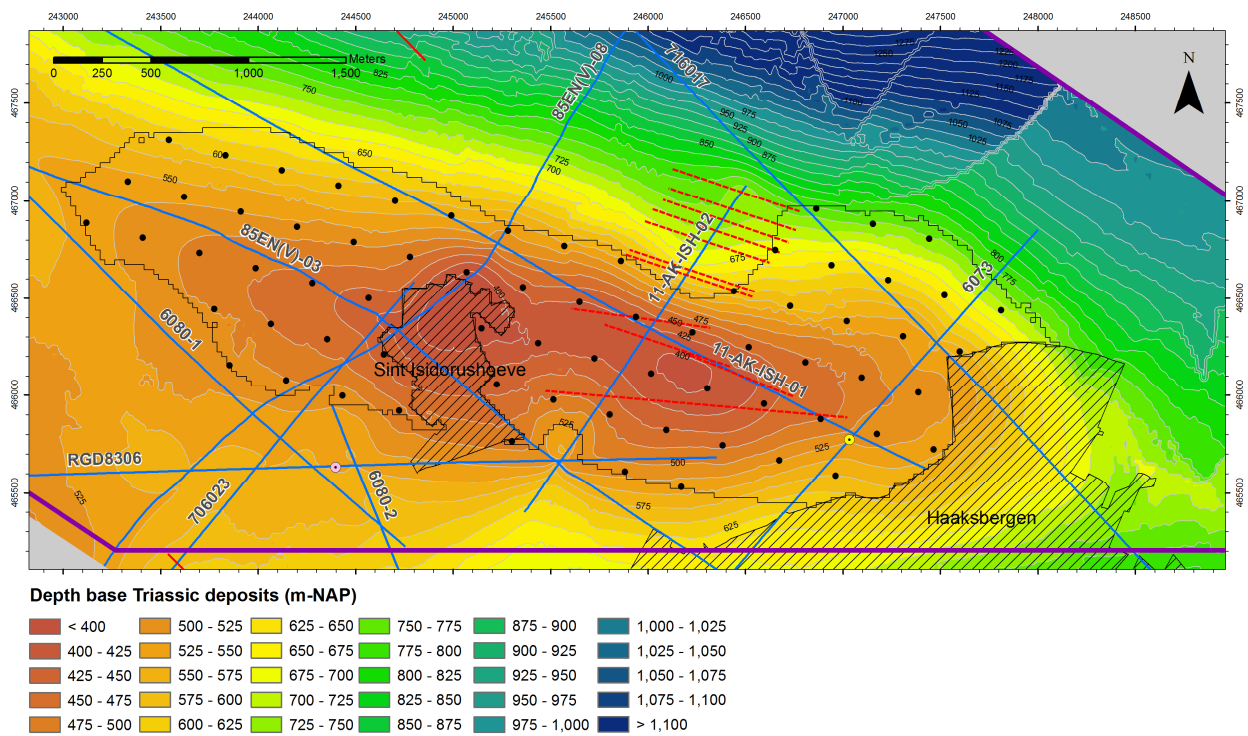


Figure 7.3: Map of the depth of the base of the Triassic (top Zechstein) with potential cavern locations as determined in chapter 7 and with estimated faults related to the top of the salt pillow.

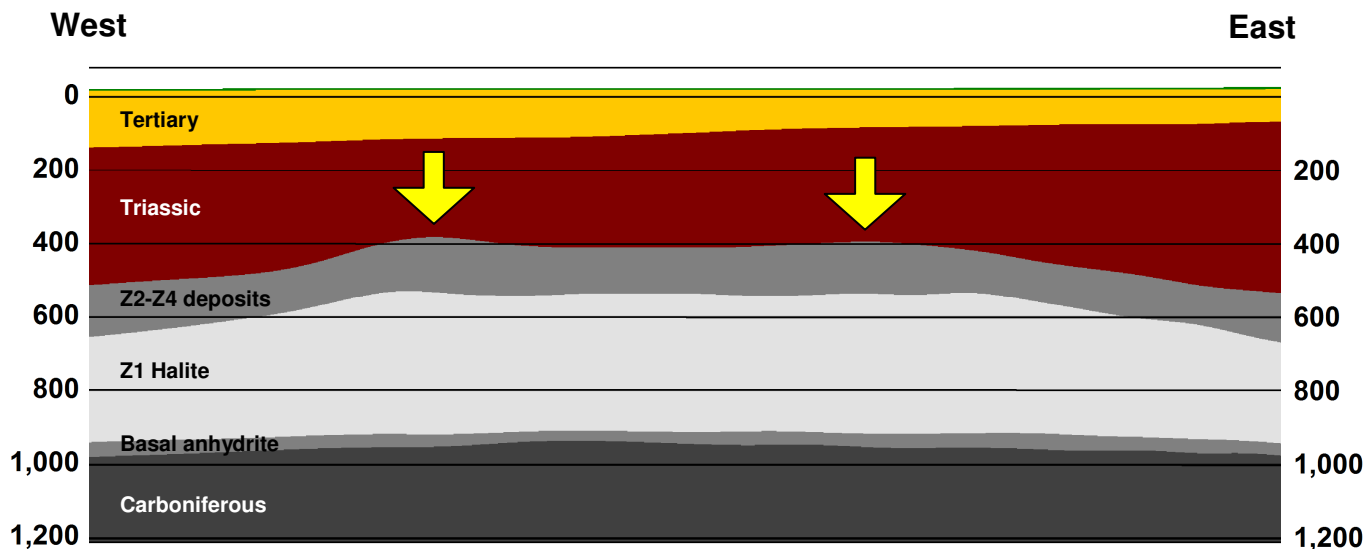


Figure 7.4: Middle part of the longitudinal west-east profile, clearly showing the two local highs in the top Zechstein deposits and the high crest in between. Note that the highs in the top of the Zechstein do not exactly coincide with the highs in the top Z1 Halite.

As a consequence mainly the two summits and the crest in-between can be considered as well locations with a (slightly) higher hydrocarbon and H<sub>2</sub>S risk. This can also be seen in the longitudinal profile, that clearly shows the two summits. Figure 7.4 shows these summits in the profile.

### 7.4.3 Top Zechstein faults

Within the concession area, some top Zechstein faults have been observed in the seismic lines, located above the Haaksbergen salt pillow. These faults may provide local highs and may provide pathways from the potential Zechstein Z2 carbonate source rocks to overlying strata. Figure 7.5 gives examples of local highs in the Zechstein deposits and of pathway creating faults in seismic line ISH-01.

Figure 7.3 shows the estimated locations and directions of faults observed in seismic lines ISH-01 and ISH-02. The group of faults seen in profile ISH-01 (see Figure 7.5) is assumed to be (sub)parallel to the seismic line itself, causing multiple intersections of this fault line with the seismic line. In seismic line ISH-02 the number of intersecting fault lines is much less, at least close to the intersection with ISH-01. Further north many faults related to the steep northern flank of the salt pillow are observed and a single fault is observed south of the crest of the salt pillow.

The faults above the Z1 salt pillow are assumed to be related to extensional stresses that occurred during the formation of the salt pillow. Although this formation (due to halokinesis) is compression related itself (Subhercynian tectonic phase; Geluk, 2005; see section 2.3.4), the stresses above the growing salt pillow should have been extensional, due to the massive uprising of the salt (see Figure 7.6).

West

East

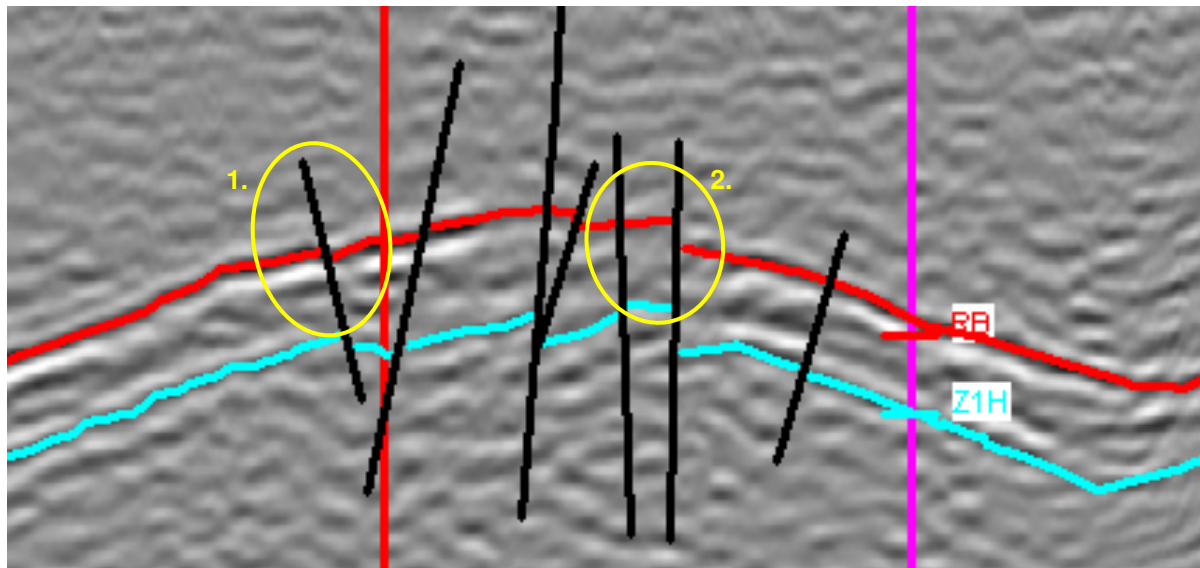


Figure 7.5: Depth profile of seismic line ISH-01 with indicated faults that might lead to local highs in the Zechstein deposits or create pathways for hydrocarbons to migrate to shallower reservoirs

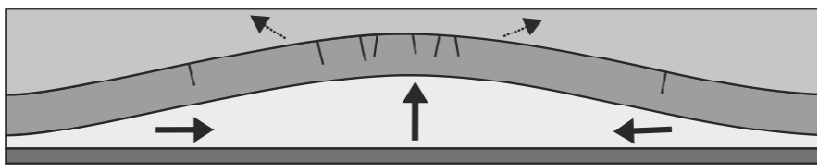


Figure 7.6: Schematic overview showing faulting in the overlying strata as a result of salt movement

#### 7.4.4 Seismic anomalies

As was stated by PanTerra, the presence of gas, as might be available from the Carboniferous hydrocarbon system, usually gives rise to seismic amplitude anomalies. Within the previously studies seismic lines, no such anomalies have been observed (Panterra, 2010a). Also within the newly shot seismic lines no such anomalies were visible.

#### 7.4.5 Conclusions

From this we can conclude that the highest risks of encountering hydrocarbons are located near the highs in the top of the Zechstein. As one of these locations is located directly beneath Sint Isidorushoeve, where no caverns are proposed, mainly the eastern local summit is of interest for locating the first well. The crest in-between these two summits forms a second potential high risk location. Finally the area where seismic lines ISH-01 and ISH-02 intersect can be identified as a high risk area, as faulting may have lead to local highs here.



## References

- Adrichem Boogaert, H.A. van and Kouwe, W.F.P. (compilers), 1993. Stratigraphic Nomenclator of the Netherlands, revision and update by RGD and NOGEPa, Mededelingen Rijks Geologische Dienst, 50.
- Buggenum, J.M. van, and D.G. den Hartog Jager, Silesian. In: Geology of the Netherlands. Royal Netherlands Academy of Arts and Sciences, 2007: p. 43-62.
- Dalfsen, W. van et al., 2006. VELMOD-1, Joint Industry Project. TNO report 2006-U-R0037/B.
- DEEP, 2010. Development of a new Brine Cavern Field for the Hengelo Salt Plant: Basic Leaching Concept and Development of the Haaksbergen Site.
- Dinoloket, TNO Utrecht : Geologische kaarten van de Diepe Ondergrond van het Nederlandse territoir Fase 1 (NCP-1) 2006.
- DMT, 2011a. Field report 2D seismic Isidorushoeve 2011. Reflection seismic vibroseis. In the area of Sint Isidorushoeve, The Netherlands. Project number: EG-EI-11-046. By: Swoboda, U., Nowaczek, S., Lukas, W. and Brenner, O.
- DMT, 2011b. Processing report 2D seismic Isidorushoeve 2011. Reflection seismic vibroseis. In the area of Isidorushoeve and Hengelo, The Netherlands. Project number: EG-EI-11-046. By: Brenner, O. and Rybarczik, G.
- Duin, E.J.T. et al., 2006. Subsurface structure of the Netherlands –result of recent on and offshore mapping. Netherlands Journal of Geosciences - Geologie en Mijnbouw, 85-4, pp. 245 -276.
- Geluk, M.C., 2005. Stratigraphy and tectonics of Permo-Triassic basins in the Netherlands and surrounding areas. PhD Thesis.
- Geluk, 2011. Website: [http://home.kpn.nl/mark.geluk/Salt\\_Index.htm](http://home.kpn.nl/mark.geluk/Salt_Index.htm)
- Geo-logic consulting services B.V., Hengelo Survey, 1988, Ordernr. 30-75321 (on behalf of AkzoNobel Chemicals BV).
- IfG, 2009. Rock Mechanical Investigation and Dimensioning for the new AkzoNobel NaCl-Bine Production Field Haaksbergen.
- Jager, J. de, 2003. Inverted basins in the Netherlands, similarities and differences. Netherlands Journal of Geosciences / Geologie en Mijnbouw 82 (4): 355-366.

Jager, J. de, 2007. Geological development. In: Geology of the Netherlands. Royal Netherlands Academy of Arts and Sciences, 2007: p. 5-26.

Kockel, F., 2003. Inversion structures in Central Europe – Expressions and reasons, an open discussion. Netherlands Journal of Geosciences / Geologie en Mijnbouw 82 (4): 367-382.

Mulder, F.J. de et al., 2003. De ondergrond van Nederland. Wolters-Noordhoff bv Groningen/Houten. The Netherlands.

MWH, 2007a. Toekomstscenario's zoutwinning Twente. Koopmans, T.P.F. and J. Wanders (in Dutch).

MWH, 2007b. Verbetering ondergrondmodel Röt- en Zechsteinzout Akzo Nobel, Twente. By: Koopmans, T.P.F. (in Dutch).

MWH, 2008a. Evaluatie Target Areas en mogelijkheden nader onderzoek ondergrond Twente. By: Koopmans, T.P.F. (in Dutch).

MWH, 2008b. Study of the salt mining possibilities in the Haaksbergen area of interest, the Netherlands, By: Koopmans, T.P.F. and Broos, M.J.

MWH, 2008c. Assessment of surface situation regarding AkzoNobel salt mining in the municipality of Haaksbergen.

MWH, 2010. Salt mining possibilities in areas adjacent to the Hengelo brine field. By: Koopmans, T.P.F. and Broos, M.J.

Oranjewoud, 2007. Ruimtelijke verkenning zoutwinning in Twente, projectnr. 64872-87. By: Wind, E. (in Dutch).

PanTerra Geoconsultants BV, 2010a. Evaluation of the hydrocarbon risk and associated volumes in the Z1 and Z2 Carbonates over the Haaksbergen Salt Pillow, Report No. G791.

PanTerra Geoconsultants BV, 2010b. Evaluation of the Blow-out Potential of the Z1 and Z2 Carbonates in the Planned Salt Exploration Well Isidorushoeve-1 (ISH-01), PanTerra Geoconsultants BV, Report No. G824, August 2010

PanTerra Geoconsultants BV, 2010c. Evaluation of some questions on the drilling program for exploration well Isidoris hoeve - 1 (ISH-01), PanTerra Geoconsultants BV, Report No. G824\_bis.

Respec, 2006. Geological characterization of the Upper Germanic Trias (Röt) and Zechstein salt members in the vicinity of the Hengelo salt production plant, Topical report RSI-1868.

Rider, M., 2002. The geological interpretation of well logs. Rider-French consulting Ltd. 2<sup>nd</sup> edition.

Rijks Geologische Dienst, Prognose van de boring “Hengevelde-1” (zuidelijk Twente). Januari 1985, rapport no GB2032.

T&A Survey BV, 2007. Seismische interpretatie van de diepe ondergrond rondom de zoutwinningsgebieden in Hengelo. Projectnummer: 0507-GPR 1191.

T&A Survey BV, 2008. Seismic interpretation of salt deposits in the subsurface of the region Haaksbergen in the Netherlands. Projectnummer: 0408 GPR1410/0708gpr1410.1.

T&A Survey BV, 2009. Seismic interpretation of Röt salt deposits in the subsurface of the region Hengelo Enschede in the Netherlands. Projectnummer: 0309-OEM1623.

T&A Survey BV, 2011a. Rapportage betreffende analyse van de Sonic log van de proefboring naar de Haaksbergen zoutstructuur. Projectnummer: 0211-OEM2444.

T&A Survey BV, 2011b. Seismic interpretation of the subsurface salt deposits in the concession Isidorushoeve. Project number: 0911-OEM2510. By: Stegers, D.

TNO, 1998. Geological Atlas of the Subsurface of the Netherlands- Onshore. Blad X: Almelo-Winterswijk.

TNO, 2004. Geological Atlas of the Subsurface of the Netherlands – Onshore.

Wong, T., Batjes, D.A.J. and J. de Jager, 2007. Geology of the Netherlands. Royal Netherlands Academy of Arts and Sciences.

Ziegler, P.A., 1978. North-Western Europe: Tectonics and Basin Development, Geologie en Mijnbouw 57 (4), p. 589-626





## Appendices

Appendix I:	Survey area and all geophone- and source positions
Appendix II:	All figures related to seismic data processing referred to in section 3.3
Appendix III:	All appendices related to related to seismic data interpretation referred to in chapter 4
Appendix IV:	Results of the manual interpolation of the depth of the base of the Zechstein Z1 Halite
Appendix V:	Results of the manual interpolation of the depth of the top of the Zechstein Z1 Halite
Appendix VI:	Modeled depth of the base of the Zechstein Z1 Halite
Appendix VII:	Modeled depth of the base of the Zechstein Z1 Halite (concession area Isidorushoeve)
Appendix VIII:	Modeled depth of the top of the Zechstein Z1 Halite
Appendix IX:	Modeled depth of the top of the Zechstein Z1 Halite (concession area Isidorushoeve)
Appendix X:	Modeled thickness of the Zechstein Z1 Halite with indicated profile lines
Appendix XI:	Modeled thickness of the Zechstein Z1 Halite with indicated profile lines (concession area Isidorushoeve)
Appendix XII:	Modeled depth of the base of the Triassic deposits
Appendix XIII:	Modeled depth of the base of the Triassic deposits (concession area Isidorushoeve)
Appendix XIV:	Modeled thickness of the Z2 to Z4 deposits
Appendix XV:	Modeled thickness of the Z2 to Z4 deposits (concession area Isidorushoeve)
Appendix XVI:	Modeled depth of the base of the Tertiary deposits
Appendix XVII:	Modeled depth of the base of the Tertiary deposits (concession area Isidorushoeve)
Appendix XVIII:	Longitudinal WNW-ESE section through the elongated salt pillow (Profile A)
Appendix XIX:	SW-NE cross section through the western part of the elongated salt pillow (Profile B)
Appendix XX:	SW-NE cross section through the middle part of the elongated salt pillow (Profile C)
Appendix XXI:	SW-NE cross section through the eastern part of the elongated salt pillow (Profile D)
Appendix XXII a-b:	Distance to closest shot point for the base (a) and the top (b) of the Zechstein Z1 Halite models
Appendix XXIII :	Shot point density for the top of the Zechstein Z1 Halite model
Appendix XXIV:	Zechstein Z1 salt thickness within the concession area for which Zechstein Z1 Halite resources are calculated, the developed areas of Sint Isidorushoeve and Haaksbergen within the concession area and indication of the 60 m buffer around seismic surveys and exploration boreholes acquired specifically for the

	purpose of salt mining
Appendix XXV:	<b>Vertrouwelijk</b>
Appendix XXVI:	Modeled depth of the top of the Zechstein Z1 Halite (reserves area)
Appendix XXVII:	<b>Vertrouwelijk</b>
Appendix XXVIII:	Calculated dip angle of the top of the Zechstein Z1 Halite within the concession area
Appendix XXIX:	Calculated dip angle of the base of the Zechstein Z1 Halite within the concession area
Appendix XXX:	Slope of the base of the Triassic combined with isopachs for the depth of the base of the Triassic with potential caverns
Appendix XXXI:	<b>Vertrouwelijk</b>